

**Electrical and Thermal Ageing of
Extruded Low Density Polyethylene
Insulation Under HVDC Conditions**

by

Frøydis Oldervoll

A dissertation submitted to

the Norwegian University of Science and Technology
Department of Electrical Power Engineering

in partial fulfilment of the
requirements for the degree of
Doctor Ingeniør

December 2000

Preface

This thesis is part of the EFFEKT project “HVDC cable insulation” at SINTEF Energy research (SEfAS). The project is financed by Nexans Norway AS (former Alcatel Kabel Norge AS), Statnett SF and the Norwegian Research Council. The work was performed at the Norwegian University of Science and Technology, Department of Electrical Power Engineering in the period from 1995 - 2000.

I would like to thank my supervisors Prof. Erling Ildstad and Dr.ing. Rolf Hegerberg for giving me support, inspiration and guidance during the work. I would also like to thank all my colleagues at the Department of Electrical Power Engineering and the Materials Science group at SEfAS for giving me help and assistance when needed.

Finally I would like to thank my husband Erik and my son Trygve, born in 1998. Erik showed a great interest in my work and always supported and encouraged me, while Trygve was a source of everyday inspiration and happiness.

Trondheim, December 2000

Frøydis Oldervoll

Abstract

After extensive research during the last decades extruded polymeric insulation is now becoming an alternative to the traditional oil-paper systems for high voltage DC (HVDC) cables. Durability is of great importance for power cables, and the main purpose of this work has been to increase the knowledge of factors controlling the endurance of an extruded polymeric insulation under HVDC conditions. The effect of electrical and thermal ageing on electrical properties like space charge accumulation, DC breakdown strength and electrical tree initiation has been investigated and related to changes in morphology, oxidation level and antioxidant concentration.

Low density polyethylene (LDPE) with and without an antioxidant additive was selected as insulating material. Test objects with plane electrodes or needle-plane electrodes were prepared by pressure moulding and equipped with aluminium electrodes. Iron particles with a diameter of 45 - 55 μm were introduced to simulate conducting contaminations in the insulation. The test objects were subjected to thermal ageing at 70°C and 90°C and the applied electrical field during ageing ranged from zero to 150 kV/mm. Ageing was conducted both with constant DC polarity and with polarity reversals. The ageing period ranged from 4 weeks to 5 months.

Thermal oxidation was observed in LDPE without antioxidant and this clearly affected the electrical properties. The DC breakdown voltage was reduced by 40% and this was explained by enhanced high-field conduction and increased joule heating due to the oxidation products. It was found that oxidation was prohibited when the thickness of the aluminium electrodes increased.

The antioxidant additive prevented thermal oxidation, but was found to cause faster space charge accumulation and larger field modifications at the electrodes. The DC breakdown voltage of test objects with needle electrodes was reduced by 16 - 26% due to the antioxidant.

Introduction of iron particles reduced the short term DC strength by 20 - 30%, but during long term ageing with constant DC voltage no difference was observed between test objects with and without particles. This was probably caused by screening of the particles by accumulated space charge.

The experiments showed that abrupt grounding or polarity reversal initiated electrical trees from the needle-electrodes. The longest trees were observed when the test objects had first been subjected to thermal and electrical ageing. The tree formation was caused by the high electrical field arising when the accumulated homocharge around the needle was converted to heterocharge at polarity reversal or grounding.

The following main conclusions were made from the work:

- Oxidation is detrimental and must be avoided in HVDC insulation.
- The antioxidant additive can have a negative influence on the electrical properties under HVDC stress.
- Polarity reversal or abrupt grounding can initiate electrical trees from protrusions present at the electrode-insulation interface of a HVDC insulation system.

Content

| | |
|---|------------|
| Preface | I |
| Abstract | III |
| Content | V |
| 1 INTRODUCTION | 1 |
| 1.1 Background | 1 |
| 1.2 Scope of Work | 2 |
| 2 LITERATURE REVIEW | 5 |
| 2.1 Basic terms | 5 |
| 2.2 Effect of thermal oxidation during DC electrical ageing | 8 |
| 2.2.1 The oxidation process | 8 |
| 2.2.2 Conduction current and space charge accumulation | 9 |
| 2.2.3 Electrical breakdown | 9 |
| 2.3 Effect of the antioxidant additive | 10 |
| 2.3.1 Space charge accumulation | 10 |
| 2.3.2 Consumption and migration of antioxidant | 11 |
| 2.4 Effect of mechanical properties | 12 |
| 2.4.1 Breakdown | 12 |
| 2.4.2 Ageing | 13 |
| 2.5 Irregularities in the insulation system | 13 |
| 2.6 Effect of DC polarity reversal | 15 |
| 2.7 Discussion | 17 |
| 3 EXPERIMENTAL TECHNIQUES | 19 |
| 3.1 Materials | 19 |
| 3.1.1 Insulating material | 19 |

| | | |
|----------|--|-----------|
| 3.1.2 | Electrodes | 20 |
| 3.1.3 | Particles | 21 |
| 3.2 | Preparation of test objects | 22 |
| 3.2.1 | Homogenous test objects | 22 |
| 3.2.2 | Test objects with included iron particles | 23 |
| 3.2.3 | Test Objects with needle prints | 24 |
| 3.3 | Characterization techniques | 25 |
| 3.3.1 | Measurement of space charge accumulation | 25 |
| 3.3.2 | Infrared spectroscopy | 28 |
| 3.3.3 | Differential Scanning Calorimetry | 30 |
| 3.3.4 | Mechanical strength | 33 |
| 4 | CHANGE IN MATERIAL PROPERTIES DUE TO THERMAL AGEING | 35 |
| 4.1 | Introduction | 35 |
| 4.2 | Experimental | 35 |
| 4.3 | Results and discussion | 36 |
| 4.3.1 | Crystallinity | 36 |
| 4.3.2 | Mechanical strength | 39 |
| 4.3.3 | Oxidation | 42 |
| 4.3.4 | Antioxidant additive | 44 |
| 4.4 | Summary of results | 47 |
| 4.5 | Conclusions | 47 |
| 5 | SPACE CHARGE ACCUMULATION DURING THERMAL AND DC ELECTRICAL AGEING | 49 |
| 5.1 | Introduction | 49 |
| 5.2 | Experimental | 50 |
| 5.3 | Results | 51 |
| 5.3.1 | Electrical ageing at 70 kV/mm | 51 |
| 5.3.2 | Thermal ageing at 70°C | 56 |
| 5.3.3 | Long term electrical and thermal ageing | 59 |
| 5.3.4 | Summary of results | 61 |
| 5.4 | Discussion | 63 |
| 5.4.1 | LDPE with antioxidant | 63 |

| | | |
|----------|--|-----------|
| 5.4.2 | LDPE without antioxidant | 65 |
| 5.5 | Conclusions | 67 |
| 6 | THE EFFECT OF IRON PARTICLES ON THE SHORT AND LONG TERM DC BREAKDOWN STRENGTH | 69 |
| 6.1 | Introduction | 69 |
| 6.2 | Experimental procedures | 70 |
| 6.3 | Results | 71 |
| 6.3.1 | Short term DC breakdown strength | 71 |
| 6.3.2 | Long term ageing | 74 |
| 6.3.3 | Characterization of the aged samples | 76 |
| 6.4 | Discussion | 79 |
| 6.4.1 | Short term DC breakdown strength | 79 |
| 6.4.2 | Long term ageing | 80 |
| 6.4.3 | Summary of discussion | 82 |
| 6.5 | Conclusions | 82 |
| 7 | DC BREAKDOWN STRENGTH OF TEST OBJECTS WITH NEEDLE-PLANE ELECTRODE GEOMETRY | 85 |
| 7.1 | Introduction | 85 |
| 7.2 | Experimental procedures | 85 |
| 7.2.1 | Short term breakdown voltage | 86 |
| 7.2.2 | Thermal and electrical ageing | 87 |
| 7.3 | Results | 88 |
| 7.3.1 | Short term breakdown voltage | 88 |
| 7.3.2 | Breakdown voltage after electrical and thermal ageing | 88 |
| 7.3.3 | Breakdown voltage after thermal ageing | 92 |
| 7.3.4 | Summary of the breakdown results | 92 |
| 7.3.5 | Electrical treeing | 94 |
| 7.4 | Discussion | 97 |
| 7.4.1 | DC breakdown voltage | 97 |
| 7.4.2 | Electrical treeing | 101 |
| 7.5 | Conclusions | 104 |

| | | |
|-----------|--|------------|
| 8 | POLARITY REVERSAL TESTING OF SAMPLES WITH NEEDLE-PLANE ELECTRODE GEOMETRY | 105 |
| 8.1 | Introduction | 105 |
| 8.2 | Experimental procedures | 105 |
| 8.3 | Results | 107 |
| | 8.3.1 DC polarity reversal breakdown test | 107 |
| | 8.3.2 4 weeks DC polarity reversal ageing | 109 |
| 8.4 | Discussion | 111 |
| | 8.4.1 Short term polarity reversal breakdown test | 111 |
| | 8.4.2 Long term ageing | 114 |
| 8.5 | Conclusions | 115 |
| 9 | DISCUSSION | 117 |
| 10 | CONCLUSIONS | 121 |
| | REFERENCES | 123 |

Chapter 1

INTRODUCTION

1.1 Background

The large majority of electric power transmissions use three-phase alternating current (AC). However, there are some situations where high voltage direct current (HVDC) transmission is more favourable. AC cables have a restricted maximum length due to the large cable capacitance and reactive power flow. For long distances and particularly for water crossing HVDC is the only possible technical solution. The world's first HVDC submarine cable was installed between the Swedish mainland and the island of Gotland in 1954 and had a capacity of 20 MW at 100 kV DC. A more recent example of a HVDC submarine cable is the Baltic cable between Sweden and Germany which was installed in 1994 [1]. The length of this cable is 250 km and the capacity is 600 MW at 450 kV DC.

The insulation system used in today's HVDC submarine cables normally consists of lapped paper insulation impregnated with either a highly viscous oil (mass impregnated) or a fluid oil (oil-filled). This technique has been used for half a century and has proven to be very reliable. Despite the success with lapped paper insulation there has been a large research and development activity on extruded polymeric insulation for HVDC purposes since the 1970s [2, 3]. There are several possible advantages of utilising an extruded insulation system [2]: An extruded cable can be operated with a higher conductor temperature which results in a higher transmission capacity compared to a mass-impregnated system. The potential environmental problems related to leakages from oil-filled cables are also removed. In addition jointing of

cables in the field may be easier with extruded compared to paper insulated cables.

In 1999 the world's first HVDC link with extruded insulation was installed on the island of Godtland [4]. This bipolar cable is 70 km long with rated voltage +/- 100 kV DC and a capacity of 50 MW. Extruded insulation systems for higher voltage ratings are also available but have not yet been installed: In Japan a crosslinked polyethylene (XLPE) insulation with an inorganic filler has been developed for 250 kV DC and work is in progress to design a cable for 500 kV DC using this extruded insulation [5]. A high density polyethylene (HDPE) material modified with a small amount of acid groups has also been found suitable for use at 500 kV DC [6]. In France a cable with low density polyethylene (LDPE) insulation has been developed for 270 kV DC [7].

In the cable systems mentioned above the extruded insulation is subjected to a mean electrical field ranging from 16 - 25 kV/mm. This is only a few percent of the intrinsic breakdown strength of polyethylene which is about 700 kV/mm [8]. The intrinsic breakdown level can only be approached for very pure, thin films. An extruded cable will inevitably contain different types of imperfections: Protrusions at the insulation - electrode interfaces or conducting or non-conducting particles in the bulk give rise to a local inhomogeneous electrical field from which breakdown can be initiated. Chemical additives and irregularities in polymer morphology lead to accumulation of electrical charge in the insulation with resulting local field enhancement. Ageing under thermal and DC electrical stress further decreases the breakdown strength, and as discussed below this will be an important topic in this work.

1.2 Scope of Work

Durability is of great importance for a HVDC submarine cable. Therefore it is necessary to investigate how extruded insulation performs under HVDC stress on a long term basis. The purpose of this work has been to obtain increased knowledge on which factors are controlling the insulation life time. Low density polyethylene was selected as insulating material since it is one of the main materials used for extruded AC cables. As mentioned above a

HVDC cable with LDPE insulation has already been developed in France and have shown promising results [7]. Cable quality LDPE always contains an antioxidant additive to prevent oxidation during production and service. In this work LDPE with and without an antioxidant was investigated in order to clarify the influence of the antioxidant under HVDC conditions.

The following hypotheses were investigated:

1. *Thermal oxidation has a negative effect on the long term electrical properties of LDPE.*
2. *The antioxidant additive prevents thermal oxidation but is a source of space charge accumulation in the insulation which may have a negative effect on the long term performance.*
3. *Inclusions in the insulation or protrusions at the electrodes are detrimental to the insulation and reduce the insulation life time under DC electrical ageing.*
4. *Defects in the insulation system are particularly critical during polarity reversal or abrupt grounding.*

In order to test the hypotheses formulated above, several types of experiments were performed:

The first step was to characterize the materials used during thermal ageing. Changes in oxidation, consumption of antioxidant, morphology and mechanical properties were monitored. These results served as a basis for further investigations and discussions and are presented in Chapter 4.

The space charge development in the material with and without antioxidant was followed during thermal and electrical ageing for a period of up to 5 months. Comparison of the two materials gave information about the role of the antioxidant additive in space charge formation. These results are presented in Chapter 5.

Conducting particles were introduced in the test objects and the short and long term DC breakdown strength was evaluated. After ageing the test objects were characterized with respect to oxidation and antioxidant concentration. The results are reported and discussed in Chapter 6.

Finally experiments were carried out on test objects with a needle-plane electrode geometry, where the needle simulated an extreme protrusion at the electrode. Reduction in breakdown strength due to electrical and/or thermal ageing was measured and the test objects were also subjected to polarity reversal tests. The area around the needle tip was closely examined to detect chemical degradation and electrical tree growth. Chapter 7 and 8 cover these results.

All experiments were performed on test objects with and without the antioxidant additive. This means that the two hypotheses concerning the antioxidant and oxidation are involved in all the described experiments.

In addition to the chapters mentioned above a review of the literature is included in Chapter 2. The review focuses on theory and findings that are related to the four hypotheses formulated above. In Chapter 3 the experimental equipment and the preparation of the test objects is described. In Chapter 9 the results are discussed with respect to the four hypotheses. Conclusions of the work are presented in Chapter 10.

Chapter 2

LITERATURE REVIEW

The subject of polymeric HVDC insulation has been extensively investigated during the last decades. The scope of this literature survey is to present theory and findings which are of importance in relation to the current work. The effect of oxidation, antioxidant additives, mechanical strength and irregularities on electrical properties like space charge accumulation, conduction current and breakdown will be discussed.

2.1 Basic terms

This section contains a brief description of some basic terms used when discussing the electrical properties of polymers with references to further reading.

Semicrystalline material: A polyethylene molecule typically consists of $10^3 - 10^5$ repeating $-\text{CH}_2$ units. These long molecules build up a semicrystalline structure consisting of crystalline and amorphous regions [9]. In the crystalline regions the polymer chains are arranged in folded structures called lamellas as shown in Figure 2.1.

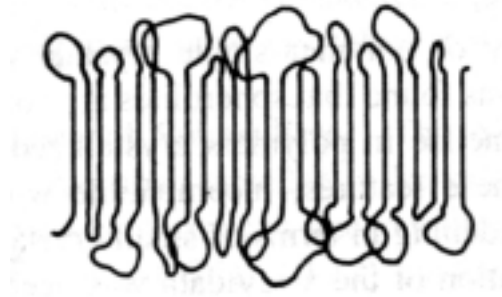


Figure 2.1 Two-dimensional model of a lamella structure. The polymer chains are folded back and forth on themselves to form a semicrystalline, ribbon-shaped region known as a lamella. Illustration from Billmeyer [9].

Charge injection: Electrons or holes entering the insulation from the electrodes must overcome an energy barrier. The height of the barrier is determined by the work function of the metal and polymer. High fields can reduce both the barrier height and width. These effects are included in the Schottky and Fowler-Norheim models for charge injections [10, 11]. The shape of the barrier will be modified by surface states arising from chemical and physical defects at the interface [12].

Charge traps: The chemical and structural defects existing in disordered regions of a polymer act as traps for electrons or holes [13]. The trap depth is given by the amount of energy required to release the charge from the trap. Thermally stimulated current measurements (TSC) on polyethylene have shown that the trap characteristics are closely related to the polymer morphology. The origin and depth of the traps in different types of polyethylene has been discussed in a review by Ieda [14].

Conduction: The conductivity of polyethylene is very low, typically less than $10^{-18} \Omega^{-1}\text{m}^{-1}$ at 40°C [15]. The conductivity increase with increasing electrical field and temperature. At low fields the conduction is ohmic but at high fields ($>10 \text{ kV/mm}$) the conduction becomes non-linear. In the high field region the charge transport can be described as a field-dependent hopping transfer of electrons between the charge traps [10, 11]. The electrons

taking part in conduction can be injected from the cathode or released from donors in the bulk of the insulation. Several electrode- and bulk-limited conduction mechanisms have been proposed for polyethylene but there is no general agreement about which model to apply. A review of the conduction mechanisms in general and the specific case of polyethylene can be found in the book by O'Dwyer [11].

Space charge: Space charge is localized charge of one polarity which is not compensated by an equal charge concentration of opposite polarity at the same location [16]. This charge causes a local field enhancement given by Poisson's equation:

$$\nabla E = \frac{\rho_c}{\epsilon} \quad (2.1)$$

where ρ_c is the charge density (Cm^{-3}) and ϵ is the permittivity. One example of space charge is ionized donors that are left behind by the electrons donated to the conduction band. Another example is electrons or holes trapped in the amorphous regions of the polymer as was discussed previously. If the electron or hole is trapped by a local arrangement of the molecular chains (cavity trap, self-trap) no counter charge is present and a space charge arises[14].

Homocharge: Space charge of the same polarity as the adjacent electrode is termed homocharge, see Figure 2.2. Homocharge is generated when charge injected from one or both electrodes is trapped in the vicinity of the injecting electrode. This can be viewed as a situation where more charge is injected from the electrodes than the insulation is able to carry off [17]. The homocharge reduces the field at the electrode, the injection decreases and the charge distribution stabilizes.

Heterocharge: Space charge of the opposite polarity as the adjacent electrode is termed heterocharge, see Figure 2.2. One possible origin of heterocharge is ionization of low molecular species. Heterocharge can also be a result of insufficient injection from the electrodes: Charge move faster through the insulation than it is supplied from the electrodes, and a layer of heterocharge is left in the electrode regions [17]. The heterocharge enhances

the field at the electrodes, the injection of charge from the electrodes increases and again the charge distribution stabilizes.

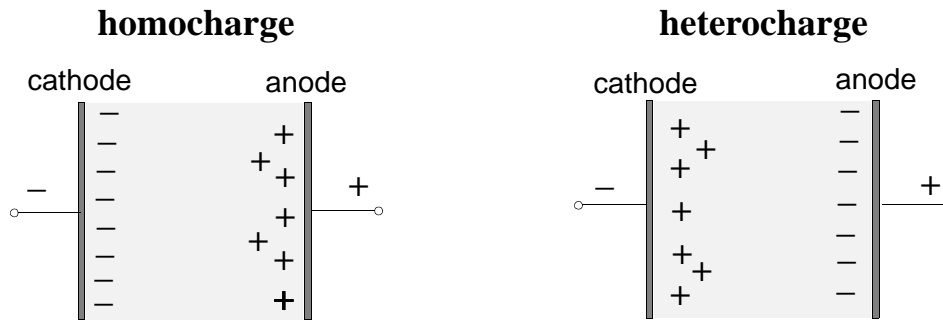


Figure 2.2 Illustration of homo- and heterocharge accumulation in the anode and cathode regions of the insulation.

2.2 Effect of thermal oxidation during DC electrical ageing

In extruded polymeric cables oxidation may take place both during production and service. Crine et al. [18] investigated a series of extruded polyethylene transmission and distribution cables. They found that all cables, even unaged ones, contained traces of oxidation and that the oxidation increased during ageing. Many investigations have been carried out to see how oxidation affects the electrical properties of polyethylene. Some important results will be summarized below.

2.2.1 The oxidation process

Oxidation is the most important mechanism giving rise to chemical degradation of polymers. It takes place when polymeric materials are exposed to elevated temperatures or UV-radiation in the presence of oxygen. Molecular oxygen attacks the hydrocarbon chains and initiates a series of reactions. This process is termed autoxidation. It is slow in the beginning, but after an induction period the rate of oxidation increases rapidly; the first formed oxidation products accelerate further degradation [19]. The autoxidation process results in formation of carbonyl groups (C=O), hydroperoxides (C-O-O-H) and carbon-carbon double bonds (C=C).

2.2.2 Conduction current and space charge accumulation

Several investigations have shown that the electrical conductivity increases with oxidation in polyethylene [20,21,22]. This increase is explained by enhanced charge injection from the electrodes and formation of localized states below the conduction band resulting in easier charge transportation.

Measurements of space charge accumulation also suggest increased charge injection from the electrodes due to oxidation. Suzuoki et al. [23] have shown that negative charge accumulates near the cathode when PE is oxidized in ozone atmosphere. They observed no positive charge near the anode, indicating that it was mainly the electron injection from the cathode that was affected by the oxidation. Dominating electron injection from the cathode is also supported by Ieda et al. [22] who measured the electric field at the electrodes in oxidized samples. They observed a large reduction in the cathode electric field but only a small decrease in the anode electric field due to accumulated charge. Both Suzuoki and Ieda found that the amount of negative charge near the cathode decreased with increasing temperature.

2.2.3 Electrical breakdown

Increased electrical current and space charge accumulation due to oxidation will affect the breakdown strength of the insulation. For thin PE films (20 - 150 μm) there seems to be a general agreement that oxidation reduces the DC breakdown strength in the temperature range from 20 - 90°C. This result is obtained both when the samples are oxidized in ozone atmosphere [20,21,24] and when thermally aged at 100°C [25]. The reduced DC breakdown strength is explained by localized Joule heating due to the increased high field conduction in oxidized samples. Tsurimoto et al. [24] have observed increased Joule heating due to oxidation. They found an inhomogeneous heating across the film area and observed that breakdown occurred at the hottest spot on the film. The inhomogeneous heating was explained by enhanced heating in weak parts of the insulation, i.e. in amorphous regions with high concentration of oxidation products.

2.3 Effect of the antioxidant additive

All extruded polymeric cables contain antioxidant additives in order to slow down the oxidation process. Chain terminating antioxidants like SantanoxR and Irganox are the most common for cable insulation. These antioxidants are hydrogen donors and replace the very reactive $-R-O_2^{\bullet}$ radicals by stable, non-reactive radicals [26]. This retards the chain reaction and slows the oxidation. Figure 2.3 shows the chemical structure of the SantanoxR molecule.

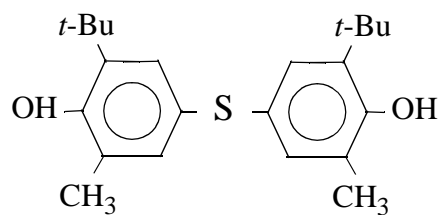


Figure 2.3 Chemical structure of SantanoxR [26]. *t*-Bu is a butyl group, i.e. a chain of four carbon atoms connected by single bonds.

The two hydroxide groups are the active parts of the SantanoxR. The chemical reaction is shown in Figure 2.4 where the SantanoxR molecule is represented as OH-A-OH.

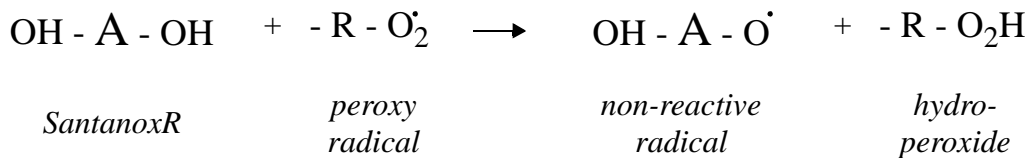


Figure 2.4 The chemical reaction between SantanoxR and the free radicals taking part in the oxidation process.

2.3.1 Space charge accumulation

The antioxidant may give rise to space charge accumulation in several ways, indirectly by altering the polymer morphology or directly by acting as a charge source or trapping site.

Cartwright et al. [27] compared LDPE with and without an antioxidant additive (unknown type) with respect to morphology and space charge accumulation. They found that in samples without antioxidant there was a considerable variation in morphology through the sample; some regions had a fine texture while others consisted of large spherulites. The samples with antioxidant on the other hand had a uniform microstructure consisting of small spherulites. This was explained by the antioxidant acting as nucleating agent for the formation of spherulites. Based on the morphology observations one would expect less charge to accumulate in LDPE with antioxidant, but this was not the case. A large amount of negative charge accumulated close to the anode in LDPE with antioxidant, no positive charge was observed. After 48 hours of ageing at 60 kV/mm and room temperature the anode electrical field was doubled due to the accumulated charge. They concluded that the antioxidant acted as a localized state trapping negative charge, while the microstructure was only a second-order effect.

A similar observation of negative charge close to the anode in LDPE with antioxidant was made by Mizutani et al. [28]. Other workers have observed both positive and negative heterocharge in LDPE with antioxidant [29, 30]. The type of antioxidant used is not given in any of the investigations referred to here. Thus different types and concentrations of antioxidant may explain the different space charge results.

2.3.2 Consumption and migration of antioxidant

During production and service the antioxidant is consumed, and thus the polymer is only protected for a certain period of time. Consumption of the antioxidant can be significant during production when the temperature is high, while at normal service temperatures (below 70°C) the consumption is a slow process. As an example a low density polyethylene sample with 0.1% antioxidant additive was protected for 100 hours at 140 °C while the protection time at 70°C was extrapolated to 200 years [31]. A protection time of 200 years is not obtained in reality since another mechanism comes into play at temperatures below the melting point of polyethylene: Most antioxidants have a very limited solubility in solid LDPE and consequently migrate out of the polymer [32]. In the example above the actual protection time at 70°C was measured to be 90 days due to the loss by migration [31].

Loss of antioxidant due to migration has also been observed in high voltage cables. Parpal et al. [33] measured the radial antioxidant profile in aged and unaged cross-linked PE (XLPE) transmission cables. They found a region depleted of antioxidant close to the semiconductive shields both in unaged and aged cables. This was not the case in LDPE cables investigated by Andreß et al. [34]. They observed a homogenous distribution of the antioxidant through the insulation shortly after fabrication, but when the cables had been stored several years at room temperature the region close to the semiconductive shield was completely depleted of antioxidant. This difference between the investigations could be due to the higher production temperature for XLPE cables compared to LDPE cables. Andreß also found that the diffusion of the antioxidant was controlled by the semiconductive shields. In samples without semiconductors no concentration gradient was observed after ageing. Thus they concluded that the antioxidant was absorbed at the insulation/semiconductor interface and that the carbon particles played an important role in the absorption due to large active surfaces.

2.4 Effect of mechanical properties

2.4.1 Breakdown

Young's modulus is a measure of the resistance to deformation of a material when an external force is applied [35], and in polyethylene this elastic modulus decreases rapidly with increasing temperature [36]. It is well known that the breakdown strength of polyethylene also shows a strong decrease with increasing temperature above 30°C [37], and in 1955 Stark and Garton [38] introduced the theory of electromechanical breakdown for polyethylene. According to this theory, compression of the polymer caused by the applied electrical stress leads to electromechanical instability and breakdown. The critical field at which the instability occurs is given by [39]:

$$E_{critical} = 0.61 \sqrt{\frac{G}{4\epsilon}} \quad (2.2)$$

where G is Young's modulus and ϵ is the static dielectric constant. The calculated critical field for temperatures above 50°C agrees well with the measured breakdown level in PE. Stark and Garton also showed that crosslinking of PE by irradiation significantly increased the breakdown level at high tem-

peratures. This was in agreement with the corresponding improvement of Young's modulus in the crosslinked polymer.

2.4.2 Ageing

When polyethylene is subjected to thermal ageing Young's modulus may change due to annealing and recrystallization [40] or degradation caused by oxidation [41, 42]. According to the electromechanical breakdown theory this will alter the breakdown level of PE at temperatures above 50°C. As an example it has been shown that the breakdown level of high density polyethylene at 90°C increased due to annealing and corresponding improvement of Young's modulus [43].

During electrical ageing the polymer is subjected to a continuous electromechanical stress. Accumulated space charge will attribute to this stress due to local enhancement of the electrical field. Dissado et al. [44] have discussed the possibility of microvoid formation and crazing in the regions with high electromechanical stress, which eventually will lead to initiation of electrical breakdown. The electrical field necessary to initiate this process will depend on the elastic modulus of the insulating material.

2.5 Irregularities in the insulation system

An extruded polymeric insulation system will inevitably contain different types of defects like conducting or non-conducting inclusions, protrusions at the semiconductive electrodes or voids. In the case of extruded AC cables it is well known that such defects reduce the endurance of the cable [45,46,47]. The defects give rise to local field enhancement and initiate electrical treeing or water treeing.

The effect of defects on the long term endurance under DC conditions has been less investigated, but work done by Chen et al. [48] indicates that defects have the same detrimental effect under DC fields. They introduced artificial defects in LDPE test samples which were aged with a constant DC voltage at room temperature. Both 50 µm copper spheres and 50 µm voids reduced the characteristic insulation life time from approximately 6000 to 2000 hours compared to control samples without defects. One should be

aware that these defects were relatively large, they made up about 30% of the total insulation thickness. Such large defects are not very likely to appear in an extruded cable. Chen et al. also performed measurements of short term DC breakdown strength. The size of the particles was varied and they found that particles with a diameter below 15 μm had little effect on the short term DC breakdown strength.

Many experiments have been performed with a needle-plane electrode configuration to simulate the inhomogenous field around a defect or protrusion in polyethylene [49-51]. This has mainly been short term experiments related to DC electrical treeing and breakdown. An advantage of needle experiments is that the electrostatic field around the needle tip is well defined. Mason [49] has showed that the maximum electrostatic field at the needle tip in the absence of space charge is given by:

$$E_{max} = \frac{2V}{r \ln\left(1 + 4\frac{d}{r}\right)} \quad (2.3)$$

where V is the applied voltage, r is the needle radius of curvature and d is the distance from needle to plane. This expression is valid when $d > 10r$.

Ieda et al. [50] performed needle experiments with $r = 5 \mu\text{m}$ and $d = 2 \text{ mm}$. They observed DC treeing for voltages above 50 kV depending on polarity and voltage rising speed. This corresponds to an electric field $> 2700 \text{ kV/mm}$ which is about 4 times the intrinsic breakdown strength of polyethylene. PE can not survive at such high fields and it was concluded that homo-space charge must accumulate around the needle tip and cause a field reduction.

The needle experiments have also shown that DC tree inception and breakdown is very dependent on the polarity of the needle tip. The breakdown and tree initiation voltage is always higher with negative polarity on the needle tip. For example, Kawamura et al. [51] found that the DC tree inception voltage in LDPE was 100% higher with negative polarity compared to positive polarity. Mason [49] and Ieda [50] explained the polarity effect by the difference in hole and electron injection: With a negative needle electrons are injected until the electrical field at the needle tip reaches a threshold value for injection. In the case of a positive needle the homo charge is created when electrons are extracted from the polymer at the anode, leaving a positive

charge behind. The number of electrons available for extraction is limited and thus less positive charge is formed and the screening of the needle is less efficient under positive polarity.

The homo-charge accumulation in the vicinity of a defect may become a serious problem if an abrupt grounding or polarity reversal takes place. This will be discussed in the next section.

2.6 Effect of DC polarity reversal

Many investigations have shown that DC polarity reversal is very critical in the case of extruded insulation [3]. This is due to the accumulation of space charge during DC voltage application giving rise to field enhancement in parts of the insulation when the polarity is reversed. Defects causing inhomogeneous fields are especially critical during polarity reversal. Homo-charge accumulates during the DC period and reduce the electric field in the vicinity of the defect (Section 2.5). If the polarity is changed abruptly the homo charge is converted to hetero charge. This results in a very high electric field exceeding the intrinsic breakdown strength of the polymer. Thus a partial breakdown takes place in the insulation.

Needle experiments can give information on the mechanisms that take place in the vicinity of a defect during polarity reversal or grounding. A common approach is to apply a DC voltage to the needle for a certain period of time before a fast grounding is performed. If an electrical tree is generated the length is recorded. Ieda et al. [50] have performed this type of grounding tree experiments on LDPE. They found that the length of the electrical tree depended on the DC prestress time. At 30°C a maximum tree length was reached after 20 minutes of prestress while this time was reduced to 5 minutes at 60°C as shown in Figure 2.5. A marked polarity effect was observed: The length of the trees formed after a positive DC prestress was only 1/6 of the tree length obtained with negative polarity. This was explained by the fact that less charge accumulates around a positive needle (Section 2.5) resulting in a weaker field enhancement at grounding. There is a general agreement

that the length of the grounding tree is closely related to the amount and distribution of the space charge accumulating during DC prestress [50 - 53].

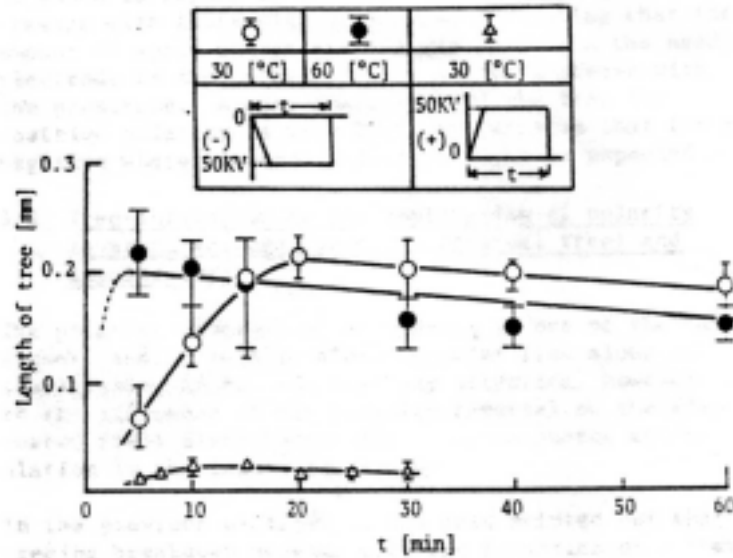


Figure 2.5 Effect of duration of DC prestress on the length of short-circuit tree. (From Ieda et al. [50])

Shimizu and Uchida [54, 55] have described electrical tree initiation in regions with inhomogeneous field from a more chemical point of view. They worked with AC voltages in their needle experiments. According to Mameri the mechanism for electrical tree initiation is very similar under AC and DC polarity reversal [52, 56] and thus the results may be relevant in these cases as well. The work of Shimizu and Uchida showed that oxidation played an important role in the electrical tree initiation. The tree initiation voltage was six times higher in samples where oxygen was removed by vacuum degassing than in samples kept in air atmosphere. This was explained in terms of an autoxidation process: chain scission caused by injected electrons from the needle was the first stage of the tree initiation. Free radicals were formed and reacted with available oxygen. New radicals were formed and an autoxidation process developed. This led to a rapid development of a tree channel. In the absence of oxygen no autoxidation took place and this resulted in a considerably higher tree initiation voltage. FTIR measurements confirmed that a higher number of C=C and C=O groups were present in the vicinity of the needle tip compared to the bulk of the material even at the very early stage of tree initiation.

2.7 Discussion

This review has summarized experimental results related to ageing of polymeric insulation under HVDC conditions. The referred results served as a basis when choosing the four working hypothesis of Section 1.2. It is clear that more work is required to make any conclusions on the hypothesis, and this will be discussed in the following sections.

Hypothesis 1. *Thermal oxidation has a negative effect on the long term HVDC properties of LDPE.*

This literature survey has shown that oxidation gives rise to enhanced charge injection from the electrodes under DC stress, which again reduces the DC breakdown strength. The majority of the experiments were performed with thin films (<100 µm) heavily oxidized after being kept in an ozone atmosphere for a few hours. In order to understand how thermal oxidation affects the long term HVDC properties it is necessary to perform experiments on thicker samples which are thermally oxidized at normal operation temperature. In addition it is not clear whether oxidation is accelerated in the vicinity of irregularities. Shimizu et al. [55] have measured enhanced oxidation around a needle tip under AC conditions, but what happens at a defect when a DC field is applied? Chen et al. [48] observed oxidation close to a particle after long term DC ageing, but this observation was done at a breakdown site, and thus the oxidation was probably caused by heat generated during breakdown. FTIR spectroscopy should be carried out systematically around defects after ageing with DC and DC polarity reversal voltage to see if defects accelerate oxidation.

Hypothesis 2: *The antioxidant additive prevents thermal oxidation but is a source of space charge accumulation in the insulation which may have a negative effect on the long term performance.*

From the literature reviewed it is clear that an antioxidant additive may give rise to large heterocharge concentrations. All these experiments were performed at room temperature during a short period of time (hours). What happens during long term ageing at higher temperatures? Migration, depletion and consumption of the antioxidant will affect the space charge generation. Long term ageing of LDPE with and without antioxidant must be carried out

in order to evaluate whether the antioxidant has a net negative effect on the HVDC properties.

Hypothesis 3: *Inclusions in the insulation or protrusions at the electrodes are detrimental to the insulation and reduce the insulation life time under DC electrical ageing.*

Few experiments have been reported concerning the influence of defects on the HVDC endurance. Chen et al. observed a reduced time to breakdown when different types of defects were included in the insulation. The particles were large compared to the insulation thickness and one should perform long term experiments with smaller particles in order to obtain a more realistic situation. The short term needle experiments reviewed here have focused on the inception voltage for DC treeing. It has been shown that electrical trees are initiated from the needle tip when the DC voltage exceeds a certain level. What happens around the needle tip if a DC stress is applied for a longer period of time? Long term experiments with needle-plane electrodes can give information on degradation in the high field area around defects in extruded insulation.

Hypothesis 4: *Polarity reversal or fast grounding accelerates the ageing process in the vicinity of particles or protrusions.*

Needle experiments have shown that defects in extruded insulation are particularly critical if the polarity is reversed or the voltage is grounded abruptly. The risk of electrical tree initiation is high since homocharge injected during the DC period is converted to hetero charge at reversal, and this results in a very high local field stress. Again it is mainly short term results that are reported and it is necessary to perform long term experiments to learn more about the ageing process in the vicinity of particles or protrusions.

Chapter 3

EXPERIMENTAL TECHNIQUES

This chapter contains two main parts. First the materials and types of test objects are described. There are three types of test objects; homogenous objects, objects with included iron particles and objects with needle prints. The first type was used for space charge measurements while the two last ones were used for breakdown tests and long term ageing. The second part deals with the different characterisation techniques used. These techniques include the PEA method for detecting accumulated space charge, FTIR for determination of oxidation degree and crystallinity and DSC measurements to reveal the melting properties and antioxidant content of the materials.

3.1 Materials

3.1.1 Insulating material

All the investigations throughout this thesis have been performed on low density polyethylene (LDPE) with and without the antioxidant additive Santanox R. LDPE was selected as insulating material since this is one of the main materials used for extruded AC cable insulation. A HVDC cable system with LDPE insulation has already been developed and has shown promising behaviour [7]. The other material widely used for AC cables is cross-linked polyethylene (XLPE). Antioxidant additive is required in XLPE due to the high cross-linking temperature of typically 180°C [58]. After manufacturing XLPE must be subjected to a degassing procedure at a temperature of typically 70 - 90°C for several days to remove volatile by-products from the cross-linking process [58]. This heat treatment may alter the polymer mor-

phology and the antioxidant concentration and distribution as discussed in Chapter 2. LDPE was thus preferred since it gave the opportunity to work with an additive free material that had not been subjected to any thermal treatment before the electrical measurements started.

The materials with product codes LE4147 and LE1800 for LDPE with and without antioxidant respectively, were supplied as pellets from Borealis. The two materials were of the same cable quality, super clean, but LE1800 was removed from the production line before the antioxidant was added. The antioxidant concentration was not given by the manufacturer but was probably in the range from 0.4 - 1.0 weight%.

3.1.2 Electrodes

The electrodes were either aluminium or gold deposited with a JEOL JEE-4X vacuum evaporator with resistive heating source. Semiconductive electrodes were considered since this would give test objects with a construction more similar to real cables. The semiconductive materials commercially available from Borealis consist of ethylbutylacetate (EBA) with added carbon black and the antioxidant additive Santanox R. Preliminary tests with such electrodes revealed diffusion of low molecular EBA components from the electrodes into the insulation. This is shown in Figure 3.1 where the absorbance of the ester group in EBA has been measured through a cross-section of test objects with and without semiconductive electrodes. The figure clearly demonstrates the diffusion of low molecular weight EBA from the semiconductive electrodes and this type of diffusion has also been observed by others [57]. The main focus of this thesis was the ageing properties of the insulating material itself, and influence of the electrodes was not desired. In addition the diffusion is difficult to control and will vary with time, temperature and sample thickness. Therefore it was decided to use metal electrodes.

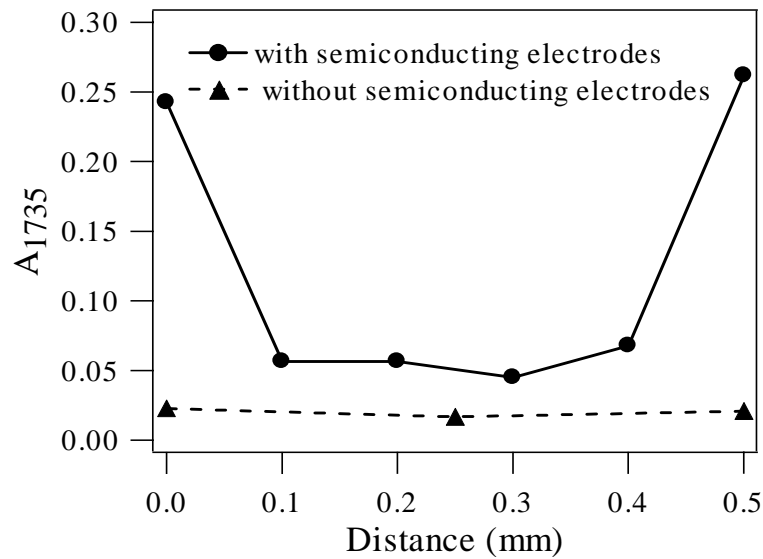


Figure 3.1 The ester absorbance at 1735 cm^{-1} through a cross-section of test objects with and without semiconductive electrodes.

3.1.3 Particles

Iron particles were selected to investigate the effect of conducting particles on the long term insulation properties. This was motivated by the fact that iron contaminations are found in medium and high voltage extruded AC cables [58]. In addition it is known that iron acts as a catalyst in the oxidation process [19] and may thus be the most critical particle type during long term ageing. The iron particles used were irregular shaped with a diameter of 45 - 55 μm , see Figure 3.2.

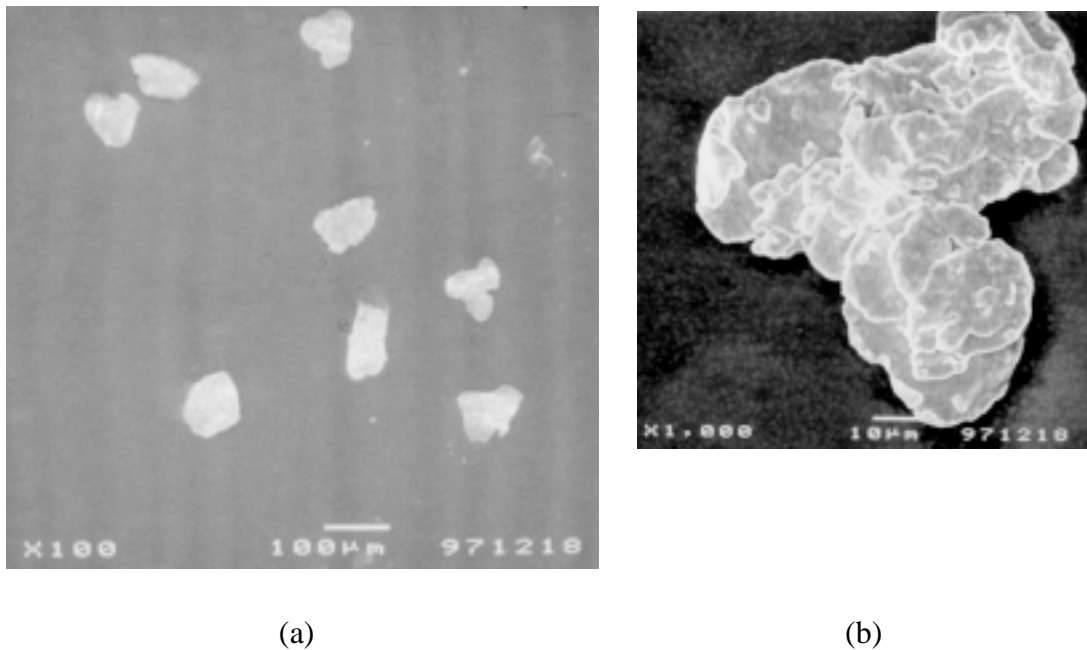


Figure 3.2 Irregular iron particles viewed with scanning electron microscope (SEM) at 100 (a) and 1000 (b) times magnification.

3.2 Preparation of test objects

3.2.1 Homogenous test objects

A laboratory twin-screw extruder was used to make an LDPE tape of the received pellets. The extruding temperature was 140°C. This extrusion process gave a homogenous material and thus effects of the pellet-interfaces were eliminated.

The tape was cut into tablets and put into moulds. Nine test objects were prepared in one batch. The nine moulds were kept in an hydraulic press at 115°C with a pressure of about 14 kPa (4-5 tons) for 30 minutes. Then the pressure was increased to 100 kPa (30 tons) and the moulds were cooled to room temperature at a rate of approximately 10°C/ minute. Hagen [58] gives a detailed description of both the extrusion process and the pressure moulding.

The resulting test objects were cup-shaped with Rogowski profiled electrodes, see figure 3.3. Due to the Rogowski profile the electric field is

homogenous and has its highest value in the centre section of the cup. The flat centre section was 42 mm in diameter. The 40 mm high skirt prevented external flashover when high voltage was applied. The insulation thickness was 0.5 ± 0.1 mm. The test objects were equipped with evaporated aluminium or gold electrodes.

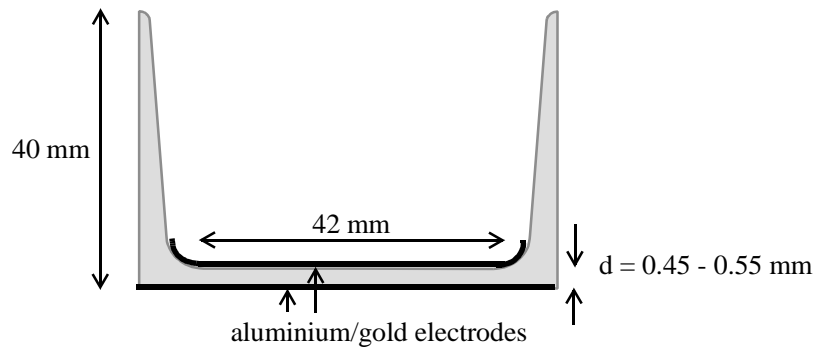


Figure 3.3 Homogenous test object

3.2.2 Test objects with included iron particles

The particles were mixed with LDPE granulate and hot rolled at 120°C to form 0.5 mm sheets containing randomly distributed iron particles. Cup-shaped objects were prepared as described in Section 3.2.1 but the flat centre area was removed. Then the remaining skirts and the sheets containing iron particles were mounted together. This was done by placing the parts in moulds and inserting them into the hydraulic press. 100 kPa (30 tons) were applied and the temperature was raised to 114°C . The moulds were kept under pressure for 45 minutes before they were cooled to room temperature at a rate of $10^{\circ}\text{C}/\text{minute}$. The resulting cup-shaped test objects with included iron particles is shown in figure 3.4. The particle concentration in the final test objects were about $4 \text{ particles}/\text{cm}^2$ and one particle made up about 17% of the total insulation thickness.

Reference test objects were also prepared following the same procedure as described above but without adding iron particles. The insulation thickness of the test objects with iron particles was 0.3 ± 0.05 mm while the reference test object had a thickness of 0.2 ± 0.05 mm.

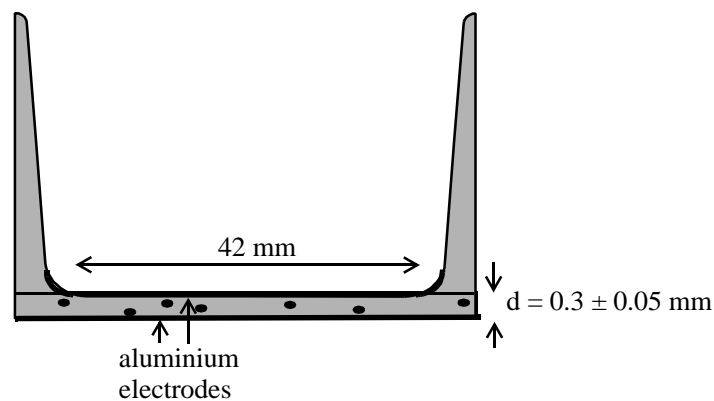


Figure 3.4 Test object with included iron particles.

3.2.3 Test Objects with needle prints

Cup-shaped test objects with an insulation thickness of 2.35 ± 0.1 mm were prepared using the same procedure as described in Section 3.2.1. Three needle prints were made in the bottom of each test object as shown in figure 3.5. This was done using the following procedure: The test object was heated to a temperature of 95°C . At this temperature the insulation was soft but not melted. Three needles were inserted into the test object under a controlled pressure. The needles were mounted on a cylindric plate to assure equal penetration depth for each needle.

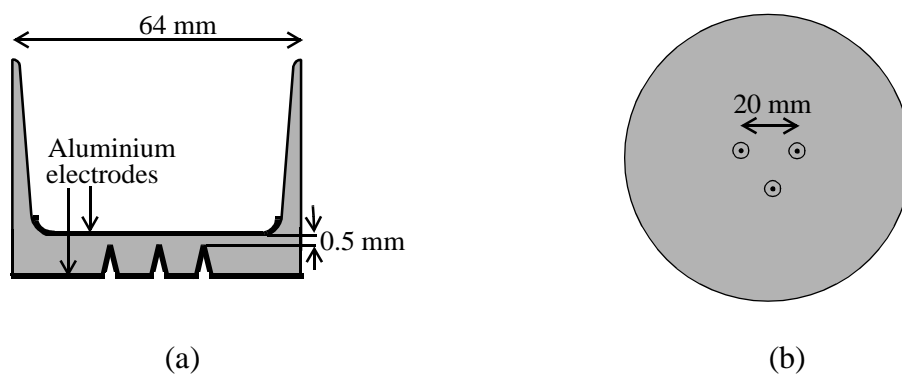


Figure 3.5 Test object with needle prints. Cross-section (a) and view from bottom (b).

The test object was cooled to room temperature at a rate of approximately $10^\circ\text{C}/\text{minute}$ before the needles were removed. The needles used were com-

mercial treeing needles from Ogura Jewel Industry Co. with a bend radius of $10\ \mu\text{m}$. The resulting needle prints had a bend radius of $6 \pm 1.5\ \mu\text{m}$ and the distance from needle to plane was $0.5 \pm 0.1\text{mm}$. Aluminium electrodes were deposited by vacuum evaporation and microscope inspection verified that aluminium covered the entire needle print, see figure 3.6.

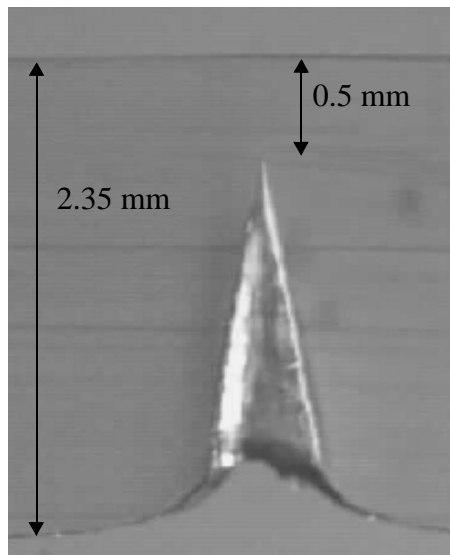


Figure 3.6 Cross-section trough needle print with aluminium electrode.

3.3 Characterization techniques

3.3.1 Measurement of space charge accumulation

During the last two decades several non-destructive methods for space charge measurements have been developed. A common feature of all these techniques is that the charged sample is subjected to a disturbance, for example a pressure wave, an electrical pulse or a thermal pulse. The material response to the disturbance is recorded and gives information about the amount and distribution of accumulated charge. The different techniques have been reviewed by several authors lately [59, 60]. In the current work the pulsed electro-acoustic method (PEA) was applied. This method was first proposed by T. Takada in 1985 [61].

Principle of the PEA method

With the PEA method a high voltage pulse is used to measure accumulated charge. The applied pulse sets up an electric field through the sample which induces a small movement of the charge. This movement generates an acoustic wave which travels through the sample and is recorded by a piezoelectric sensor. Deconvolution and calibration of the recorded signal is necessary to obtain the space charge distribution. A detailed description of the PEA principles have been given by several authors, for example Maeno et al. [62] and Sanden [63].

Experimental setup

The experimental apparatus used was delivered by Potential Cooperation. Figure 3.7 gives a schematic view of the experimental layout. The geometrical resolution of the instrument is $70\ \mu\text{m}$ and the sensitivity is $0.1\ \text{nC}/\text{mm}^3$. The applied pulse has an amplitude of 300V, the pulse width is 28 ns and is applied repeatedly every 23 ms. A DC voltage up to $\pm 12\text{kV}$ can be applied during measurement. The output signal was recorded with a digitizing oscilloscope. Further data processing like deconvolution and calibration is performed using the computer program Igor Pro. The data processing steps have been presented in more detail by Sanden [63].

Figure 3.8 (a) and (b) shows two examples of calibrated space charge profiles, one without and one with internal space charge respectively. The test object without internal space charge was subjected to a DC voltage of 4 kV during measurement. The applied voltage induced surface charges at the electrodes as can be seen from the graph. We observe that the second charge peak has an amplitude which is almost twice as large as the amplitude of the first peak. This is caused by a reflection of the acoustic wave at the upper electrode in the setup. After 4 weeks of electrical ageing a negative charge had accumulated in the bulk of the test object as can be seen from Figure 3.8 (b). This negative charge induced positive image charges at the electrodes to ensure neutrality. No DC voltage was applied during measurement and this was in general the case for all the space charge profiles presented in this thesis.

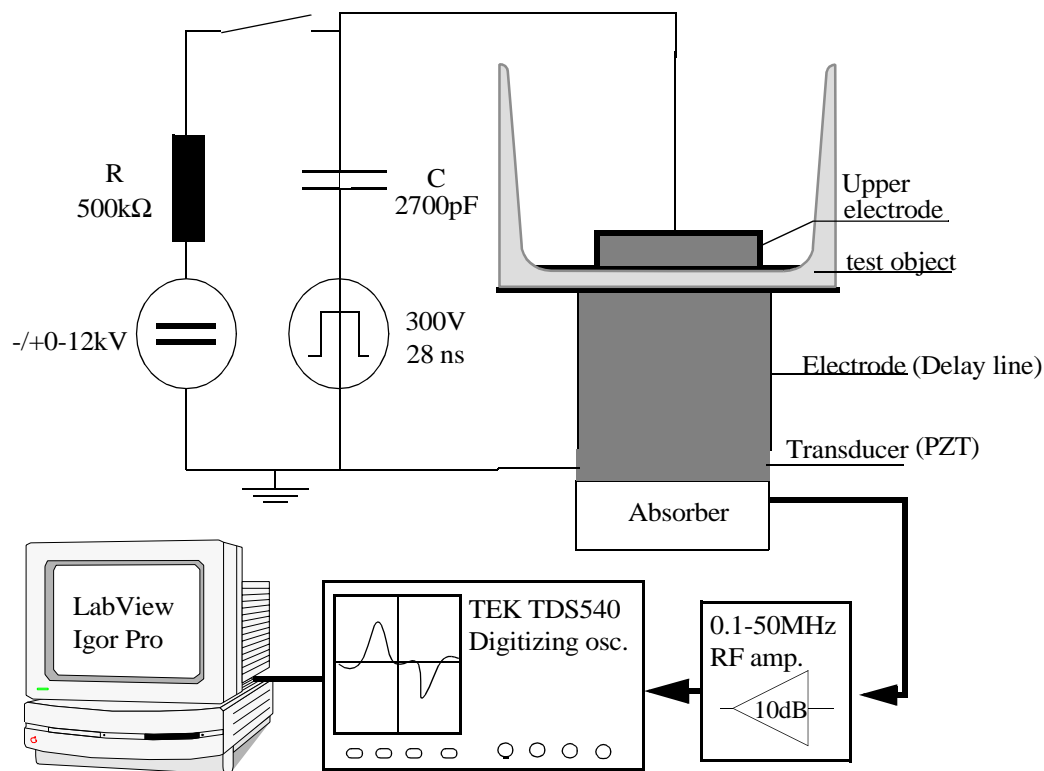


Figure 3.7 Experimental setup for space charge measurements

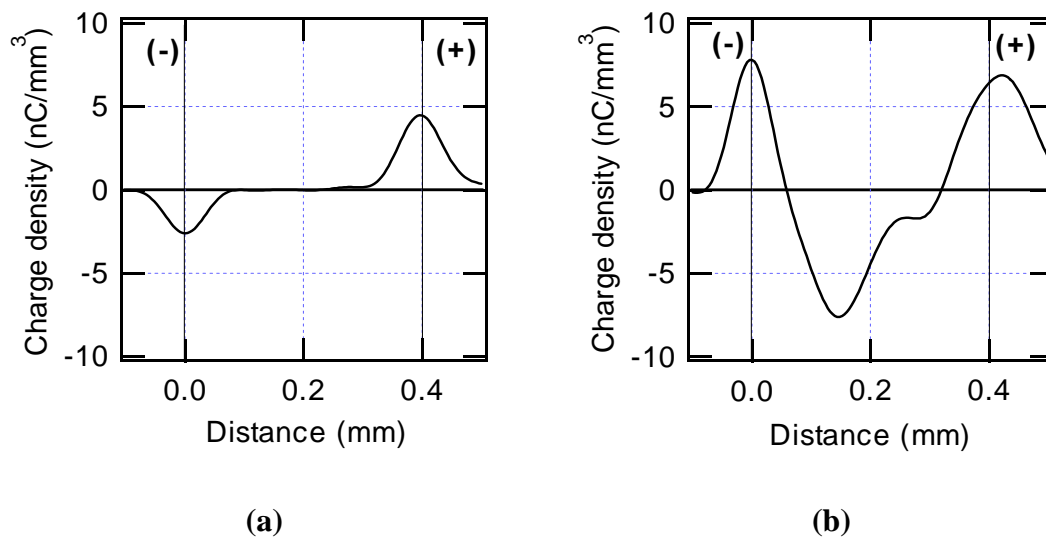


Figure 3.8 Example of space charge profiles recorded with the PEA method. (a) Test object with no internal space charge subjected to an applied voltage of 4 kV during measurement. (b) Test object with negative space charge in the bulk, no voltage applied during measurement.

Measuring procedure

The test objects were aged in an oven at elevated temperatures but were cooled to room temperature with the aid of a water circulating plate before the voltage was turned off and the space charge measurements carried out. A small drop of silicon oil was placed on the bottom electrode of the test object to assure acoustic coupling towards the PEA sensor. To increase the signal to noise ratio the signal was measured 2000 times and averaged.

3.3.2 Infrared spectroscopy

The oxidation level in the aged test objects was measured with a Fourier Transform Infrared (FTIR) microscope [64]. The instrument used was a Perkin-Elmer micro-FTIR equipped with a liquid nitrogen cooled MCT detector. The ketonic carbonyl absorption at 1720 cm^{-1} was used as a measure of the oxidation level [66]. The concentration of carbonyl groups was calculated from the obtained spectra by applying Beer's law [65]:

$$\log \frac{I_0}{I} = \alpha d C = A \quad (3.1)$$

Here I_0 is the background intensity and I is the band intensity at the wavelength of interest as shown in Figure 3.9. A is the absorption, C is the concentration of absorbing groups, d is the sample thickness and α is the absorption coefficient. For the ketonic carbonyl absorption α is $5.88\text{ (weight\% * mm)}^{-1}$ [66].

The sample thickness at the measuring point was obtained from the absorption at 1895 cm^{-1} indicated in the figure above. This absorption is characteristic of the polymer itself (C-H deformation modes in polyethylene) and is not influenced by oxidation or morphology changes [67]. A calibration curve showing the relationship between the absorbance at 1895 cm^{-1} and sample thickness was established based on measurements on specimens with known thickness, see Figure 3.10.

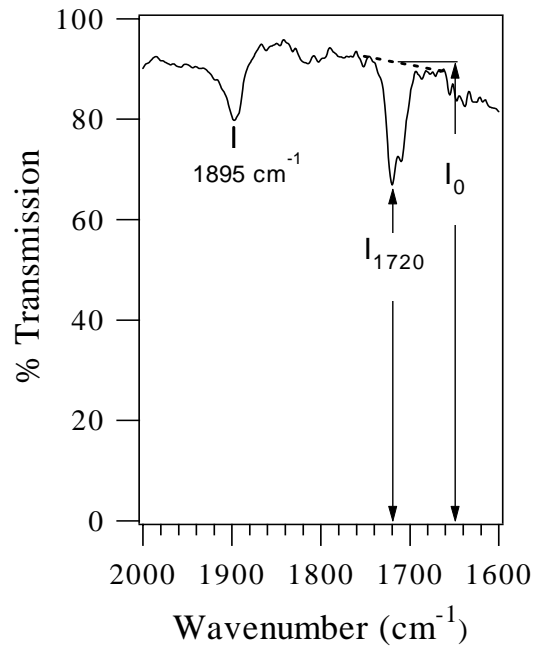


Figure 3.9 The band intensity and the background intensity is shown for the carbonyl absorption at 1720 cm^{-1} .

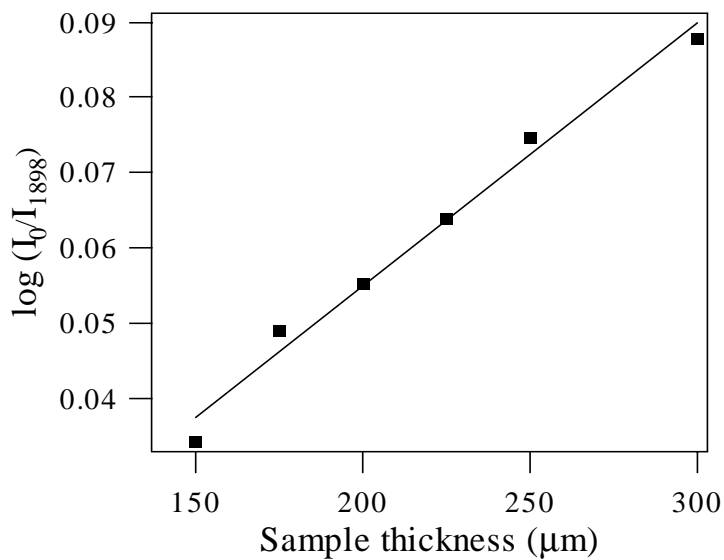


Figure 3.10 Calibration curve for determination of sample thickness.

3.3.3 Differential Scanning Calorimetry

The principle of Differential Scanning Calorimetry (DSC) is to heat the polymer material following a pre-defined time-temperature ramp. When the material undergoes a thermal transition more or less energy is required to follow the ramp depending on whether the transition is endothermic or exothermic respectively. This change in energy demand is recorded and is a direct measure of the heat of transition [68]. DSC was used for two different purposes: To estimate the degree of crystallinity in the test objects and to determine the antioxidant concentration. The instrument used was a Perkin Elmer DSC7.

Degree of crystallinity

The experimental parameters used are shown in table 3.1. The nitrogen gas flow was adjusted by purging the gas-outlet through water and counting the gas bubbles. 1 bubble per second corresponding to approximately 1 cm³/minute was found suitable to achieve reproducible measurements. Figure 3.11 shows a typical melting characteristic of extruded LDPE. The integral of the curve from onset to baseline return gives the melting enthalpy, ΔH_m , of the material. The percentage crystallinity, W_c , is proportional to ΔH_m :

$$W_c = \frac{100\Delta H_m}{\Delta H_c}$$

where ΔH_c is the melting enthalpy of 100% crystalline material. For polyethylene ΔH_c has been determined to 277 J/g [76].

Table 3.1: Experimental parameters, DSC

| Parameter | Crystallinity measurement | Oxidation Temperature |
|-------------------|---------------------------|-----------------------|
| Heating rate | 10°C/min. | 10°C/min. |
| Temperature range | 50 - 150°C | 50 - 300°C |
| Sample weight | 5 - 15 mg | 5 - 15 mg |
| Gas purge | Nitrogen | Oxygen |
| pan | closed aluminium pan | open aluminium pan |

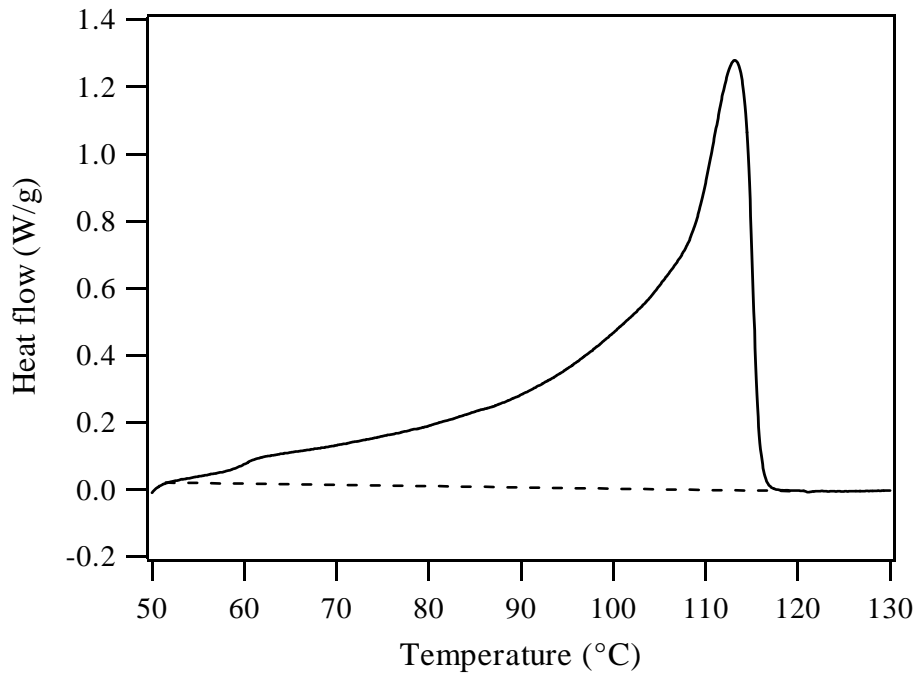


Figure 3.11 Melting characteristic of extruded LDPE with antioxidant. $\Delta H_m = 106 \text{ J/g}$ which is equivalent to 38% crystallinity.

Antioxidant concentration

The antioxidant concentration is related to the onset of the exothermic oxidation process. Two different approaches can be used to measure this onset, the isothermal or dynamic method:

1. Isothermal: The sample is heated to a temperature well above the melting point under nitrogen atmosphere. When isothermal conditions are achieved the atmosphere is changed to oxygen and the time to onset of the oxidative reaction is measured. The onset time is termed *oxidation induction time, oit*.
2. Dynamic: The sample is purged with oxygen while the temperature of the sample is raised at a constant rate. The temperature for the start of the exothermic reaction is recorded. This temperature is termed the *oxidation temperature, T_{ox}* .

The dynamic method was chosen in this work since it was best suited for the available DSC equipment and software. In addition, Crine et al. [18] have

shown that both methods gave a good indication on the antioxidant concentration in aged polyethylene cables. The experimental parameters used are listed in table 3.1. The selection of the parameters was based on the recommendations given by Karlsson et al. [69] who have performed a thorough study of the dynamic method. The oxygen gas flow was adjusted upwards until the oxidation temperature stabilized at a minimum level. According to Karlsson this minimum level is obtained when the gas flow is above $50 \text{ cm}^3/\text{min}$. Figure 3.12 shows a typical dynamic run of LDPE with and without antioxidant.

The exact concentration of Santanox R in the LDPE granulate was not given by the manufacturer, and thus it was not possible to correlate the obtained T_{ox} values to real concentration values. The relative comparison of the T_{ox} values of the material before and after ageing still gives information on how much antioxidant that has been consumed during ageing. One should just be aware that the relationship between T_{ox} and the antioxidant concentration is not linear. In the case of Irganox 1010 which is an antioxidant of the same type as Santanox R, Karlsson et al. [69] found a strong increase in T_{ox} at antioxidant concentrations below 0.2 weight% followed by a weaker increase at higher concentrations.

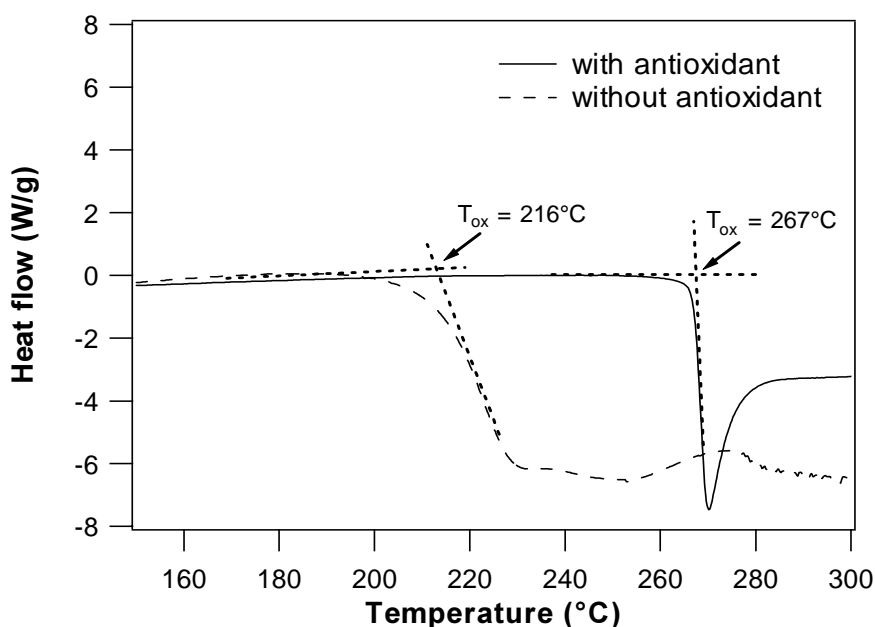


Figure 3.12 Dynamic measurement of oxidation onset.

3.3.4 Mechanical strength

A tensile stress-strain test was performed to obtain Young's modulus of elasticity for unaged and aged materials. A tensile testing apparatus of type Lloyd LR5K was used for these measurements. The apparatus was equipped with an oven and tests were performed in the temperature range from 20 to 70°C.

0.8 mm slabs of LDPE with and without antioxidant additive were used for the mechanical testing. The slabs were prepared by pressure moulding of pre-extruded material following the same procedure as described in Section 3.2.1. Dumbbell shaped specimens were cut from the slabs and mounted in the tensile apparatus. The specimens were stretched at a constant speed of 20 mm/minute and the applied stress was continuously monitored with a PC.

Figure 3.13 shows a typical mechanical run with applied stress vs. time. Young's modulus was calculated from the slope in the initial period:

$$Y = \frac{\Delta S}{l_{relative}} = \frac{\Delta S}{\frac{v \cdot \Delta t}{l_0}} \quad [\text{Pa}] \quad (3.2)$$

Here ΔS is the change in applied stress during the time period Δt as shown in Figure 3.13, $l_{relative}$ is the relative elongation, v is the pulling speed and l_0 is the original length of the specimen.

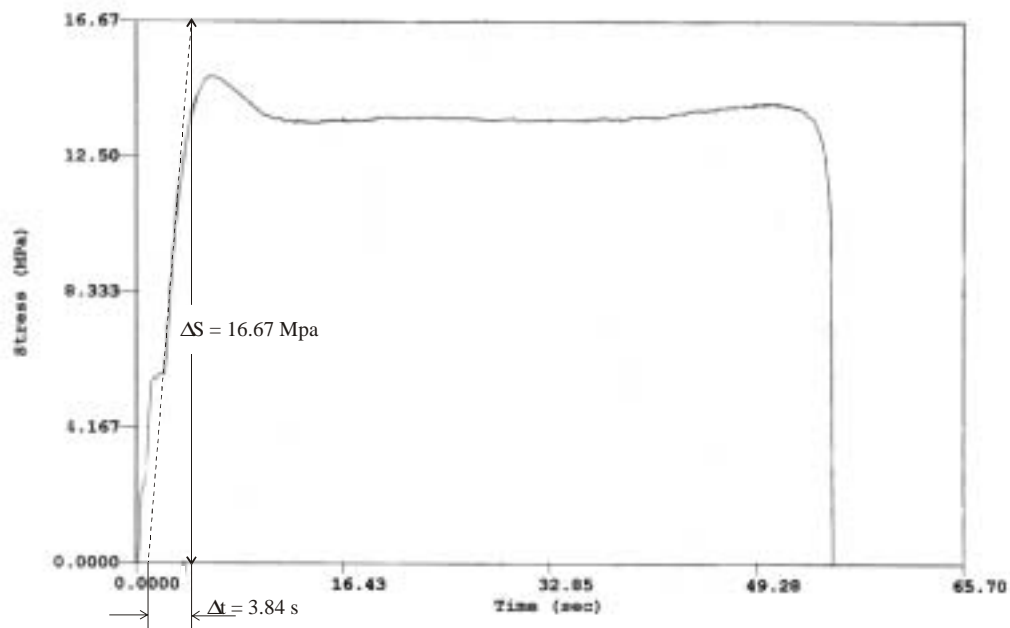


Figure 3.13 Tensile stress-strain test of LDPE specimen at 20°C.

Chapter 4

CHANGE IN MATERIAL PROPERTIES DUE TO THERMAL AGEING

4.1 Introduction

When low density polyethylene is subjected to thermal ageing the material undergoes several changes which can affect the electrical properties. In this chapter results from experiments performed to investigate the effect of thermal ageing on crystallinity, mechanical strength and oxidation will be presented. The results obtained will serve as a fundament when discussing the results from the electrical tests in the following chapters.

4.2 Experimental

The experimental techniques used for the characterization are described in Section 3.3. The measurements were mainly performed on the same cup shaped test objects as were used in the electrical tests, and the manufacturing procedure is given in Section 3.2. One exception are the mechanical tests which were performed on 0.8 mm circular slabs prepared for this purpose, see Section 3.3.4. Crystallinity measurements were also performed on these slabs in order to examine the correlation between changes in mechanical strength and crystallinity after thermal ageing.

The thermal ageing was performed at 70 and 90°C which are the main ageing temperatures used in the experiments presented throughout this thesis. The

choice of 70°C was based on this being the maximum service temperature for LDPE AC cables, while 90°C was selected to accelerate the thermal degradation processes.

4.3 Results and discussion

4.3.1 Crystallinity

Initial morphology

The DSC measurements revealed quite large variations in the melting behaviour from test object to test object, and the degree of crystallinity varied from 35 - 40%. This variation can be subscribed to the manufacturing process where a complete control with the processing parameters was not achieved. The heating and cooling rate varied across the area of the hydraulic press where nine test objects were prepared in each batch, and this was probably the main factor causing morphology variations. As an example the mould in the centre position clearly experienced the slowest cooling rate since it was surrounded by eight warm neighbours and thus there was more time available for crystallization.

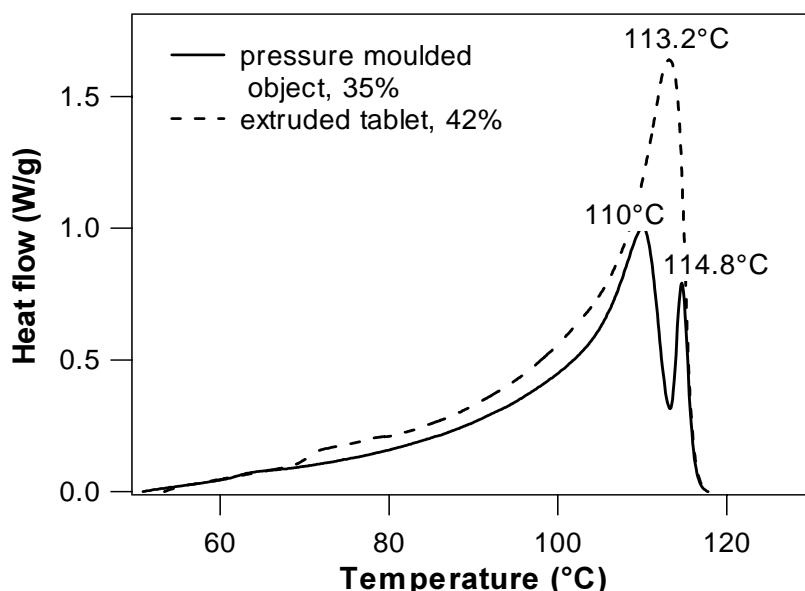


Figure 4.1 Melting endotherm of the extruded material compared to the pressure moulded test object. The crystallinity is given in the legend.

Figure 4.1 shows a typical melting endotherm of a pressure moulded test object compared to the melting endotherm of the material before pressure moulding. After moulding the melting peak separated into two peaks and the crystallinity decreased. The formation of the two peaks is probably a result of a recrystallization taking place both at the moulding temperature and during the subsequent cooling. Basset [40] has recrystallized polyethylene at a range of different temperatures and discuss the phenomena in detail. Two melting peaks were observed in all the pressure moulded test objects, but the proportion between the low and high temperature peak varied from object to object. As discussed above this variation can be subscribed to a variation in the heating and cooling sequence at different positions of the hydraulic press.

Development during ageing

The development of the crystallinity during thermal ageing at 70°C is shown in Figure 4.2. For each material all measuring points were from one specific test object. Both in LDPE with and without antioxidant the crystallinity increased with time. The test object without antioxidant was less crystalline before ageing but after 4 weeks at 70°C both materials arrived at a crystallinity level of 44%.

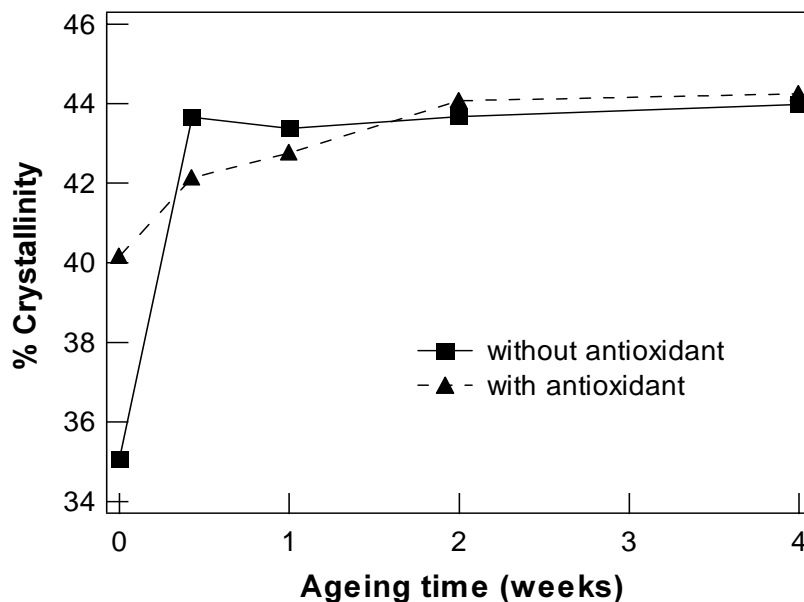


Figure 4.2 Development of crystallinity during thermal ageing at 70°C.

The crystallinity increase is a result of a recrystallization process taking place in the material. Components with low molecular weight which failed to crystallize in the manufacturing process are allowed to organize when the temperature is kept constantly at 70°C for a longer period of time. The development of the melting endotherm displayed in Figure 4.3 very clearly shows the recrystallization taking place. After ageing a shoulder appeared around 80°C which corresponds to the melting of the recrystallized material. In addition the number of larger sized crystallites with higher melting point also grew during the ageing. In general a crystallinity of $43 \pm 1\%$ was obtained for all objects after 4 weeks of ageing and thus the large variation in crystallinity due to the manufacturing was eliminated in the annealing process.

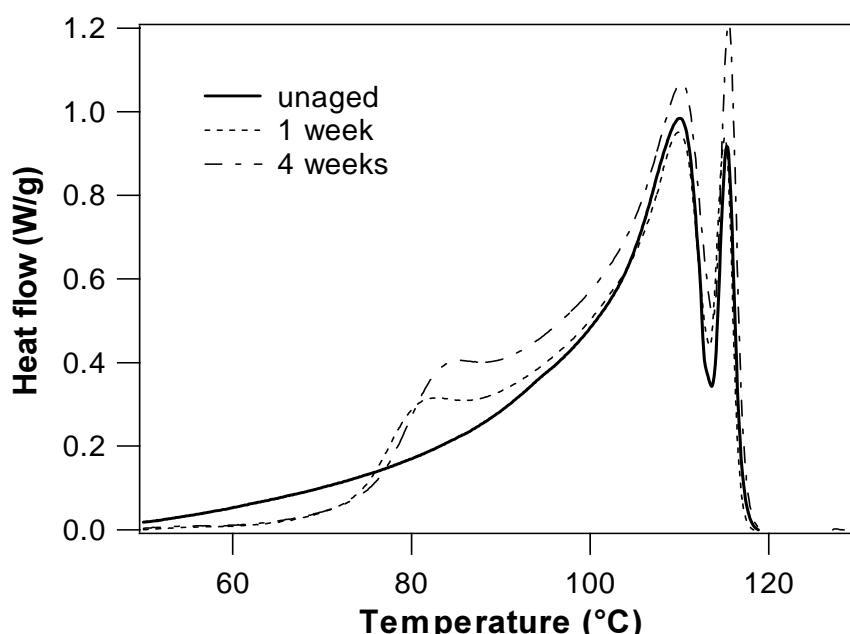


Figure 4.3 Development of the melting endotherm of LDPE with antioxidant during thermal ageing at 70°C.

Even if the total crystallinity was equal the size distribution of the crystallites varied after the thermal ageing. This can be seen in Figure 4.4 where the melting endotherm of two test objects without antioxidant aged 4 weeks at 70°C is displayed. Both test objects had a crystallinity of 44% but the proportion between the two melting peaks differed, indicating a higher amount of large crystallites in one of the objects.

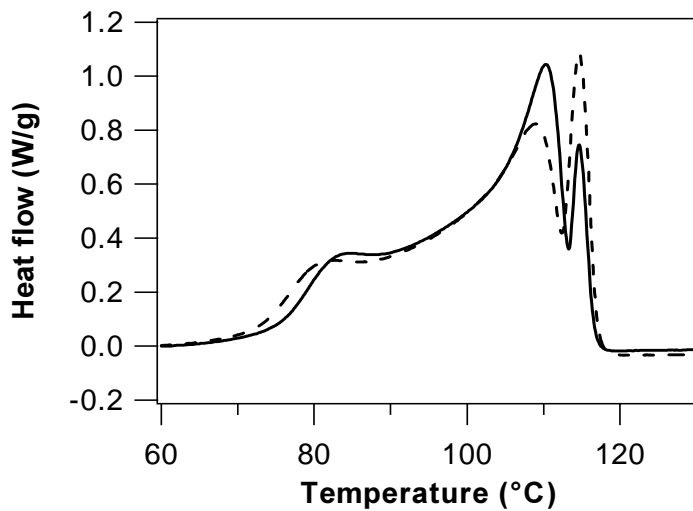


Figure 4.4 Melting characteristics of two test objects without antioxidant subjected to 4 weeks ageing at 70°C.

4.3.2 Mechanical strength

Young's modulus of elasticity was measured with a tensile stress-strain test as described in Section 3.3.4. The modulus is given by the initial slope of the stress strain curve and is a measure of the resistance to deformation when an external force is applied [35]. Young's modulus was selected as mechanical parameter since it is included in the electromechanical breakdown theory presented in Section 2.4 and may have an influence on the electrical strength of LDPE at high temperatures.

Figure 4.5 shows the development of Young's modulus with increasing test temperature. Both LDPE with and without antioxidant was tested and showed exactly the same behaviour: The elastic modulus decreased by nearly a factor of ten when the temperature was increased from 20°C to 70°C. The obtained results are in good agreement with the results by Moll et al. [36]. The decrease in Young's modulus is caused by a softening of the polymer as the temperature increases towards the melting point.

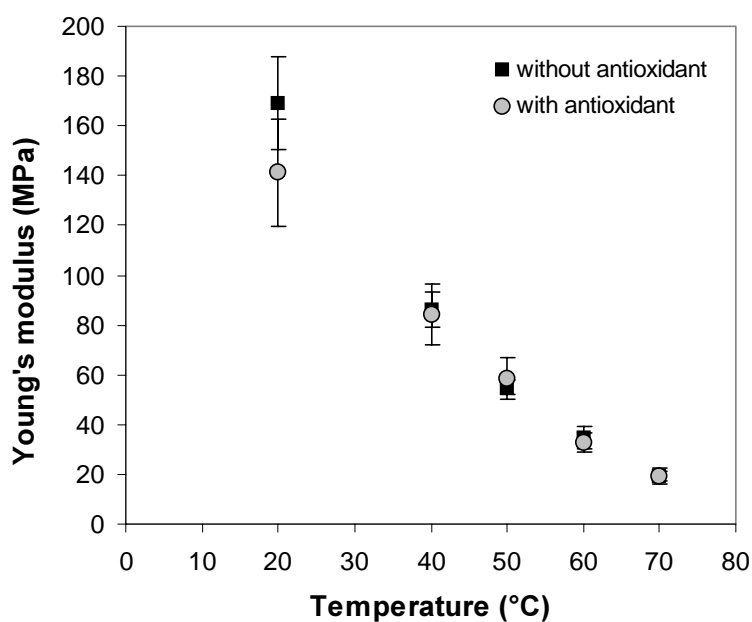


Figure 4.5 Young's modulus measured as a function of temperature for LDPE without antioxidant. Each point represent a mean of 8 values and the standard deviation is indicated.

The effect of thermal ageing on Young's modulus was investigated by keeping the 0.8 mm thick circular slabs at a temperature of 70°C or 90°C for a period of 4 weeks. 4 slabs of LDPE with and without antioxidant were kept at each temperature and two dumbbell shaped specimens were taken from each slab. The test was performed at 70°C since the majority of the electrical tests were performed at this temperature. Figure 4.6 shows the change in Young's modulus due to the ageing. After 4 weeks at 70°C the modulus increased by 53 and 74% in LDPE without and with antioxidant respectively. 4 weeks at 90°C did not result in any significant change in the modulus compared to the unaged value. The increased resistance towards deformation after ageing at 70°C was probably caused by the recrystallization process discussed in the previous section. The crystallinity of the slabs after ageing is shown in Figure 4.7 and we see that the crystallinity shows a very similar behaviour as the elastic modulus: The crystallinity increased after ageing at 70°C but was unaltered after ageing at 90°C.

The lack of crystallinity increase after ageing at 90°C can be explained as follows: During ageing at 90°C the low molecular weight fraction of the polymer was in a melted state and did not crystallize. When the slabs were

removed from the oven a relatively fast cooling took place, the low molecular components failed to crystallize and thus the degree of crystallinity remained unchanged.

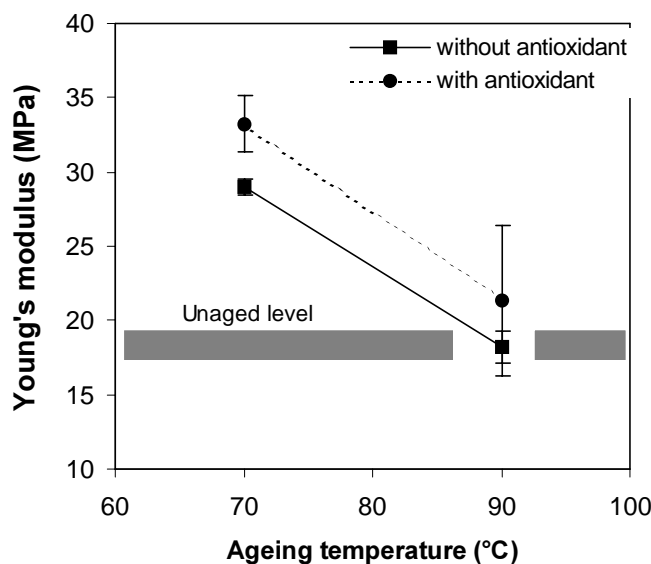


Figure 4.6 Young's modulus measured after 4 weeks ageing at 70 and 90°C. Each point is a mean of 8 values, the standard deviation is indicated.

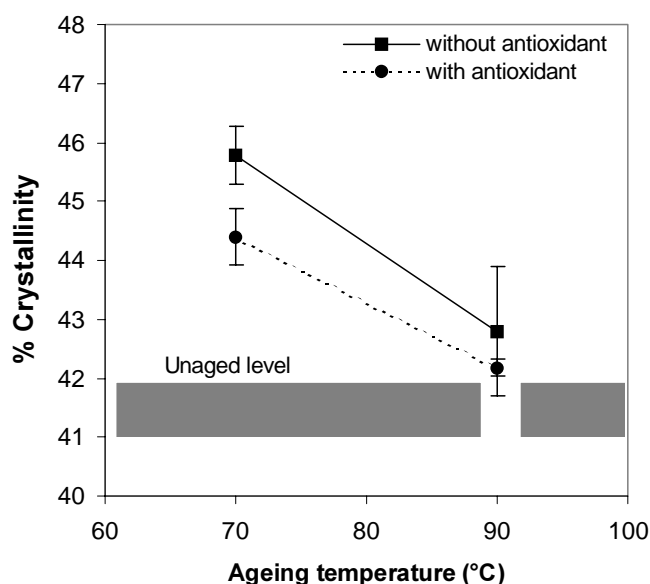


Figure 4.7 Crystallinity measured after 4 weeks ageing at 70 and 90°C. Each point is a mean of 8 values, the standard deviation is indicated.

4.3.3 Oxidation

The oxidation level of the test objects was estimated from the carbonyl group absorption at 1720 cm^{-1} as described in Section 3.3.2. The results presented in this section were obtained from the cup shaped test objects with needle-plane electrode. The measurements were performed after the objects had been subjected to short or long term electrical and thermal ageing. FTIR measurements were also performed on the other type of test objects used throughout this thesis and the same trends were observed in these objects. $250\text{ }\mu\text{m}$ thick cross-sections were microtomed from the test objects and Figure 4.8 shows the typical number of measuring points taken at one cross-section. At each point an area of $25\text{ X }25\text{ }\mu\text{m}$ was measured.

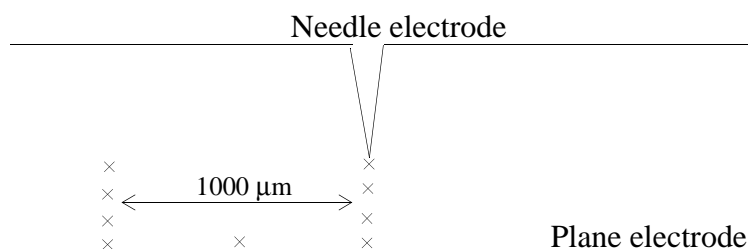


Figure 4.8 FTIR measuring points in a $250\text{ }\mu\text{m}$ cross-section

Figure 4.9 shows the carbonyl concentration before and after 4 weeks ageing at 70 and 90°C . The presented values are a mean of the measurements taken close to the plane electrode and the standard deviation is indicated. After 4 weeks of ageing at 70°C no change in the carbonyl content was observed in any of the test objects, but when the ageing temperature was raised to 90°C the carbonyl content in many of the LDPE test objects without antioxidant increased by a factor of 10. In the test objects with antioxidant the carbonyl content remained at the same value as before ageing. Figure 4.10 shows the distribution of the carbonyl groups from the plane electrode towards the needle tip in a heavily oxidized test object. We see that the carbonyl concentration was highest close to the plane electrode and decreased when moving into the insulation.

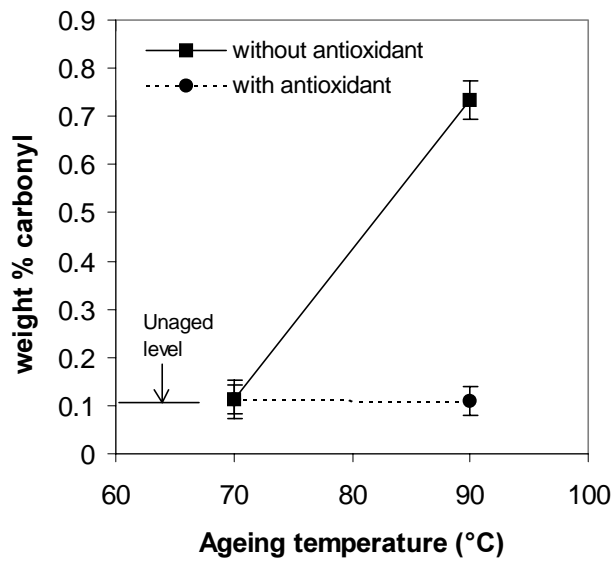


Figure 4.9 Carbonyl concentration measured after 4 weeks ageing at 70 and 90°C.

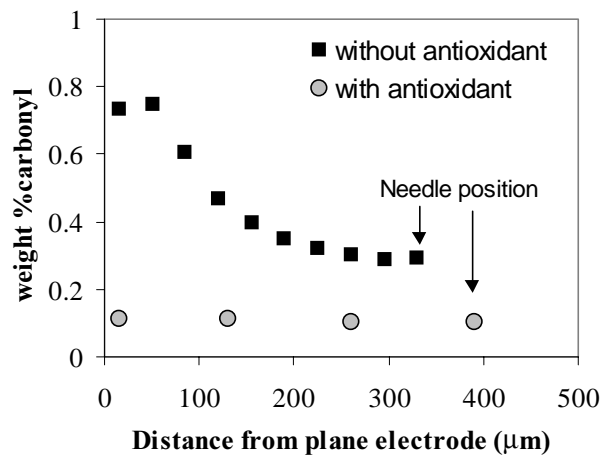


Figure 4.10 Carbonyl content in cross-sections of test object with and without antioxidant measured after 4 weeks ageing at 90°C versus the distance from plane electrode towards the needle tip.

Two of the five test objects aged 4 weeks at 90°C did not show any increase in the carbonyl content. Probably this large scatter in the degree of oxidation was related to variation in the thickness of the aluminium electrodes. If the aluminium layer is thicker and more compact, longer time is needed for oxygen to diffuse into the insulation. Cross-sections from the five test objects

were inspected in an optical microscope and the thickness of the aluminium electrodes were measured. Carbonyl concentration vs. electrode thickness at the plane electrode is shown in Figure 4.11 which shows a clear trend of higher carbonyl content when the amount of deposited aluminium decreases.

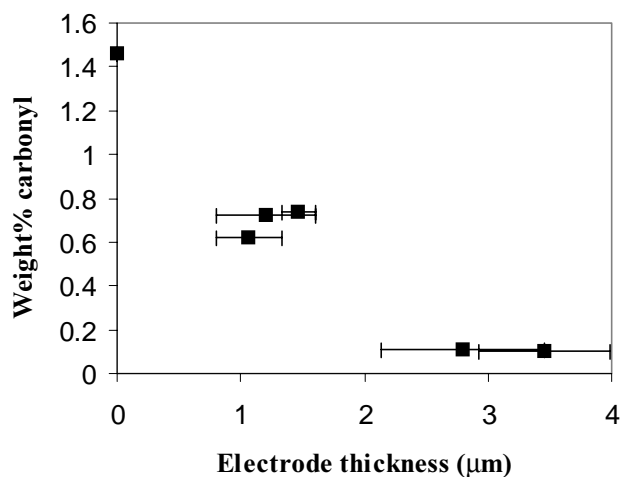


Figure 4.11 Carbonyl content measured close to the plane electrode vs. thickness of the aluminium electrode. Test objects aged 4 weeks at 90°C. The point at zero is taken from a test object aged without electrodes.

4.3.4 Antioxidant additive

The oxidation temperature was used as a measure of the antioxidant concentration in the test objects with antioxidant before and after thermal ageing. The temperature was obtained with the dynamic DSC method described in Section 3.3.3. The measurements were performed after the electrical and thermal ageing experiments. The different test objects had an insulation thickness ranging from 0.2 mm to 2 mm and thus the influence of the sample thickness on the oxidation temperature could be investigated. A cross-section from the centre part of the insulation was always used in the DSC measurements, i.e. the obtained oxidation temperature was a mean value for the whole insulation thickness.

Figure 4.12 shows the change in oxidation temperature due to 4 weeks of thermal ageing at 70 or 90°C. The oxidation temperature remained at the initial level of 267°C in the test objects with 2 mm insulation thickness, while in the 0.5 mm thick object the temperature was reduced to 239°C after 4

weeks at 90°C. As a reference the oxidation temperature in LDPE without antioxidant was 216°C (see Figure 3.12). Based on the results by Karlsson et al. [69] an oxidation temperature of 239°C indicate a reduction of the mean antioxidant concentration from 0.5 - 1% before ageing to less than 0.1% after ageing.

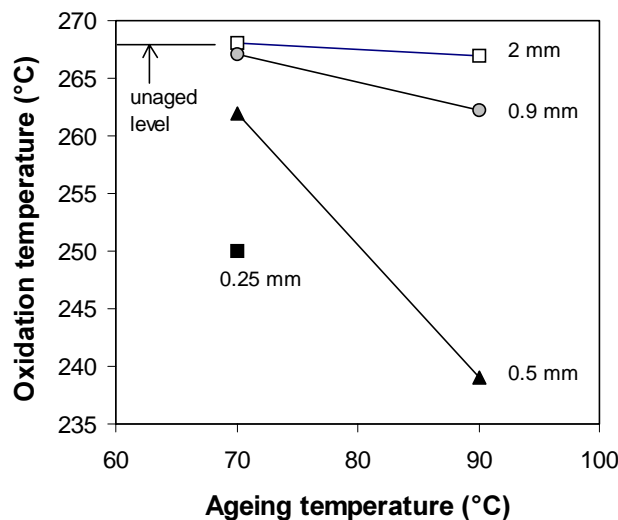


Figure 4.12 Oxidation temperature in LDPE with antioxidant after 4 weeks ageing at 70 and 90°C. Test objects with different insulation thickness.

The strong dependence on sample thickness is related to the inhomogeneous distribution of the antioxidant through the sample. As discussed in Section 2.3.2 the antioxidant additive may disappear in two ways: It is consumed by free radicals taking part in the oxidation process and it migrates out of the material. Both these processes lead to a depletion of antioxidant near the surface. In a thick insulation the depleted regions make up a small percentage of the total volume while in a thin insulation the whole insulation may be depleted. The obtained oxidation temperatures can be converted to approximate concentration values by using the results from Karlsson et al. [69]. In Figure 4.13 the concentration values are plotted against the inverse of the insulation thickness and we see that a linear relationship is obtained. This is reasonable since the average antioxidant concentration in a cross-section will depend on the ratio of the depleted region to the total insulation thickness. If the straight lines are extrapolated to zero antioxidant concentration a thickness of 0.22 mm and 0.45 mm is obtained for $T = 70^\circ\text{C}$ and 90°C respectively.

Thus a 0.22 mm thick sample will be completely depleted of antioxidant after 4 weeks at 70°C. In the thicker samples the size of the depleted regions can then be estimated to be 0.11 mm and 0.23 mm at each electrode after 4 weeks at 70°C and 90°C respectively.

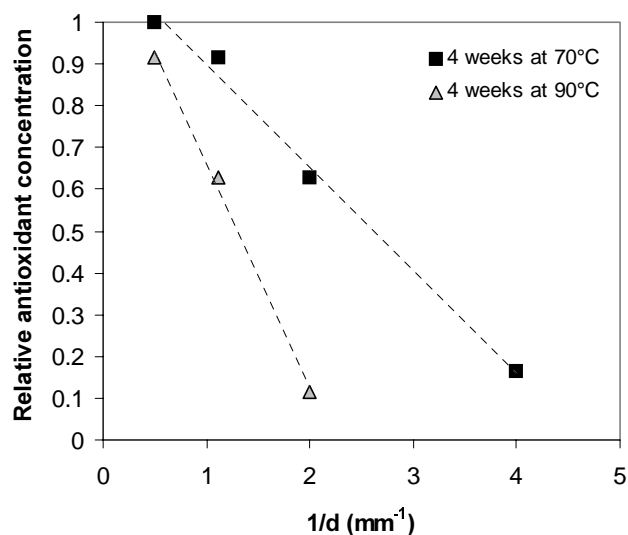


Figure 4.13 Relative antioxidant concentrations, $C/C_{initial}$, estimated from the measured oxidation temperatures versus the inverse of the sample thickness. $C_{initial}$ is assumed to be in the range from 0.4 - 0.6 weight%.

4.4 Summary of results

The effect of 4 weeks of thermal ageing on the material properties investigated in this chapter is summarized in Table 4.1.

Table 4.1: Change in material properties after 4 weeks of thermal ageing.

| Material property | Type of material | 4 weeks at 70°C | 4 weeks at 90°C |
|---------------------------|------------------|--|--|
| Crystallinity | both materials | 10 - 23% increase | no significant increase |
| Young's modulus | both materials | 50 - 70% increase | no significant increase |
| Antioxidant concentration | with antiox. | 0.11 mm thick region depleted of antioxidant | 0.23 mm thick region depleted of antioxidant |
| Oxidation level | without antiox. | unaltered | heavy oxidation |
| | with antiox. | unaltered | unaltered |

4.5 Conclusions

The following conclusions can be made from the material characterization presented in this chapter:

The degree of crystallinity and the size distribution of the crystallites varied from test object to test object. This was subscribed to the manufacturing process. After ageing there was less variation in degree of crystallinity but there was still a scatter in the crystallite size distribution.

Young's modulus decreased by a factor of 10 when the test temperature was increased from 20 to 70°C. Recrystallization during thermal ageing resulted in an increase of the elastic modulus.

The oxidation level was unaltered after 4 weeks at 70°C but heavy oxidation was observed after 4 weeks at 90°C. The thickness of the evaporated aluminium electrodes were found to have a major influence on the carbonyl content.

The antioxidant concentration decreased during thermal ageing due to loss by diffusion and loss by reaction with free radicals. A depletion region arose close to the surfaces and the size of this region increased with increasing ageing temperature.

Chapter 5

SPACE CHARGE ACCUMULATION DURING THERMAL AND DC ELECTRICAL AGEING

5.1 Introduction

In this chapter results from experimental investigations of space charge formation in LDPE insulation during thermal and DC electrical ageing will be presented. The presence of space charge gives rise to local field enhancement which may result in a lowered breakdown level and reduced time to failure. The role of the antioxidant additive in the generation of space charge will be an important issue. The literature reviewed in Chapter 2 indicated that the antioxidant additive may be a source of space charge, but the referred experiments were all performed at room temperature with an ageing period limited to some hours [27 - 30]. The following hypothesis was formulated concerning the antioxidant additive:

The antioxidant additive prevents thermal oxidation but is a source of space charge accumulation in the insulation which may have a negative effect on the long term performance.

To test this hypothesis polyethylene samples with and without antioxidant additive were subjected to thermal and/or electrical ageing for up to six months. Space charge profiles were recorded during ageing and comparison of the profiles for the two materials gave information about the role of the antioxidant additive.

Another important issue is the effect of oxidation on the space charge characteristics. The literature reviewed in Chapter 2 showed that oxidation resulted in enhanced charge injection from the electrodes [20 - 23]. Long

term ageing at 70°C may therefore reveal changes in the space charge profiles due to the oxidation process.

5.2 Experimental

Cup shaped test objects with and without antioxidant additive were prepared following the procedure described in Section 3.2.1. The majority of the test objects were equipped with aluminium electrodes while in a few cases gold was applied. The test objects were subjected to thermal and electrical ageing and the development of the space charge distribution was monitored with the PEA method described in Section 3.3.1. Three different ageing schemes described below were followed:

i) Electrical ageing in the temperature range from 25 - 70°C

The test objects were kept in air atmosphere at temperatures varying from 25 to 70°C for a period of four weeks. During the whole ageing period the objects were subjected to an electrical field of approximately 70 kV/mm. Space charge profiles were recorded after 1 hour, 24 hours, 1 week and 4 weeks. As explained in Section 3.3.1 the space charge measurements were performed with the voltage off after having cooled the energized test objects to room temperature.

ii) Thermal ageing at $T = 70^\circ\text{C}$

The test objects were kept in air atmosphere at a temperature of 70°C and were not subjected to electrical stress during the majority of the ageing period. In order to monitor changes in the space charge characteristics during thermal ageing the following procedure was adapted: The objects were charged at 70 kV/mm for 1 hour prior to space charge measurements performed before and after 1 week and 4 weeks of ageing. After this charge measurement the objects were kept short-circuited at 70°C for 24 hours to remove the accumulated charge. In some cases the thermal ageing period was followed by a subsequent electrical ageing with $E = 70 \text{ kV/mm}$ and $T = 70^\circ\text{C}$. Space charge profiles were recorded after 24 hours, 1 week and 4 weeks.

iii) Long term electrical ageing at 70°C

The test objects were kept in air atmosphere at 70°C for a period of five months. They were subjected to an electrical field of about 100 kV/mm during the whole ageing period and space charge profiles were recorded after 1 hour, 24 hours and 1, 4, 6, 8, 12 and 21 weeks of ageing.

5.3 Results

In the following section space charge profiles from the different ageing cases will be presented. Two or three test objects were subjected to each of the ageing conditions. There was a variation in the space charge pattern from test object to test object, especially for ageing temperatures below 70°C. This can be seen from Figure 5.3 where the scatter in the maximum charge value is shown for ageing temperatures from 25 - 70°C. The profiles must therefore be taken as examples of observed space charge patterns, and the focus in the presentation will be on the main characteristics for each material not on details in each specific space charge plot.

5.3.1 Electrical ageing at 70 kV/mm

Figure 5.1 shows the development of the space charge profiles in test objects without and with antioxidant during electrical ageing at 25°C. After 1 hour there were only small amounts of charge present in both materials, but after 24 hours a large negative charge was observed in the material with antioxidant. The negative charge was distributed throughout the sample with a maximum close to the anode. The enhancement of the applied field at the anode due to this negative charge was about 60%. After 4 weeks the negative charge had been replaced by positive charge at the anode and a homocharge distribution appeared. In LDPE without antioxidant negative charge was present close to the cathode while positive charge appeared in the bulk of the material. The amount of charge after 4 weeks ageing at 25°C was comparable in the two materials as can be seen from Figure 5.3.

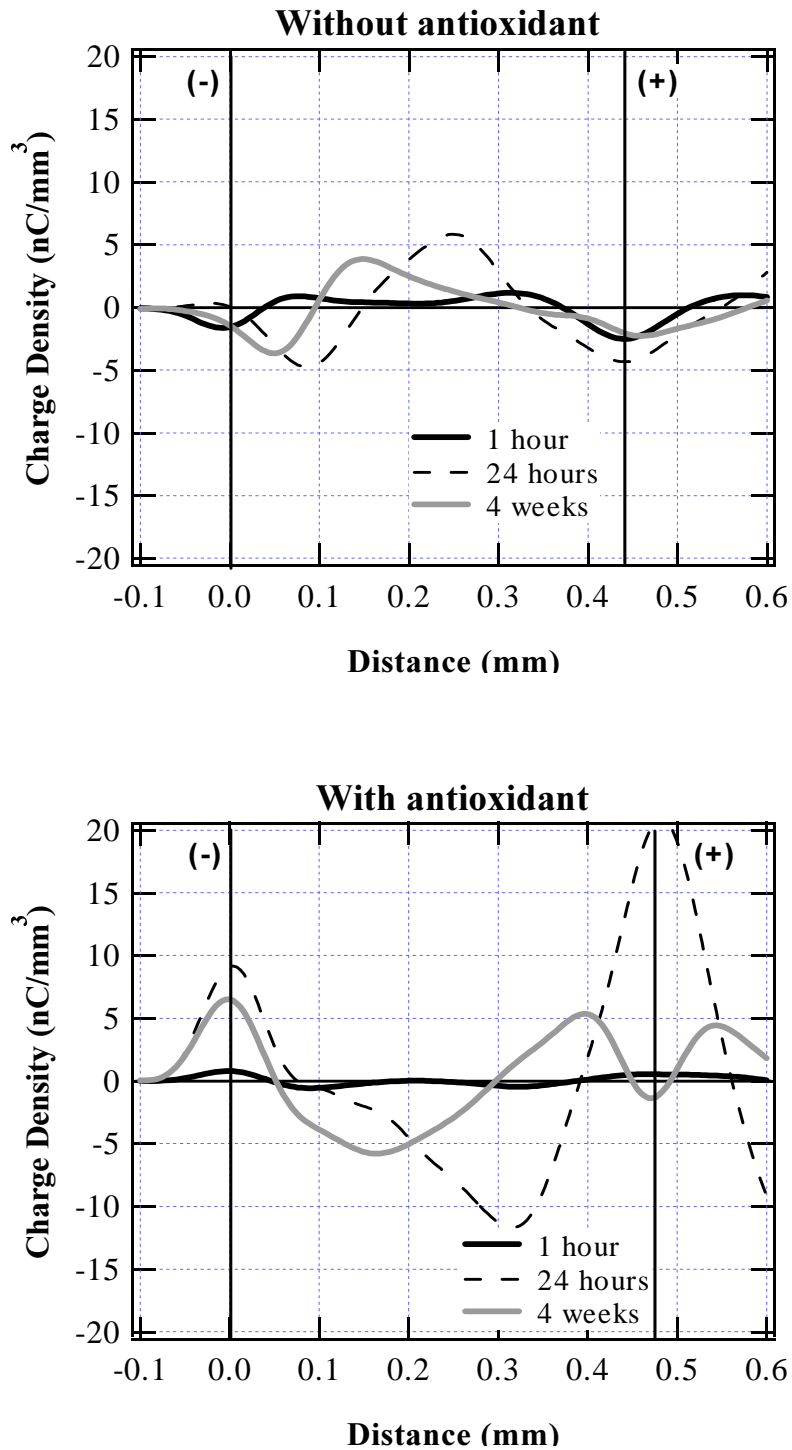
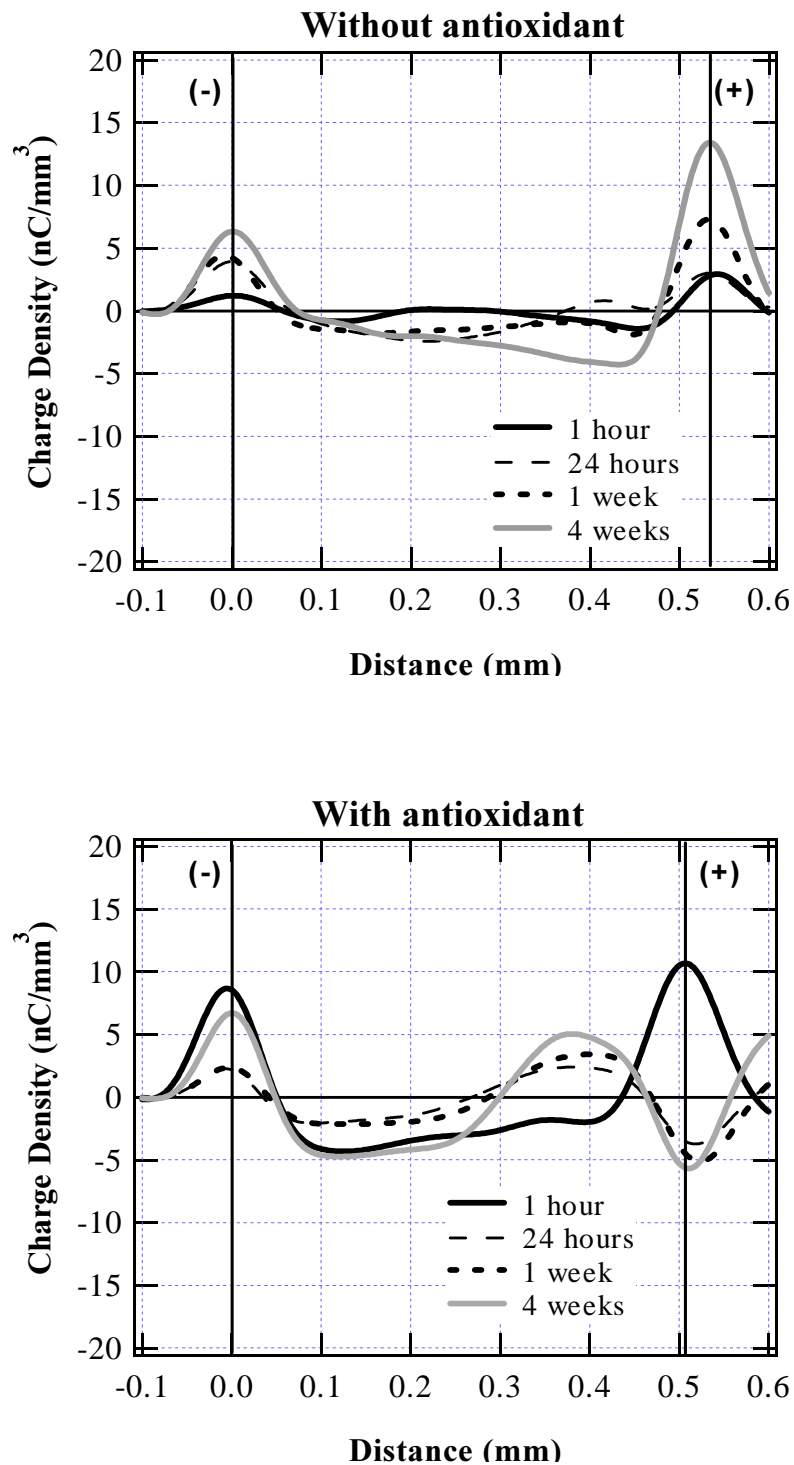


Figure 5.1 Space charge distribution in LDPE measured during electrical ageing. $T = 25^{\circ}\text{C}$, $E = 70 \text{ kV/mm}$. Aluminium electrodes.



Space charge accumulated at a higher initial rate in LDPE with antioxidant when the ageing temperature was increased from 25 to 40°C. Already after 1 hour at 40°C a large amount of negative charge was observed throughout the bulk, corresponding to an anode field enhancement of about 40%. This is illustrated in Figure 5.3 where the maximum charge concentration obtained after 1 hour is plotted against temperature. After 4 weeks ageing a homocharge distribution comparable to that observed at 25°C was again present. When the ageing temperature was increased to 55°C and 70°C the same trend was repeated, but the homocharge distribution was present within the first 24 hours of ageing. This can be seen from Figure 5.2 which shows the space charge development in a test object with antioxidant at 70°C.

In LDPE without antioxidant the effect of increasing the temperature on the initial space charge accumulation was less pronounced as can be seen from Figure 5.3. But after 4 weeks ageing the amount of charge increased and became comparable to LDPE with antioxidant. At 40 and 55°C positive charge was dominating throughout the bulk while at 70°C only negative charge developed. This can be seen from Figure 5.2 which shows the space charge development in a test object without antioxidant at 70°C.

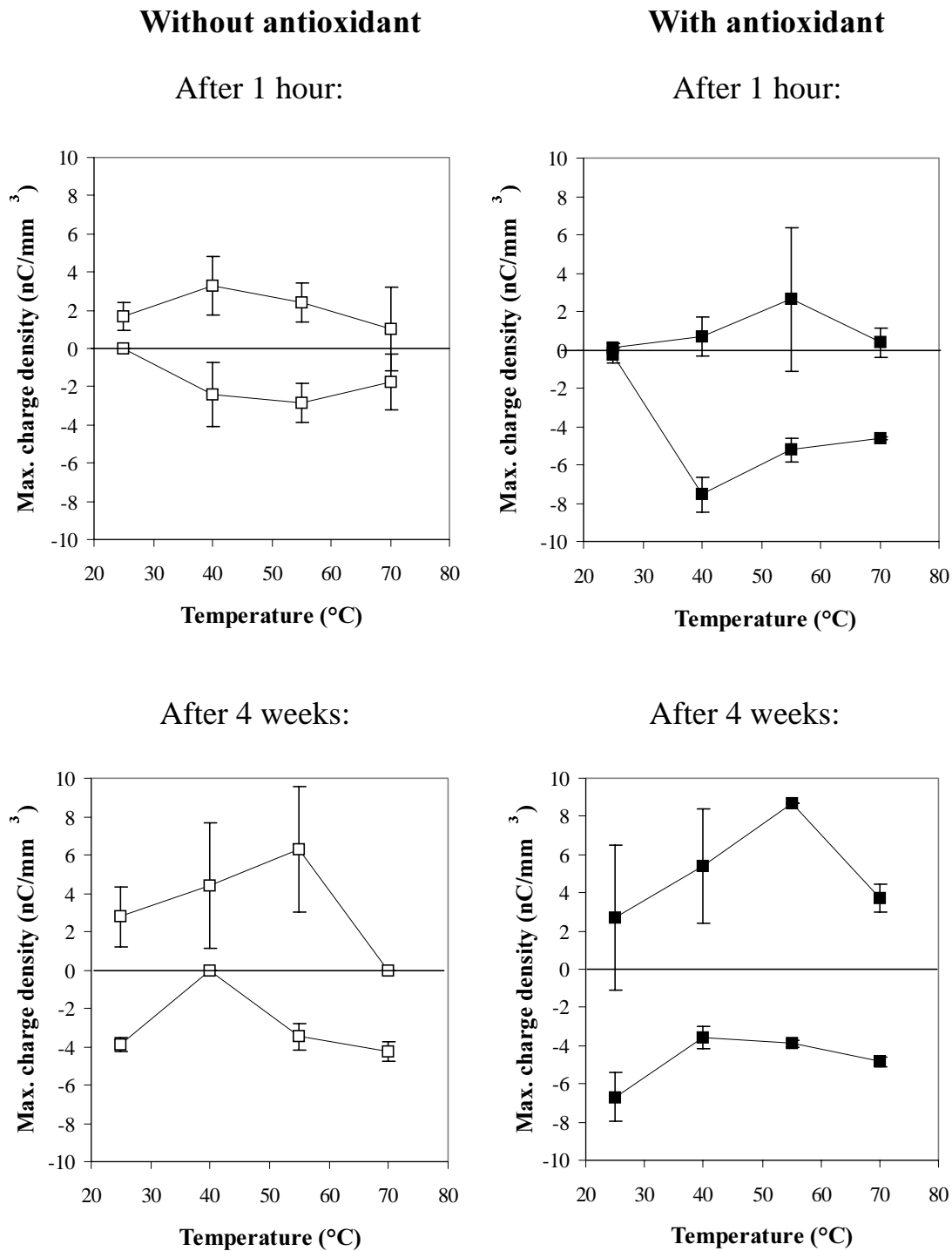


Figure 5.3 Maximum positive and negative charge values obtained after 1 hour and 4 weeks at $E = 70 \text{ kV/mm}$. The values are a mean of measurements on 2 - 3 different test objects and the scatter is shown.

5.3.2 Thermal ageing at 70°C

Figure 5.4 and 5.5 show the space charge profiles for thermally aged test objects without and with antioxidant respectively. The difference between the two materials was very pronounced; in LDPE without antioxidant only small amounts of charge accumulated, while in LDPE with antioxidant the charge close to the cathode changed from negative to positive after 4 weeks with thermal ageing. The positive charge gave rise to a 67% enhancement of the cathode electrical field. The test object with antioxidant was subjected to a subsequent electrical ageing and the development of the space charge during this period is shown in Figure 5.5. After 24 hours the positive charge at the cathode side was reduced by about 1/3, but as the ageing continued the positive charge started to increase again and the field enhancement was 59% after 4 weeks with applied field.

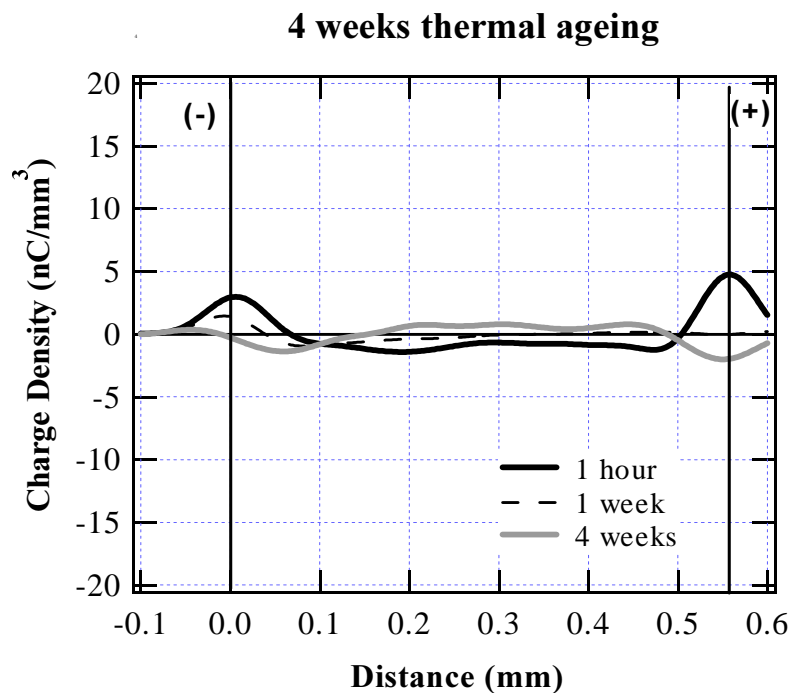


Figure 5.4 Measured space charge distribution in LDPE without antioxidant during thermal ageing at 70°C. Sample stressed 1 hour at 70 kV/mm before measuring. Aluminium electrodes.

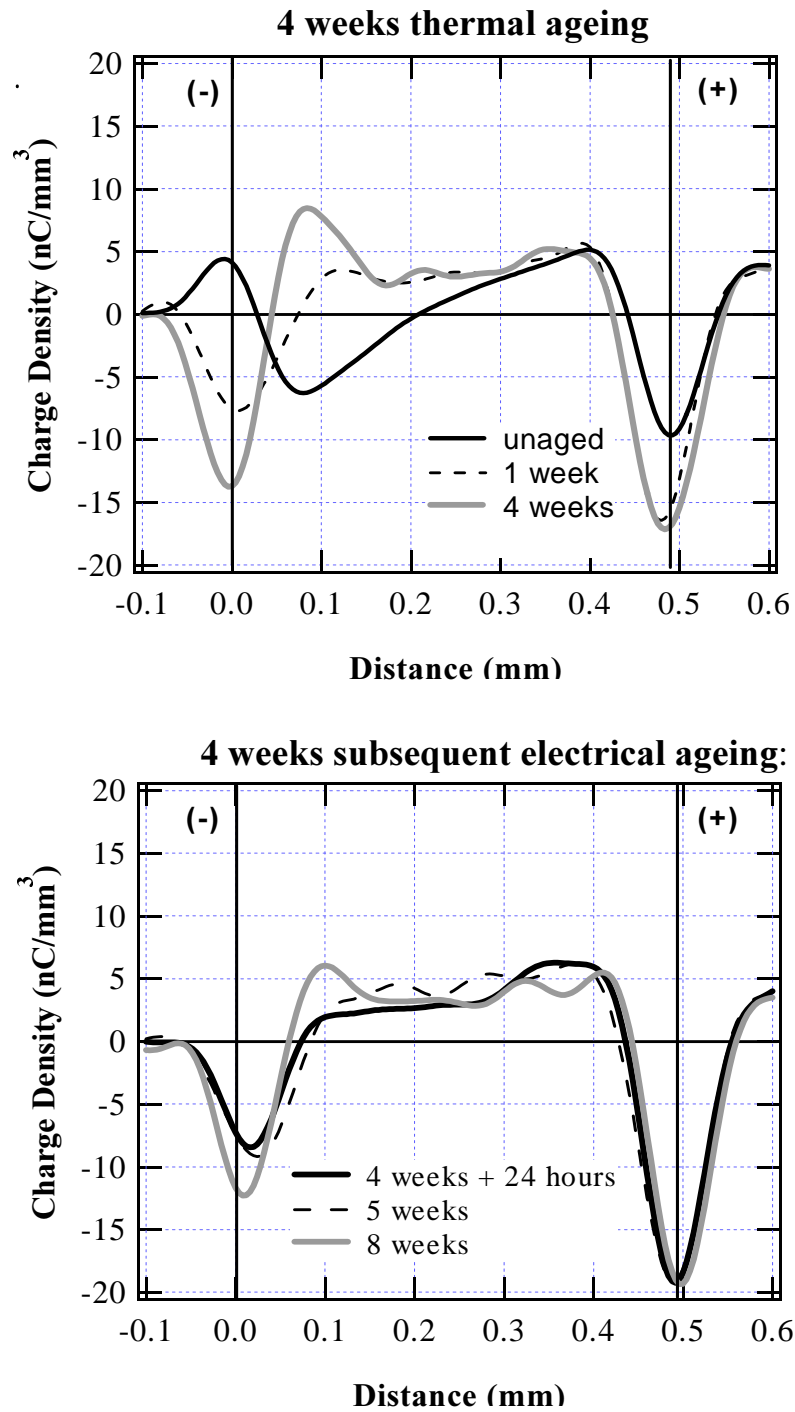


Figure 5.5 Measured space charge distribution in LDPE test object with antioxidant during thermal and subsequent electrical ageing. $T = 70^{\circ}\text{C}$. Thermal ageing: Sample stressed 1 hour at 70 kV/mm before measuring. Subsequent electrical ageing: $E = 70\text{ kV/mm}$ applied continuously. Aluminium electrodes.

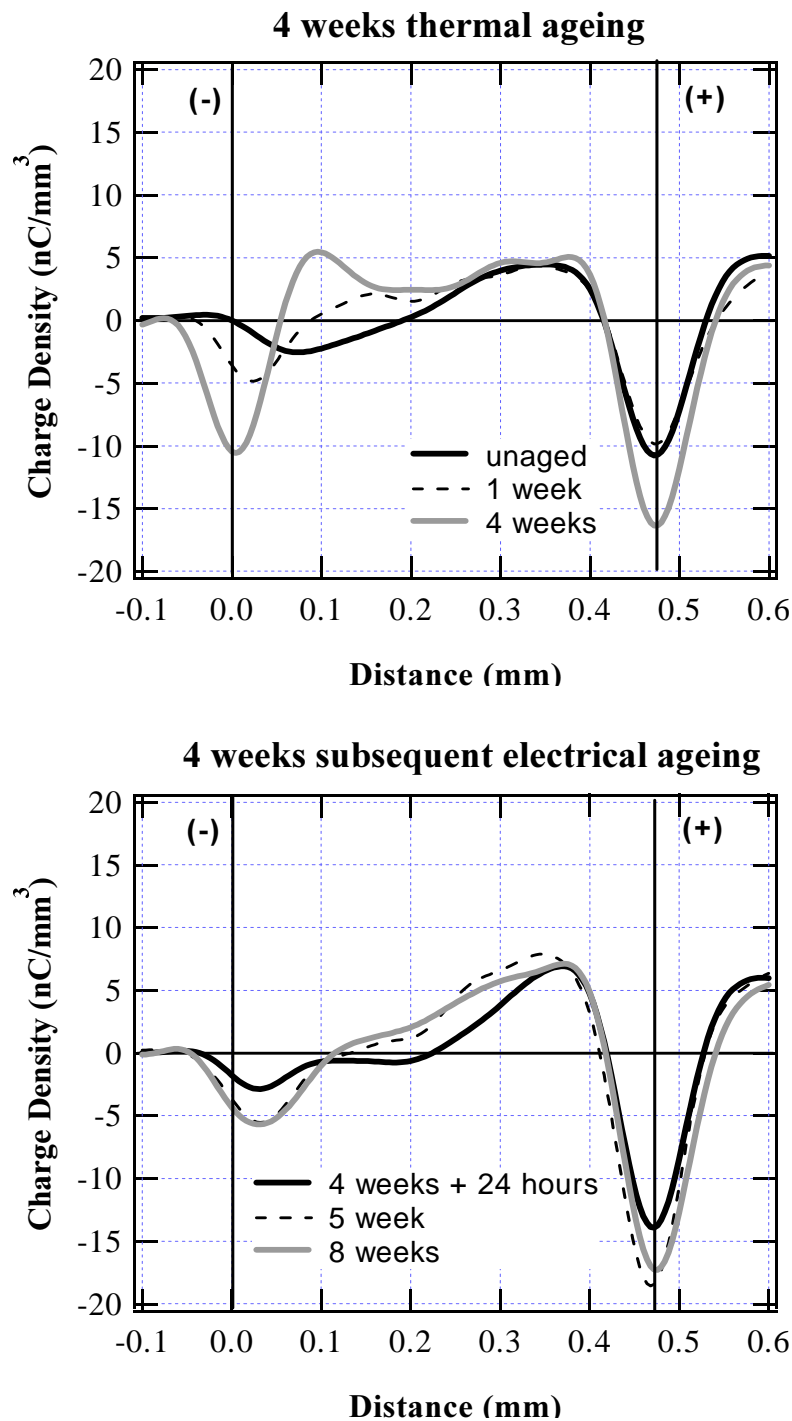


Figure 5.6 Measured space charge distribution in LDPE test object with antioxidant during thermal and subsequent electrical ageing. $T = 70^{\circ}\text{C}$. Thermal ageing: Sample stressed 1 hour at 70 kV/mm before measuring. Subsequent electrical ageing: $E = 70\text{ kV/mm}$ applied continuously. Gold electrodes.

To investigate whether the positive charge formation in LDPE with antioxidant was related to the electrode material, the same ageing experiment was performed on test objects with gold electrodes. The space charge profiles during the thermal and the subsequent electrical ageing are shown in Figure 5.6. The development of the space charge distribution during thermal ageing followed the same pattern as the test objects with aluminium electrodes, and a 50% enhancement of the cathode electrical field was reached after 4 weeks. In the subsequent electrical ageing the positive charge in the cathode region disappeared after 24 hours and did not return as the ageing proceeded. Thus the behaviour differed from the case with aluminium electrodes where the positive charge in the cathode region was maintained during the subsequent electrical ageing.

5.3.3 Long term electrical and thermal ageing

Figure 5.7 shows the space charge development from 1 hour to 21 weeks in test objects without and with antioxidant. In LDPE without antioxidant negative charge was present in the majority of the insulation after 1 hour with some positive charge close to the anode. During ageing the positive charge was growing and after 4 weeks the negative charge was completely replaced by positive charge. From 4 to 6 weeks the distribution changed once more and negative charge was again dominating in the cathode region. In the test object with antioxidant the initial distribution consisted of large homo-charges at both electrodes. When the ageing proceeded positive charge became dominating throughout the object with a maximum close to the cathode. This type of distribution was very similar to those observed after 4 weeks thermal ageing (see Figure 5.5) and resulted in a field enhancement of about 50% at the cathode.

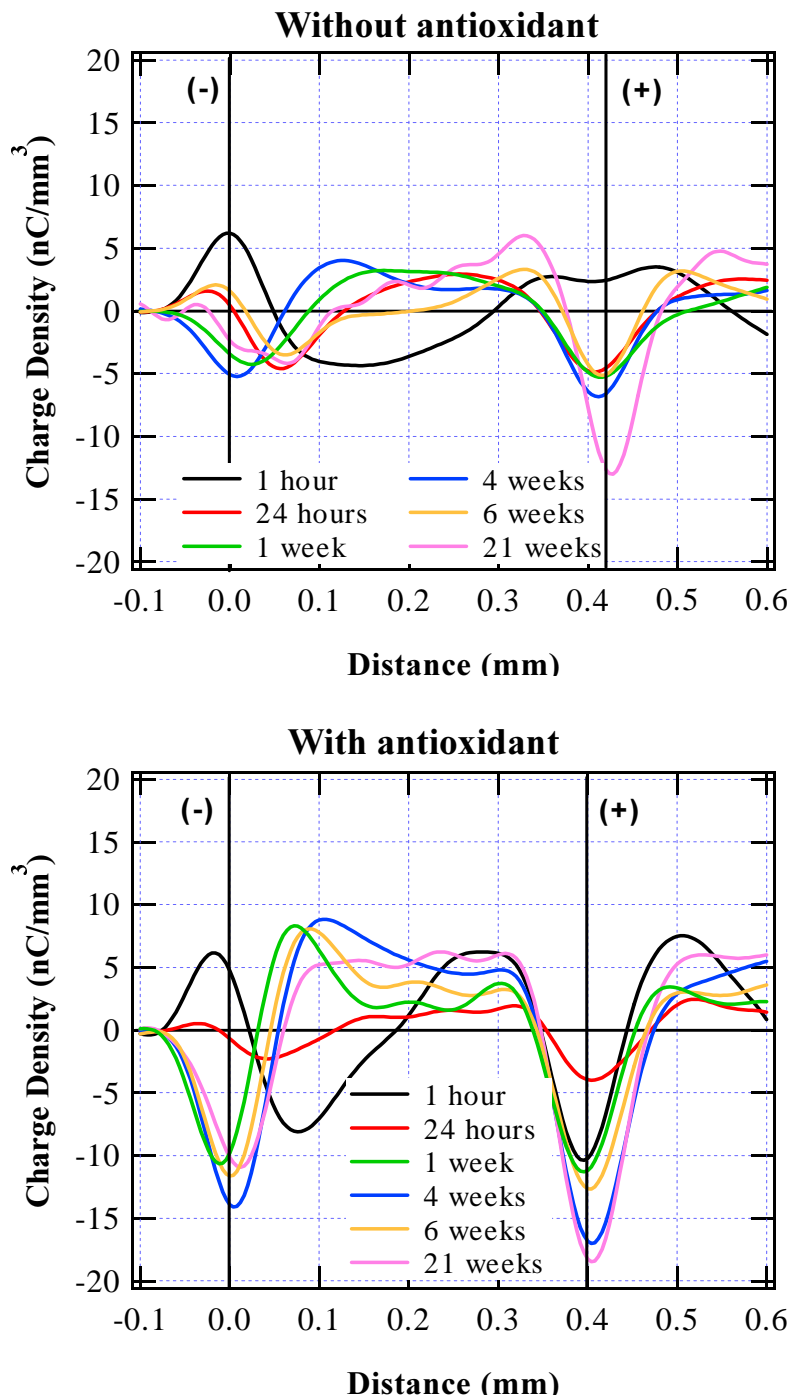


Figure 5.7 Space charge distribution in LDPE measured during long term ageing. Aluminium electrodes. $E = 100 \text{ kV/mm}$, $T = 70^\circ\text{C}$.

5.3.4 Summary of results

Figure 5.8 shows the development of the cathode electrical field in test objects without and with antioxidant subjected to the different ageing conditions. From this figure it is clear that there were differences between the two materials. The highest field modifications were obtained in material with antioxidant. It is also evident that the development of the space charge was very dependent on the applied electrical field and temperature during ageing.

Electrical ageing at 25°C did not result in any significant modification of the applied field in LDPE without antioxidant, while in LDPE with antioxidant a 40% reduction of the applied field was reached after 24 hours. When the ageing temperature was raised to 70°C, negative charge accumulated in LDPE without antioxidant and a 40% reduction of the cathode field was reached after 4 weeks of ageing. In LDPE with antioxidant the increased temperature mainly seemed to increase the rate of charge accumulation; a field reduction of 40% was reached after only 1 hour at 70°C.

Thermal ageing at 70°C with zero applied field except for one hour prior to the space charge measurements had a major effect on the charge characteristics of the material with antioxidant. There was a change from a field reduction of 20% to a field enhancement of about 60% during the 4 week ageing period due to positive charge accumulation in the cathode region.

Increase of the electrical field from 70 to 100 kV/mm also resulted in a change from negative to positive charge accumulation in the cathode region. After 4 weeks at 100 kV/mm a 40% enhancement of the applied field was obtained in LDPE with antioxidant compared to a 40% reduction in the case of 4 weeks at 70 kV/mm.

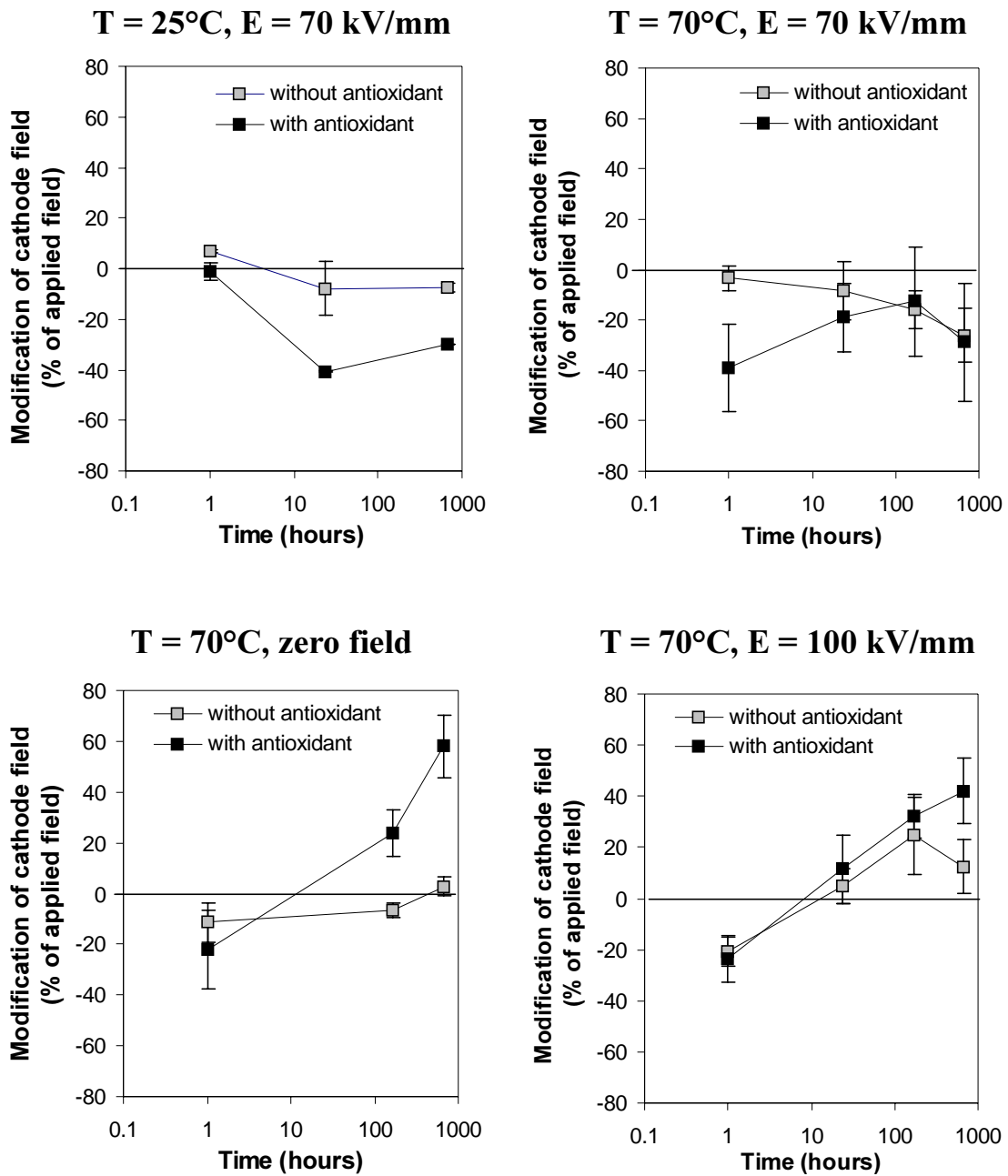


Figure 5.8 Development of the cathode field modification with ageing time under different ageing conditions. The values are a mean of measurements on 2 - 4 different test objects and the scatter is indicated.

5.4 Discussion

5.4.1 LDPE with antioxidant

Electrical ageing at 70 kV/mm

In LDPE with antioxidant the electrical ageing at 70 kV/mm resulted in a homocharge distribution at all ageing temperatures. Previously several authors have reported heterocharge formation in LDPE with antioxidant [27 - 30]. The referred experiments were performed at room temperature after a few hours of electrical stress which may explain the disagreement. If Figure 5.1 is examined we see that negative charge was present at the anode after 24 hours at 25°C. This result agrees with the results of both Mizutani et al. [28] and Cartwright et al. [27] who observed heterocharge only at the anode after 3 hours at 120 kV/mm and 48 hours at 40 kV/mm respectively.

As the ageing proceeded the negative charge at the anode was replaced by homocharge. This transition may be explained as follows: The negative charge caused a 60% enhancement of the anode electrical field and the extraction of electrons at the anode increased due to this enhancement. In addition the electron injection from the cathode decreased due to the reduced cathode field. This development continued until a more stable situation with field reduction at both electrodes was reached, i.e. a homocharge distribution was formed. When the temperature was raised to 40°C and above the homocharge distribution was observed already after 1 - 24 hours of ageing. The faster development may be explained by the increased charge injection and charge mobility with increasing temperature [10].

Thermal ageing at 70°C

After 4 weeks at 70°C and zero electrical field, one hour with applied electrical stress resulted in positive charge throughout the sample with a maximum close to the cathode. Before the thermal ageing one hour with applied stress gave a homocharge distribution as discussed above. Which changes in the material during thermal ageing could be responsible for this major change in charge trapping characteristics? The literature referred in Section 2.3.2 showed that the antioxidant molecules diffuse easily through the material at 70°C. In a previous publication it was suggested that antioxidant mol-

ecules arriving at the aluminium-LDPE surface reacted with aluminium and caused the positive charge formation [72]. In order to test this model some objects were equipped with gold electrodes since gold was expected to be less reactive towards the antioxidant. The same positive charge formation was observed in test objects with gold electrodes and this contradicted the proposed model.

The oxidation temperature measurements presented in Section 4.3.4 showed a decrease in the amount of antioxidant after 4 weeks at 70°C. Thus used antioxidant molecules that had donated one or two hydrogen atoms (see Figure 2.4) were present in the test object, especially close to the surfaces where oxygen diffuse into the material. Mizutani et al. [73] have shown that a thin layer of used antioxidant molecules on the surface of a LDPE sample enhanced the conduction current of the sample. The increased conduction current was explained by enhanced electron injection and extraction at the cathode and anode respectively. The positive charge distribution after thermal ageing may be related to this effect of the used antioxidant. If the extraction of electrons from the anode becomes more efficient than the injection at the cathode a net positive charge will be left in the insulation.

Consumption of the antioxidant was clearly also occurring when the test objects were subjected to an applied electrical field of 70 kV/mm during the whole ageing period, but no transition from homocharge to a positive charge distribution was observed in this case. The homocharge reduced the field at the electrodes by about 40% and it is possible that this reduced field was too low to induce any effect of the used antioxidant molecules. This is in correspondence with the result by Mizutani et al. [73] showing a significantly lower charge injection/extraction at the electrodes with $E = 40$ kV/mm compared to $E = 80$ kV/mm in LDPE containing used antioxidant.

When the thermally aged test objects with aluminium electrodes were subjected to subsequent electrical ageing the positive charge in the cathode region initially decreased but then started to increase again, i.e. there was no return to the homocharge distribution obtained when the electrical field was applied during the whole ageing period. The field at the cathode never dropped below about 100 kV/mm and this field was probably high enough to maintain the positive charge distribution. In the test object with gold electrodes the positive charge in the cathode region disappeared. It is not clear

whether this was a result of the different electrode material or just a result of object-to-object variation.

Electrical ageing at 100 kV/mm, $T = 70^{\circ}\text{C}$

Increasing the ageing field from 70 to 100 kV/mm resulted in a positive space charge distribution very similar to the one obtained after thermal ageing. This is another indication that a high field at the electrodes is necessary to obtain the transition from homocharge to positive charge accumulation. The initial homocharge reduced the field at the electrodes to about 80 kV/mm, but this was still high enough to initiate the positive charge generation as the antioxidant was being consumed.

5.4.2 LDPE without antioxidant

Electrical ageing at 70 kV/mm

In LDPE without antioxidant there was no apparent trend in the space charge development. The obtained distributions varied with temperature and there were also large variations from test object to test object under equal conditions. The object-to-object variation was probably a result of morphology variations between the test objects. The DSC measurements presented in Section 4.3.1 showed that the pressure moulded test objects contained a fraction of larger crystallites and that the amount of these crystallites was very variable. Uchida et al. [70] have shown that the crystallite size can affect both the distribution and amount of charge in polyethylene. Uchida also found that the crystallite size had a large influence on how the space charge pattern changed with increasing temperature. This may explain the lack of a clear trend in the space charge development of the test objects without antioxidant when increasing the ageing temperature. LDPE with antioxidant had a more consistent development in the space charge distribution from test object to test object and with increasing temperature. There was a variation in the amount of charge accumulating, but the trend with negative charge throughout the bulk followed by a homocharge distribution was always observed. This indicates that the antioxidant additive had a dominating influence on the injection and accumulation of charge while morphology became a second order effect. This is in agreement with the conclusion made by Cartwright et

al. [27] when comparing morphology and space charge accumulation in LDPE with and without antioxidant.

Above room temperature the amount of charge accumulating in LDPE without antioxidant was comparable to the amount present in test objects with antioxidant although the charge accumulated at a slower rate. The formation of charge in LDPE without antioxidant was probably related to components with low molecular weight. Suh et al. [71] have shown that when these components were removed by xylene extraction the amount of space charge was reduced to 1/3. At an ageing temperature of 70°C formation of oxidation products close to the electrodes may also have contributed to the space charge formation. Negative charge was observed throughout the sample and Ieda et al. [22] have shown that a thin layer of oxidized PE on the surfaces of unoxidized PE caused negative charge accumulation at both electrodes.

Thermal ageing at 70°C

Only small amounts of charge accumulated both before and after the 4 week period with thermal ageing. Again this illustrates the slower rate of charge accumulation in LDPE without antioxidant compared to the material with antioxidant. One hour of field application prior to measuring space charge was too short to get any substantial amount of charge in the insulation, and therefore no information about the effect of thermal ageing was obtained.

Electrical ageing at 100 kV/mm, $T = 70^{\circ}\text{C}$

When the ageing field was increased to 100 kV/mm a positive space charge very similar to that of LDPE with antioxidant developed throughout the material, although the charge concentration was about 50% lower. The positive charge formation could be a result of oxidation products close to the surface altering the balance between charge injection and extraction as discussed above for the case of used antioxidant molecules. From four to six weeks of ageing there was a change from positive to negative charge in the cathode region. The material characterization presented in Chapter 4 showed that the auto-oxidation process accelerated after about six weeks at 70°C resulting in a fast increase of oxidation products throughout the whole material. The transitions to negative charge may be related to the accelerated oxidation.

5.5 Conclusions

The antioxidant additive caused a faster rate of space charge accumulation in the initial period of the ageing. 1 hour with applied electrical stress gave rise to a 30 - 40% reduction of the cathode electrical field in LDPE with antioxidant compared to a 2 - 10% modification in LDPE without antioxidant.

The antioxidant additive seemed to stimulate charge injection from the electrodes and in general a homocharge distribution arose after ageing at 70 kV/mm. In LDPE without antioxidant there were large object-to-object variations in the space charge distributions and this was probably related to morphology differences.

When LDPE with antioxidant was subjected to thermal ageing or electrical ageing at 100 kV/mm positive space charge with a maximum close to the cathode developed. The positive space charge caused a cathode field enhancement of up to 70%. It was proposed that used antioxidant molecules altered the balance between charge injection and extraction at the electrodes and caused the positive charge formation. This type of development was also observed in LDPE without antioxidant, probably due to the formation of oxidation products in the electrode regions.

Chapter 6

THE EFFECT OF IRON PARTICLES ON THE SHORT AND LONG TERM DC BREAKDOWN STRENGTH

6.1 Introduction

The experiments presented in this chapter are concerned with the effect of inclusions in the insulation system. Defects can not be completely eliminated in a practical extruded insulation system, and it is important to investigate the consequences of defects on the insulation durability. As discussed in section 2.5 it is well known that defects reduce the insulation life time under AC conditions, and work done by Chen et al. [48] indicate that this is also the case for HVDC. On this basis the following hypothesis was formulated in Chapter 1:

Inclusions in the insulation or protrusions at the electrodes are detrimental to the insulation and reduce the insulation life time under DC electrical ageing.

To investigate this hypothesis iron particles were included in LDPE test objects, and both the short and long term DC breakdown strength was evaluated. Iron particles were selected since iron contaminations have been found in medium and high voltage extruded AC cables [58], probably due to wear of the extruder tools. In addition it is known that iron acts as a catalyst in the oxidation process [19] and may thus be the most critical particle type during long term ageing. All experiments were performed on LDPE with and without the antioxidant additive SantanoxR. The first two hypotheses formulated in Section 1.2 concerning the effect of oxidation and antioxidant are therefore also involved in this chapter.

6.2 Experimental procedures

Test objects with iron particles and reference test objects without particles were prepared as described in Section 3.2.2. Measurements of the short term DC breakdown strength were performed at 23°C and 70°C. The test objects were immersed in silicone oil to prevent external flashover. The voltage was raised to a starting level and then increased stepwise every 5 minute as shown in Figure 6.1. Table 6.1 shows the ramp parameters used in the two different temperature cases. 4 - 9 repetitions were performed in each testing case and 85% of all breakdowns occurred during the 5 minute period with constant voltage.

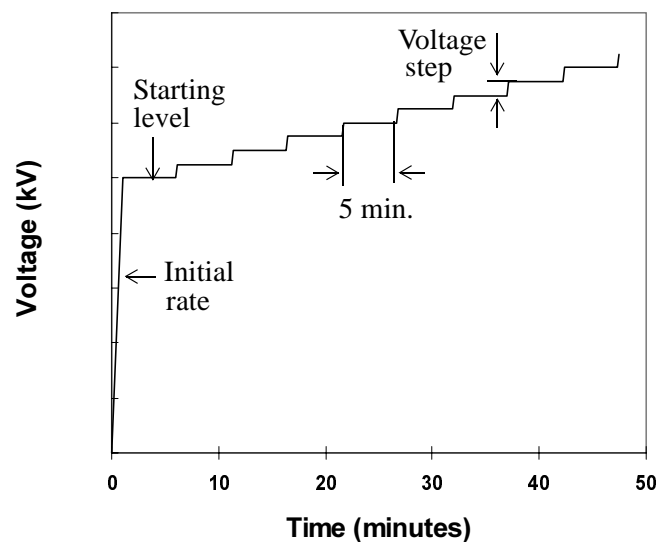


Figure 6.1 DC ramp test with stepwise increase of voltage

Table 6.1 Parameters used in the DC ramp test

| T | Test object | Initial rate | Starting level | Voltage step |
|------|-----------------|--------------|----------------|--------------|
| 23°C | reference, iron | 0.5 kV/s | 350 kV/mm | 5 kV |
| 70°C | reference | 0.7 kV/s | 150 kV/mm | 7 kV |
| 70°C | iron | 0.7 kV/s | 100 kV/mm | 7 kV |

The long term endurance test was performed at 70°C with a DC electrical field of 90 - 200 kV/mm. Time to breakdown was recorded until the experiment was terminated. Breakdown occurred in 80% of the test objects through the experimental period. During ageing the test objects were exposed to the ventilated air of the oven. Due to lower voltage it was found unnecessary to keep the samples immersed in silicone oil. After ageing the test objects were characterized with respect to oxidation level and consumption of antioxidant. The oxidation level was determined by FTIR spectroscopy while the antioxidant concentration was measured with the dynamic DSC method, both methods are described in Section 3.3.

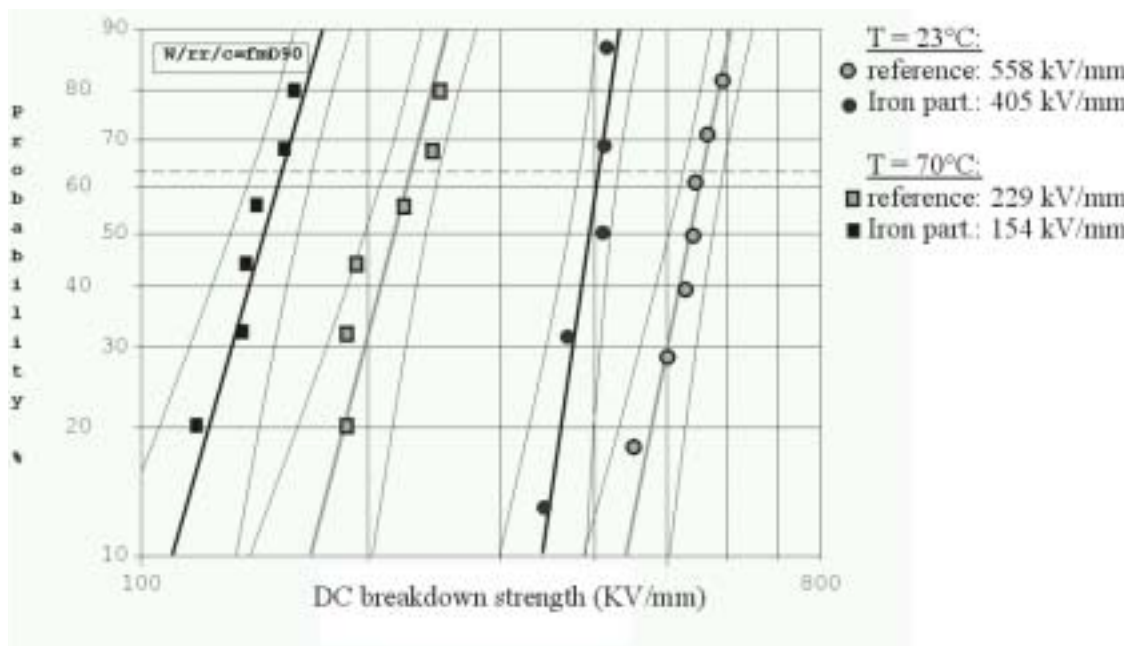
6.3 Results

6.3.1 Short term DC breakdown strength

The breakdown values obtained were analysed using Weibull statistics and the resulting Weibull plots for LDPE without and with antioxidant are shown in Figure 6.2. Table 6.2 summarizes the 63% breakdown strength values for the different cases. For both materials a strong temperature effect is evident, the characteristic breakdown strength was reduced by about 60% when the temperature was raised from 23°C to 70°C.

From Figure 6.2 it is also clear that the iron particles led to a significant reduction of the DC breakdown strength and Table 6.3 gives the percentage reduction. We see that the effect of the particles was most pronounced in the material without the antioxidant with a maximum reduction of 33% at 70°C. The material without the antioxidant additive in general had a lower breakdown strength compared to the material with antioxidant, especially at room temperature as can be seen from Table 6.4.

LDPE without antioxidant



LDPE with antioxidant

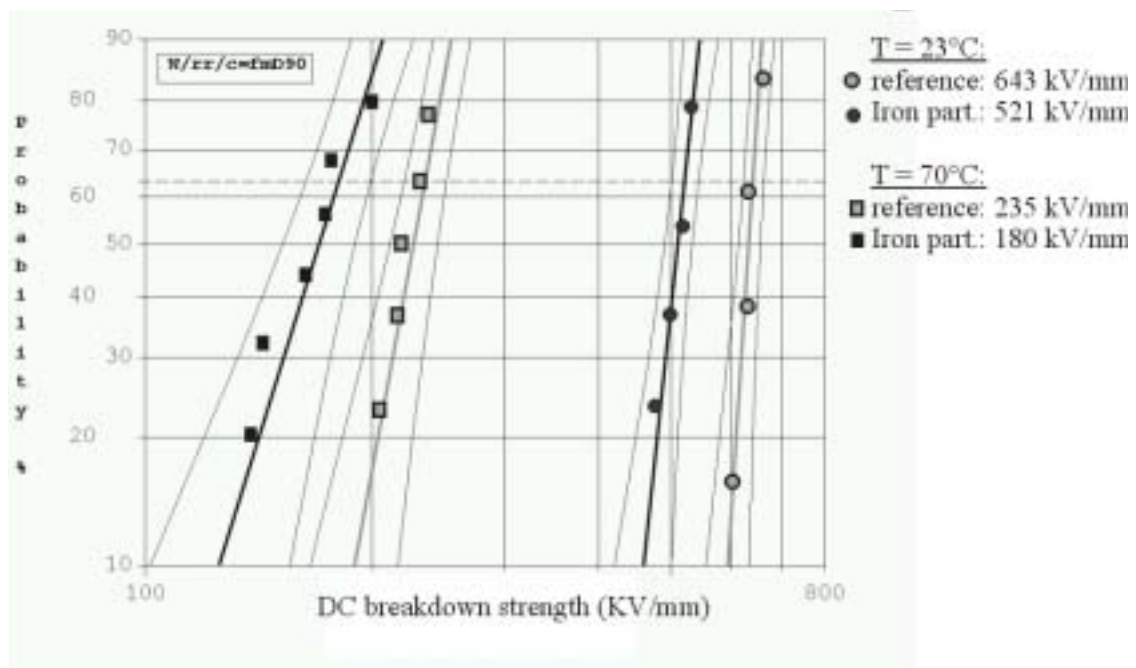


Figure 6.2 Weibull plot of the short term DC breakdown values obtained in LDPE without and with antioxidant. The 90% confidence limits are shown and the 63% breakdown voltage is given in the legend.

Table 6.2 Summary of the short term DC breakdown tests.

$E_{63\%}$: characteristic breakdown strength, β : Weibull shape factor, n/s: total number of data/ suspended data

| Material | T (°C) | Test object | $E_{63\%}$ (kV/mm) | β | n/s |
|--------------------------|--------|----------------|-----------------------|---------|-----|
| LDPE without antioxidant | 23 | reference | 558 | 9.6 | 9/0 |
| | | iron particles | 405 | 13.2 | 5/0 |
| | 70 | reference | 229 | 7.3 | 8/0 |
| | | iron particles | 154 | 6.7 | 8/0 |
| LDPE with antioxidant | 23 | reference | 643 | 28.4 | 4/0 |
| | | iron particles | 521 | 17.4 | 8/3 |
| | 70 | reference | 235 | 10.2 | 7/0 |
| | | iron particles | 180 | 6.2 | 8/0 |

Table 6.3 Percentage reduction of the DC breakdown strength due to the iron particles; $(E_{\text{iron}} - E_{\text{reference}})100\% / E_{\text{reference}}$

| Material | T (°C) | Effect of particles |
|--------------------------|--------|---------------------|
| LDPE without antioxidant | 23 | -27% |
| | 70 | -33% |
| LDPE with antioxidant | 23 | -19% |
| | 70 | -23% |

Table 6.4 Percentage improvement of the DC breakdown strength due to the antioxidant additive; $(E_{\text{with antiox.}} - E_{\text{without antiox.}})100\% / E_{\text{without antiox.}}$

| Test object | T (°C) | Effect of antioxidant |
|---------------------|--------|-----------------------|
| reference | 23 | 15% |
| | 70 | 3% |
| with iron particles | 23 | 29% |
| | 70 | 17% |

6.3.2 Long term ageing

The results of the DC endurance experiments are summarized in Figure 6.3. There were no significant differences between reference samples and samples with iron particles neither in test objects without or with antioxidant. In samples with antioxidant there was a large scatter in the time to breakdown, as an example the time to breakdown at 100 kV/mm ranged from 20 minutes to 3000 hours. In LDPE without antioxidant the majority of the breakdowns occurred either during the first hour of ageing or later than about 800 hours.

If the applied electrical field exceeded a certain limit none of the test objects survived more than 24 hours. For test objects with and without antioxidant this limit was 110 kV/mm and 130 kV/mm respectively as can be seen from Figure 6.4. From this figure we also see that 70% of all the test objects without antioxidant survived more than 24 hours, while only 40% of the test objects with antioxidant did the same.

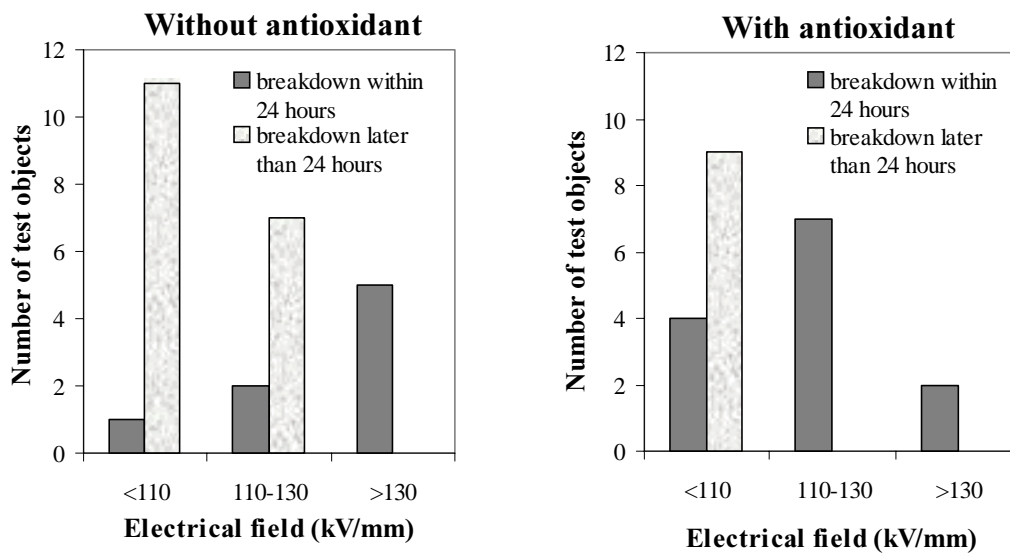


Figure 6.4 Number of test objects with breakdown before or after 24 hours for three electrical field intervals.

6.3.3 Characterization of the aged samples

Oxidation level

Figure 6.5 shows the infrared spectra of two reference test objects with and without antioxidant after 1400 hours of ageing compared to the spectra of the unaged materials. In the object without antioxidant a very strong absorption around 1720 cm^{-1} was observed after ageing, indicating oxidative degradation of the material. In LDPE with antioxidant there was no sign of changes in the oxidation level after 1400 hours of ageing.

Figure 6.6 shows the ketonic carbonyl content in several aged test objects with and without antioxidant. The carbonyl content is calculated from the IR-spectras with the aid of Beers law as described in Section 3.3.2. Each point represents a mean of 5 measurements taken at different positions throughout the bottom area of the test object and the standard deviation is indicated. At each position an area of $25 \times 25\text{ }\mu\text{m}$ was measured. Both reference and iron particle test objects are represented in the figure. In the test objects with iron particles IR-spectra were recorded both in the vicinity of the iron particles and in the bulk of the material, but no difference in the oxidation level was observed due to the particles. We see that in test objects without antioxidant the carbonyl content started to increase after about 1000 hours of ageing. In

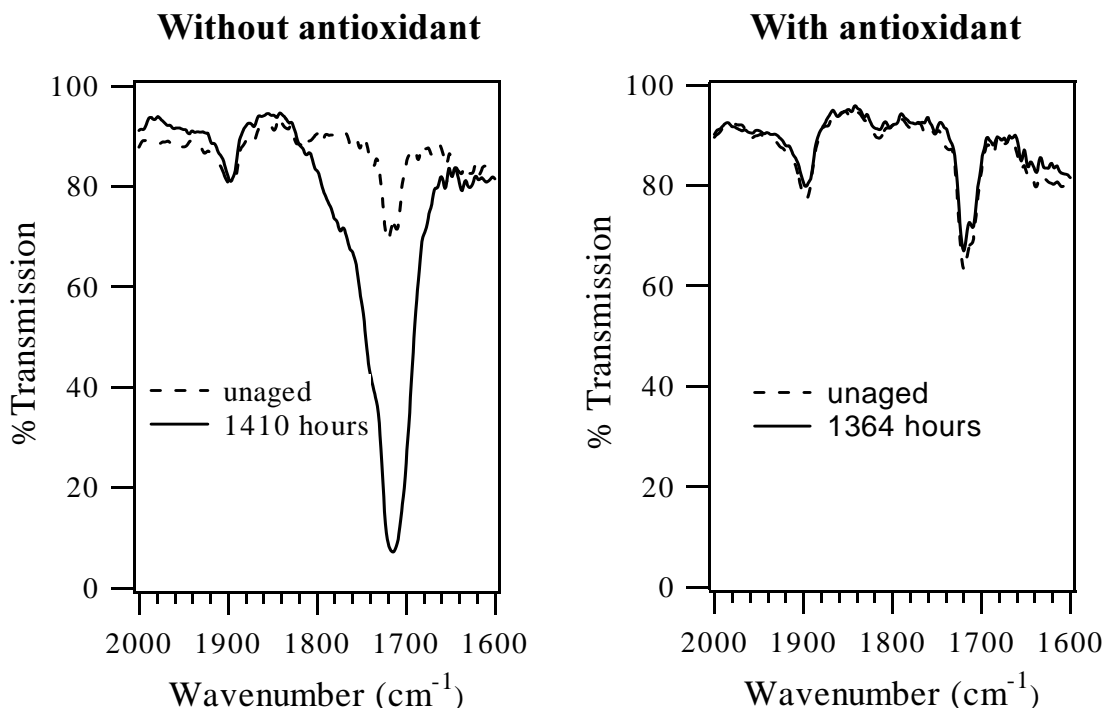


Figure 6.5 Infrared spectras of aged and unaged reference test objects with and without antioxidant.

LDPE with antioxidant the carbonyl content remained stable at 0.1 weight% even after 3000 hours of ageing.

Consumption of antioxidant

Figure 6.7 shows the oxidation temperature of aged test objects recorded by DSC. In the test objects with antioxidant the oxidation temperature started to decrease after 400 hours of ageing. As discussed in Section 4.3.4 the reduced oxidation temperature is caused by migration and consume of the antioxidant leaving depleted regions close to the surfaces. After 1300 hours the oxidation temperature was reduced from 267°C to 222°C which is only 10°C higher than the value obtained in LDPE without antioxidant. Based on the results by Karlsson et al. [69] this indicate that less than 1/10 of the original antioxidant concentration was left in the material. LDPE without antioxidant had an oxidation temperature of 212°C before ageing. When the oxidation process accelerated the oxidation temperature decreased further as can be seen from Figure 6.7.

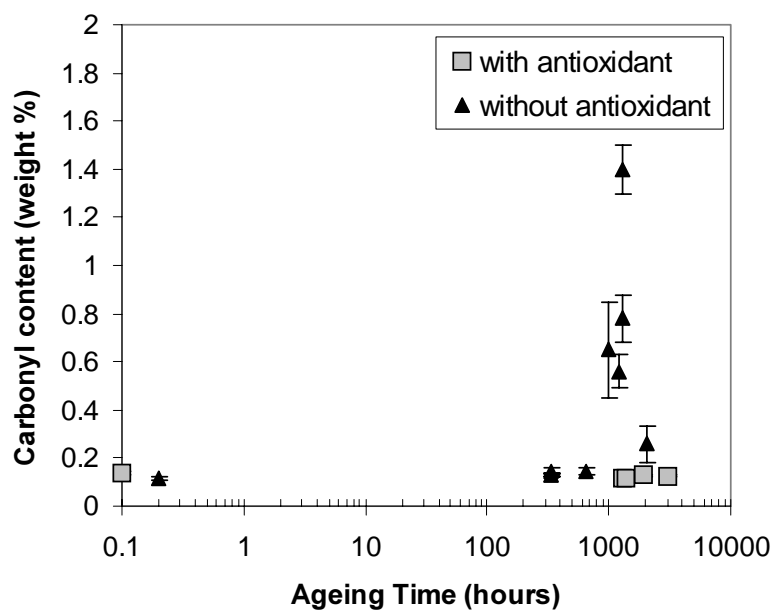


Figure 6.6 Measured carbonyl content in test objects with and without antioxidant aged until breakdown occurred.

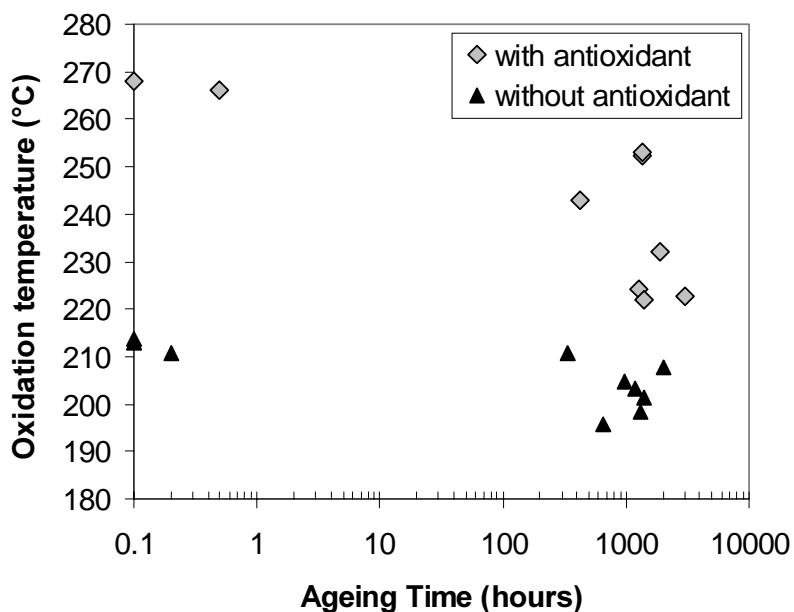


Figure 6.7 Oxidation temperature in aged test objects with and without antioxidant measured with the dynamic DSC method.

6.4 Discussion

6.4.1 Short term DC breakdown strength

Strong temperature dependence of the DC breakdown strength

The short term DC tests revealed that the breakdown strength of the test objects was highly temperature dependent, with a reduction of about 60% when the temperature was increased from 23°C to 70°C. This behaviour of polyethylene is well known from the literature where many experiments have shown that the breakdown strength is almost constant up to 20°C and then falls off rapidly [37,77]. As discussed in Section 2.4 breakdown in LDPE above room temperature can be caused by electromechanical instability due to the decrease in Young's modulus with increasing temperature [38, 39]. In Figure 6.8 the critical electrical field for electromechanical breakdown in LDPE without antioxidant has been calculated from the values of Young's modulus obtained in Section 4.3.2 using equation 2.1. We see that at room temperature breakdown occurred at 60% of the electromechanical critical field, while at 70°C the calculated and measured values are very similar. This indicates an electromechanical breakdown mechanism at 70°C in accordance with the literature referred above.

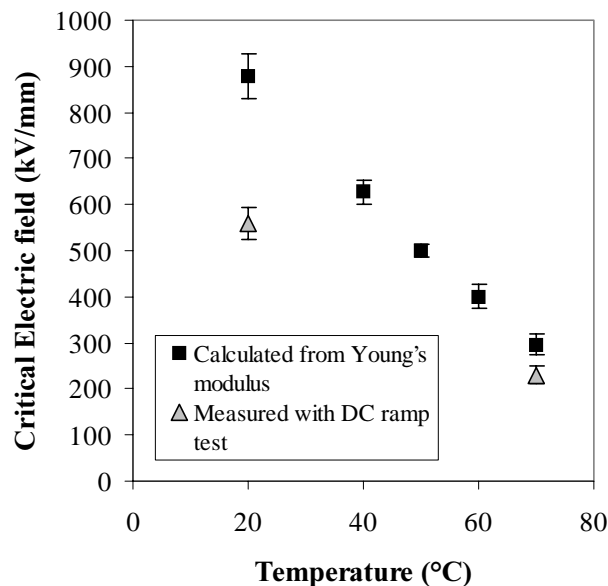


Figure 6.8 Critical electrical field in LDPE calculated from Young's modulus at different temperatures. The breakdown values obtained in the DC ramp test are also shown.

Short term breakdown strength improved by the antioxidant additive

The material with antioxidant had a significantly higher short term breakdown strength than the material without antioxidant at 23°C. Previous investigations have shown that both the DC and impulse breakdown strength of LDPE was increased by homocharge accumulation due to the reduced electrical field at the electrodes [28, 74, 75]. All space charge measurements presented in Chapter 5 showed a faster charge build-up in LDPE with antioxidant compared to LDPE without antioxidant. A larger reduction of the electrical field at the electrodes may therefore have been obtained in LDPE with antioxidant during the test period, and this may explain the observed difference in breakdown strength between the materials. At 70°C electromechanical breakdown was probably the dominating mechanism and differences in space charge accumulation had less influence.

Introduction of iron particles reduced the DC breakdown strength

Introduction of iron particles resulted in a significant reduction of the DC breakdown strength for all test conditions. The iron particles made up about 17% of the total insulation thickness and in LDPE with antioxidant the reduction due to the particles was in this range. This indicates that the particles acted as a partial short circuit of the insulation and reduced the actual insulation thickness. In LDPE without antioxidant the reduction in breakdown strength was about 30%, i.e. larger than the reduction in insulation thickness. This may be caused by electrical field enhancement in the proximity of the irregular iron particles initiating breakdown at a lower electrical field. Accumulation of space charge around the particles will smooth the electrical field and reduce this field effect of the particles. As shown in Chapter 5, there was a faster space charge accumulation in LDPE with antioxidant which may explain why this material was less sensitive to the particles.

6.4.2 Long term ageing*No influence of included iron particles during long term ageing*

The long term ageing showed no effect of the included iron particles on time to breakdown neither in samples with or without antioxidant. This was not expected based on the short term results and also the results obtained by Chen et al. [48]. The lack of particle influence may be explained by accumulation of charge around the particles during ageing. The charge reduced the effect

of the particles as discussed above and other factors may have controlled the time to breakdown. These factors will be discussed in the two following sections for LDPE without and with antioxidant respectively.

Failure after 800 hours in LDPE without antioxidant - related to oxidation

In the case of LDPE without antioxidant 70% of the breakdowns occurred later than 800 hours. The infrared measurements showed that most of the test objects aged more than 800 hours were heavy oxidized, and it seems likely that the breakdowns occurring were related to this oxidation. As discussed in Section 2.2.3 previous investigations have shown that the DC breakdown strength of PE decreases with oxidation, probably due to enhanced high field conduction and increased Joule heating [20, 21, 24, 25]. The time to reach a critical oxidation level depends on the thickness of the aluminium electrodes as shown in Section 4.3.3 and this may explain the scatter in time to breakdown.

60% of the failures in LDPE with antioxidant occurred within 24 hours

In test objects with antioxidant 60% of the breakdowns occurred during the first 24 hours of ageing. The space charge measurements presented in Chapter 4 showed a fast charge build-up in LDPE with antioxidant and this may explain the breakdown behaviour of the material. After only one hour at 100 kV/mm a large homocharge was present as can be seen from Figure 5.7 and this distribution caused a field enhancement of 23% in the centre of the sample. The actual field enhancement was probably higher since the space charge measurement was performed after cooling down the sample and switching off the voltage. Some of the accumulated charge probably disappears during this procedure. With a field enhancement in this range the local field begins to approach the short term breakdown strength of the material and breakdown may be initiated. The test objects that survived this first ageing period lasted more than 400 hours. This may also be related to the development of the space charge distribution. From Figure 5.7 we see that at some point between 1 hour and 24 hours the homocharge decreased and a positive charge started to develop. After 4 weeks the field enhancement at the cathode due to this positive charge had reached 50%. Again the local electrical field is in a range which may have initiated breakdown.

When the electrical field exceeded 110 kV/mm none of the test objects with antioxidant survived more than 24 hours while in LDPE without antioxidant this limit was 130 kV/mm. This difference is in agreement with the space charge measurements in Chapter 5 showing that the amount of space charge in LDPE without antioxidant was approximately 60% lower compared to LDPE with antioxidant after one hour of voltage application (see Figure 5.7).

6.4.3 Summary of discussion

The suggested breakdown mechanisms for the different test cases are summarized in the table below.

| Short term DC breakdown strength | |
|---|---|
| T = 23°C | T = 70°C |
| <ul style="list-style-type: none"> • Space charge affects the breakdown strength • iron particles -> reduced strength • antioxidant -> enhanced strength | <ul style="list-style-type: none"> • Electro-mechanical breakdown due to reduction in Young's modulus • space charge is a second order effect • iron particles -> reduced strength • antioxidant -> no effect |
| Long term DC breakdown strength at 70°C | |
| <ul style="list-style-type: none"> • No particle effect, the particles screened by accumulated space charge. • Other dominating mechanisms: • LDPE <i>without</i> antioxidant: Oxidation enhances the high field conduction and cause breakdown. • LDPE <i>with</i> antioxidant: Large amount of space charge accumulates during ageing. Field enhancement at the electrodes or in the bulk causes breakdown. Insulation life time reduced by the antioxidant additive. | |

6.5 Conclusions

Introduction of irregular iron particles reduced the short term DC breakdown strength of LDPE but did not affect the long term performance. The particles

were probably screened by injected space charge and other mechanisms controlled the insulation life time.

The antioxidant additive enhanced the short term performance at room temperature but reduced the long term performance. These results were explained by the space charge behaviour of LDPE with antioxidant.

In LDPE without antioxidant the majority of the breakdowns occurred after 800 hours in the long term test. This was explained by the accelerated oxidation with corresponding enhancement of high field conduction causing breakdown.

Chapter 7

DC BREAKDOWN STRENGTH OF TEST OBJECTS WITH NEEDLE-PLANE ELECTRODE GEOMETRY

7.1 Introduction

In the previous chapter the effect of conducting inclusions in the insulation system was investigated. Another type of defect which may appear in an extruded insulation system is protrusions at the electrodes. Such protrusions give rise to areas with local field enhancement where the ageing process may be accelerated. Protrusions at the electrodes are particularly critical during fast grounding or polarity reversal as discussed in Chapter 2.6. Homocharge accumulates around the protrusion during the DC period. Immediately after grounding or polarity reversal a large electrical field arises due to this homocharge, and partial breakdown of the insulation may be initiated.

To investigate the effect of protrusions experiments have been performed on test objects with a needle-plane electrode geometry. The objects were subjected to thermal and DC electrical ageing and changes in the DC breakdown strength due to this ageing were observed. The four hypotheses proposed in Section 1.2 are all discussed in connection with the results obtained here.

7.2 Experimental procedures

Cup-shaped test objects with three needle prints were prepared from LDPE with and without antioxidant as described in Section 3.2.3. The tip of the needle print had a bend radius of $6 \pm 1.5 \mu\text{m}$ and the distance from needle to plane was $0.5 \pm 0.1 \text{mm}$.

7.2.1 Short term breakdown voltage

The short term DC breakdown voltage was measured at a temperature of 70°C using a ramp test of the same type as previously shown in Figure 6.1. The starting level was 10 kV in the case of positive polarity and 25 kV for negative polarity. The polarity given always refers to the needle electrode. The voltage was increased in steps of 3 kV every 5 minute at a rate of 0.1 kV/s. 5 repetitions were performed and 80% of the breakdowns occurred during the 5 minute period with constant voltage.

The breakdown values are always given as applied voltage, not as the average electrical field between needle and plane. The reason for this is that the needle to plane distance varied from 0.4 - 0.6 mm. This variation in insulation thickness has a large effect on the average electrical field but little influence on the electrostatic field at the needle tip as illustrated in Figure 7.1. Therefore, if we assume that the conditions around the needle tip control the breakdown strength the applied voltage is the relevant parameter.

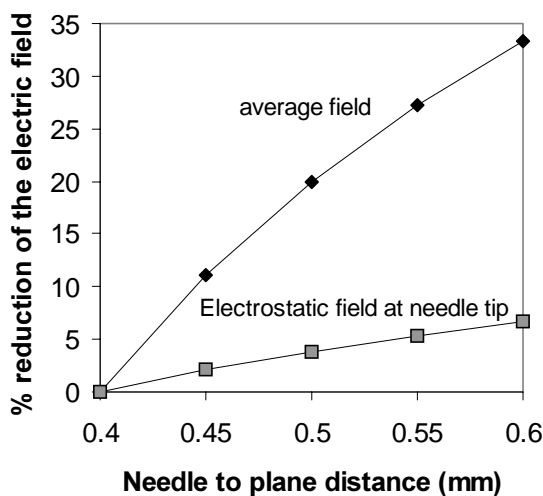


Figure 7.1 Reduction of the average electrical field and the electrostatic field at the needle tip with increasing needle to plane distance. $U = 40$ kV. The static electrical field was calculated from Equation 2.5.

7.2.2 Thermal and electrical ageing

The needle print objects were subjected to 4 weeks ageing, and the ageing parameters varied were temperature, voltage and needle polarity. Table 7.1 shows the seven different parameter combinations used. 10 objects were subjected to each set of conditions, 5 with and 5 without antioxidant additive. When the ageing was initiated and terminated the voltage was turned on and off at a slow rate of 0.1 kV/second to prevent electrical tree initiation. After ageing the DC breakdown strength was measured following exactly the short term procedure described in the previous section. The test objects which had been subjected to an electrical field during ageing were kept short-circuited at the ageing temperature for one hour before the breakdown test was performed. This was done to remove accumulated charge from the test objects. The same voltage polarity was applied both during ageing and testing. All breakdown tests were performed at 70°C, also when the test objects had been aged at 90°C. This was necessary since the effect of the different ageing conditions should be compared against each other.

After the breakdown tests had been performed the objects were microtomed in 250 µm thick slices and the area around the needles were investigated with optical and infrared microscopy.

Table 7.1 Ageing conditions.

| Ageing scheme | Ageing Temperature (°C) | Ageing Voltage (kV) | Polarity (ageing and testing) |
|---------------|-------------------------|---------------------|-------------------------------|
| 1 | 70 | 13 | + |
| 2 | 70 | 13 | ÷ |
| 3 | 70 | zero field | + |
| 4 | 70 | zero field | ÷ |
| 5 | 90 | 13 | + |
| 6 | 90 | 13 | ÷ |
| 7 | 90 | zero field | ÷ |

7.3 Results

7.3.1 Short term breakdown voltage

The breakdown values obtained were analysed using Weibull statistics and the resulting Weibull plot for unaged test objects with and without antioxidant is shown in Figure 7.2. The breakdown voltage was significantly higher with negative compared to positive polarity for both materials. The strongest polarity effect was observed in LDPE without antioxidant where 85% higher breakdown voltage was obtained with negative polarity. If the two materials are compared we see that the breakdown levels were equal for positive polarity while LDPE without antioxidant had a 20% higher breakdown voltage than LDPE with antioxidant in the case of negative polarity.

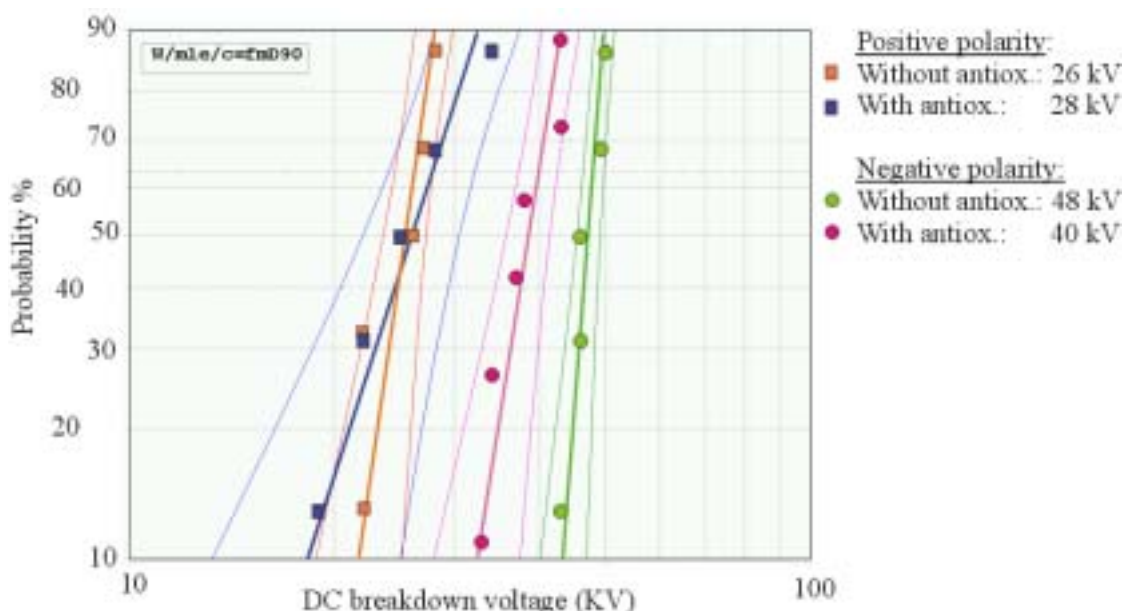


Figure 7.2 Weibull plot of DC breakdown voltage obtained for unaged test objects at 70°C. The 90% confidence limits are shown and the 63% breakdown voltage is given in the legend.

7.3.2 Breakdown voltage after electrical and thermal ageing

Figure 7.4 shows the Weibull plot obtained after 4 weeks of electrical ageing at 70°C (ageing scheme 1 and 2). There was no significant change in the breakdown level in the case of positive polarity. For negative polarity the

breakdown level of the material with antioxidant remained unchanged while the characteristic breakdown voltage of LDPE without antioxidant increased with 18% after ageing. This increase gave an even more pronounced polarity effect in LDPE without antioxidant by 148% higher breakdown strength for negative compared to positive polarity.

When the ageing temperature was increased to 90°C a more dramatic change in the DC breakdown strength was observed for LDPE without antioxidant. With negative polarity three of the five test objects had a breakdown voltage of about 29 kV while for the two others breakdown occurred at 59 kV. The oxidation level of these test objects was measured by FTIR (see Section 4.3.3) and the measured carbonyl concentration is plotted against the DC breakdown voltage in Figure 7.3. From this figure it is clear that the separation in two breakdown levels was related to the degree of oxidation, the two test objects with high breakdown values had an unaltered carbonyl content, while a large increase was observed in the objects with a low breakdown level. The Weibull plot for all the breakdown values obtained after 4 weeks ageing at 90°C and +/- 13 kV is shown in Figure 7.4. We see that for oxidized LDPE without antioxidant the breakdown level with negative polarity was reduced to about the same level as for positive polarity, i.e. the polarity effect was eliminated after ageing. For LDPE with antioxidant there was no significant change in the breakdown voltage.

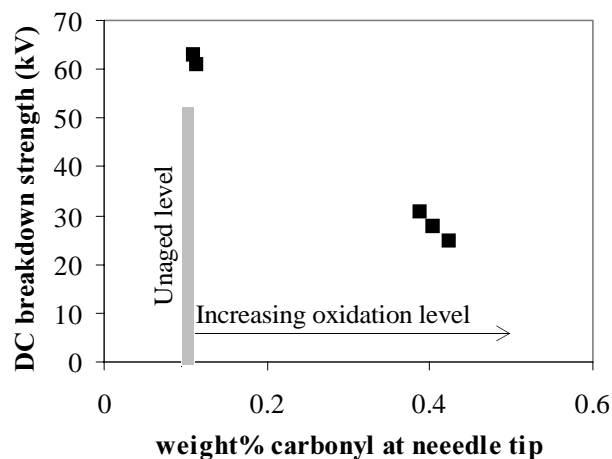


Figure 7.3 DC breakdown values of aged test objects without antioxidant plotted against measured carbonyl content at the needle. Ageing conditions: 4 weeks at $U = -13$ kV, $T = 90^\circ$.

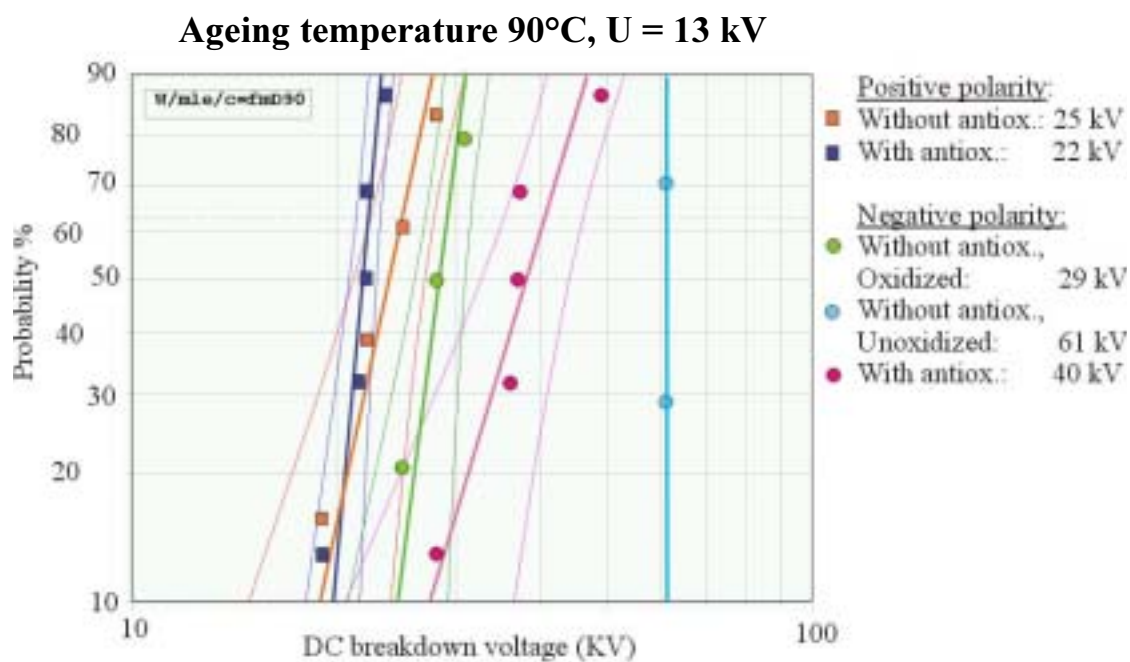
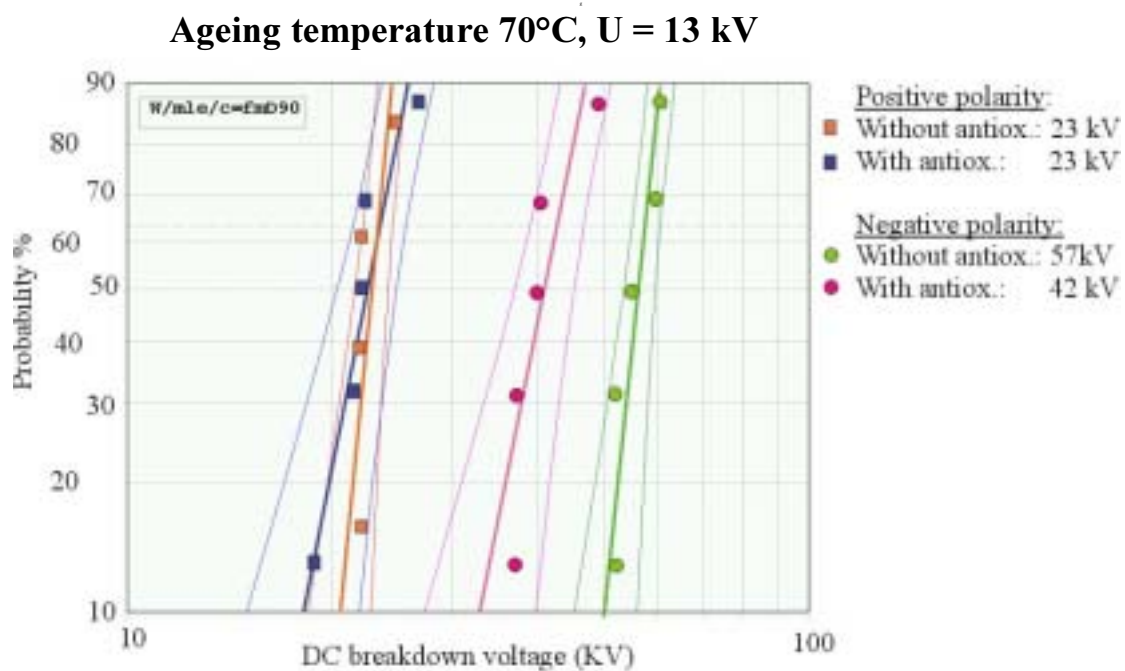


Figure 7.4 Weibull plot of DC breakdown values obtained after 4 weeks electrical and thermal ageing. The 90% confidence limits are shown and the 63% breakdown voltage is given in the legend.

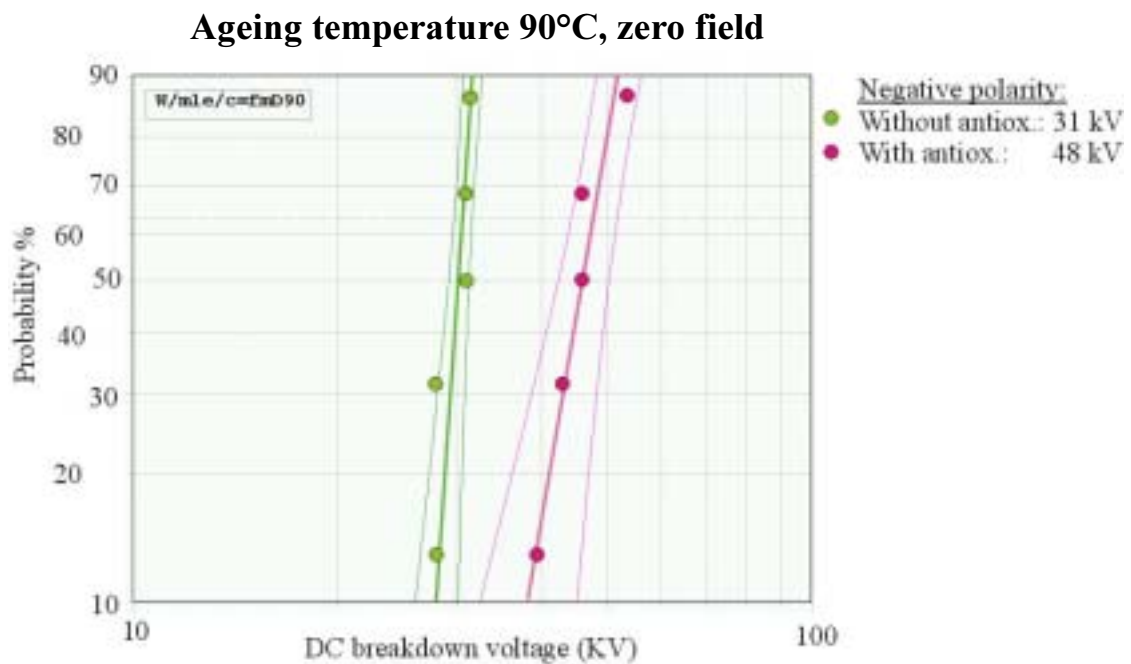
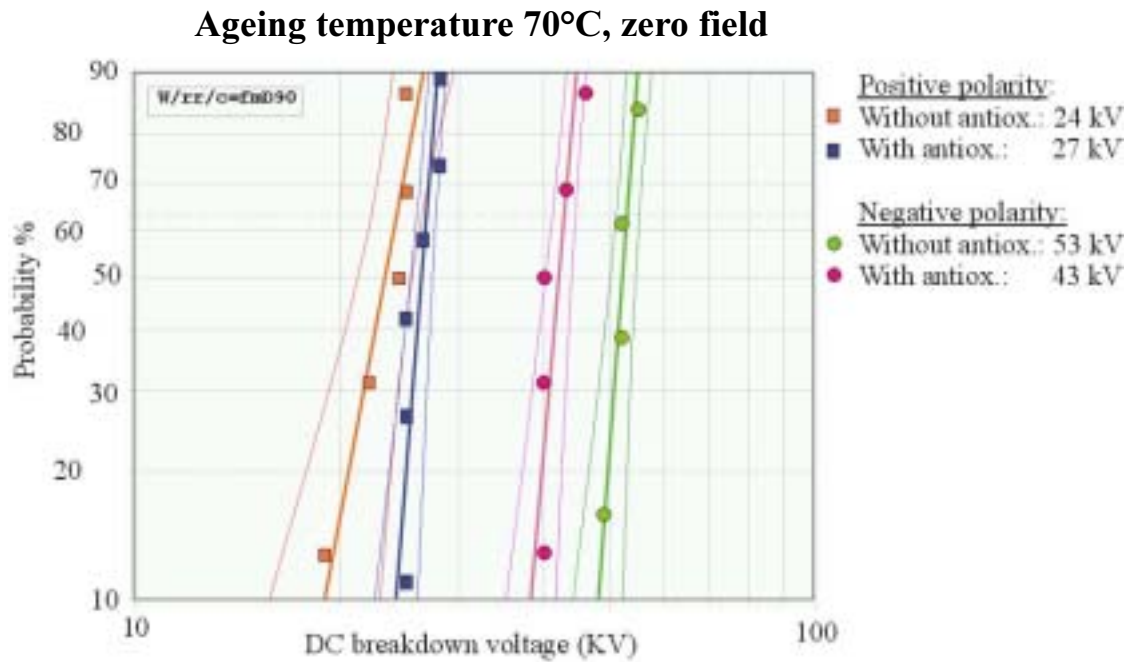


Figure 7.5 Weibull plot of DC breakdown values obtained after 4 weeks thermal ageing. Zero electric field, The 90% confidence limits are shown and the 63% breakdown voltage is given in the legend.

7.3.3 Breakdown voltage after thermal ageing

The result of the thermal ageing with zero electric field is shown in Figure 7.5. After 4 weeks at 70°C the only significant change in breakdown level was observed for LDPE without antioxidant in the case of negative polarity where the level had increased by 10%. This result is very similar to what was obtained after electrical ageing at 70°C.

When the ageing temperature was increased to 90°C a large reduction in the breakdown voltage of LDPE without antioxidant was again observed in the case of negative polarity. For LDPE with antioxidant on the other hand the 63% breakdown level increased by 20% after ageing. Tests with positive polarity were not carried out for this ageing temperature.

7.3.4 Summary of the breakdown results

The obtained 63% values for all the breakdown tests are summarized in Figure 7.6. The following main results are well displayed in these figures:

- Polarity effect: 40 - 150% higher breakdown voltage obtained with negative compared to positive polarity.
- Antioxidant effect: 20 - 36% higher negative breakdown voltage obtained for LDPE without than with antioxidant. (Except after ageing at 90°C)
- Oxidation effect: 40% reduction in the negative breakdown voltage of LDPE without antioxidant after 4 weeks ageing at 90°C.
- Very similar development in the DC breakdown strength with and without applied electrical field during ageing.

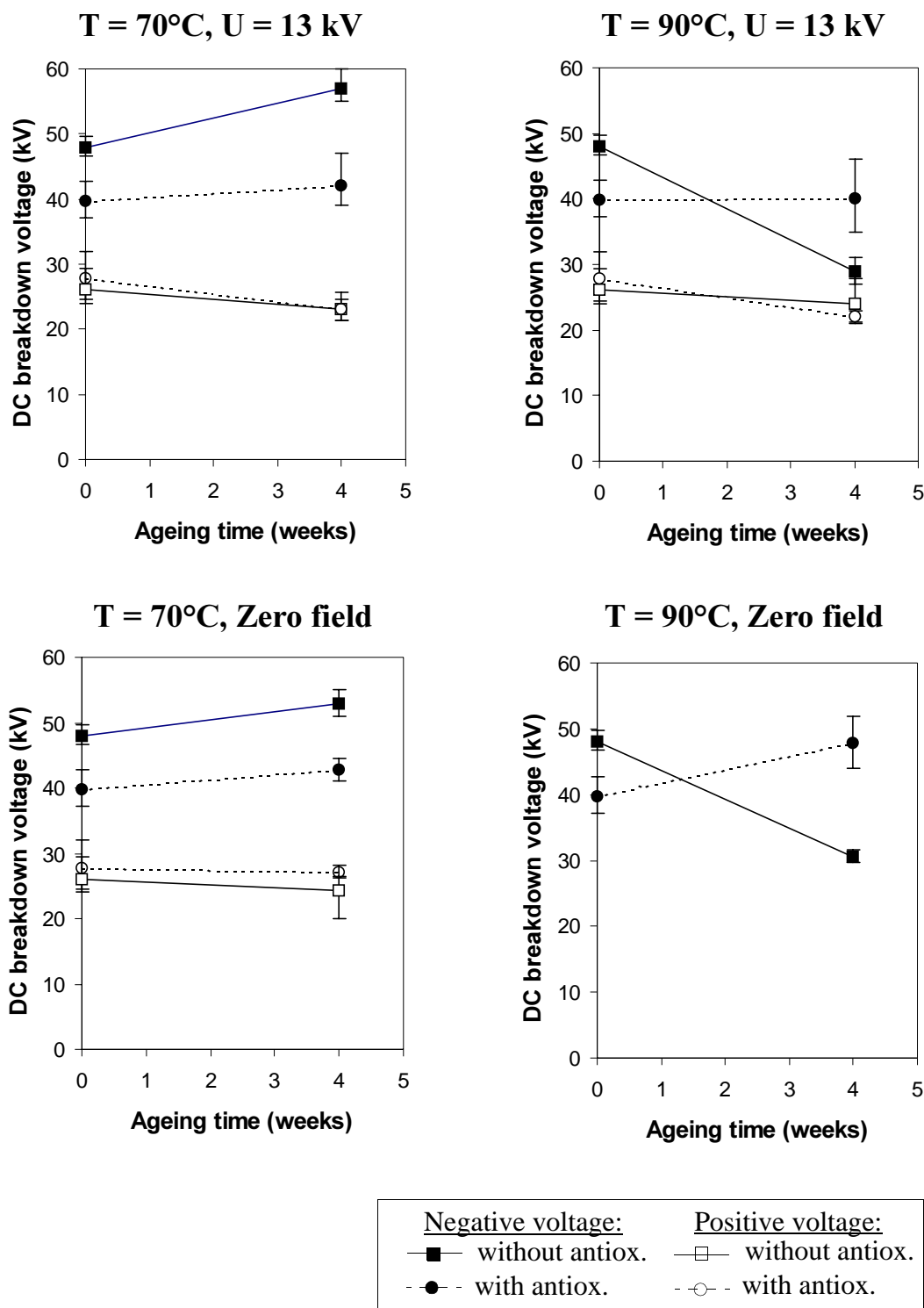


Figure 7.6 DC breakdown voltage before and after 4 weeks electrical and/or thermal ageing at 70 and 90°C.

7.3.5 Electrical treeing

Breakdown was initiated from one of the three needles in a test object. A large breakdown channel was formed from this needle and it was not possible to observe electrical trees. However electrical trees were often present from the two needles where breakdown did not occur during the DC breakdown test. Figure 7.7 shows an example of electrical tree growth from a needle tip. The length of the trees was measured in the direction of the electrical field as shown in the figure.

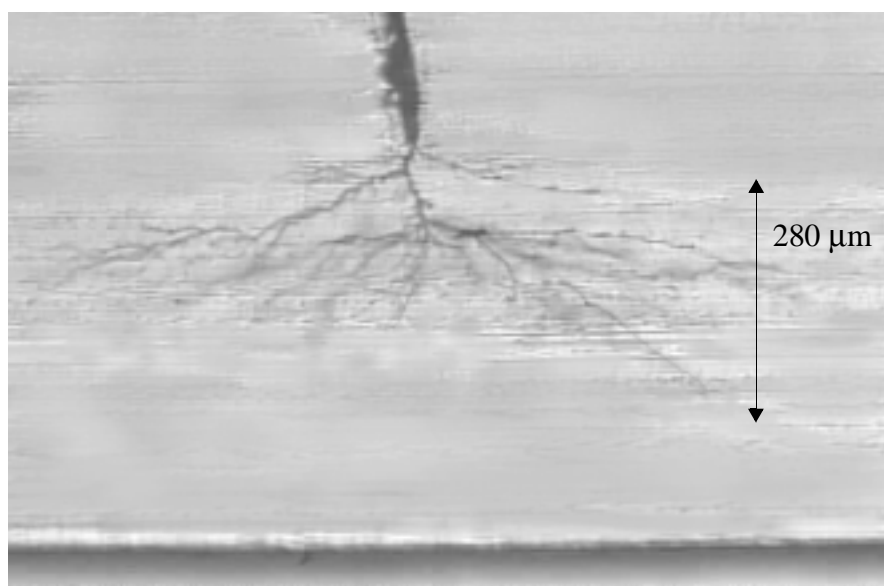


Figure 7.7 Microscope image of electrical tree growth. LDPE without antioxidant aged 4 weeks at 70°C with negative voltage applied at the needle.

Table 7.2 shows the number of needles with observed electrical trees and the total number of needles investigated for each ageing case. For the unaged test objects only a few trees were observed with positive polarity. In the case of negative polarity electrical trees were present at all needles. The number of trees increased after the test objects had been subjected to electrical and thermal ageing. The highest number of electrical trees were observed after 4 weeks of electrical ageing at 90°C where trees were present at all inspected needles irrespective of polarity.

Table 7.2 The ratio of needles with observed electrical tree to the total number of needles inspected. The numbers in parentheses refers to the ageing set number in Table 6.1.

| Ageing conditions: | Positive polarity | | Negative polarity | |
|--------------------------------|-------------------|--------------|-------------------|--------------|
| | without antiox. | with antiox. | without antiox. | with antiox. |
| unaged | 3/12 | 1/10 | 10/10 | 10/10 |
| 4 week, electrical 70°C (1,2) | 3/7 | 8/10 | 10/10 | 10/10 |
| 4 week, electrical, 90°C (5,6) | 6/6 | 10/10 | 10/10 | 9/9 |
| 4 week thermal, 70°C (3,4) | 1/10 | 5/10 | 10/10 | 8/10 |
| 4 week thermal 90°C (7) | - | - | 6/8 | 9/10 |

The length of all the electrical trees was measured and the mean tree length for each of the ageing cases are displayed in Figure 7.8. The mean was calculated from all the inspected needles, i.e. zero length was ascribed to the needles with no electrical tree. The results presented in Figure 7.8 show that there was a trend towards longer electrical trees after the test objects had been subjected to combined electrical and thermal ageing. The scatter in the measured tree lengths was large and an analysis of variance was performed for each set of parameters to see if the change in tree length with ageing was significant [78]. The calculated significance levels for the different ageing cases are shown in Table 7.3, and it is clear that there was a significant increase in the tree length after combined electrical and thermal ageing. One exception was the test objects with antioxidant aged 4 weeks with negative voltage at 90°C. In this case the treelength was unaltered. The most pronounced change took place in LDPE without antioxidant after 4 weeks ageing with positive voltage at 90°C. A mean tree length of 280 μm was observed which is significantly higher than for any of the other ageing cases.

When the test objects were aged thermally with zero electric field there were less changes in the tree lengths as can be seen both from Figure 7.8 and Table 7.3. In LDPE without antioxidant there were no significant changes while in the material with antioxidant the tree length increased by 80% after 4 weeks at 90°C in the case of negative polarity. It is interesting to note that in this particular case the tree length increased after thermal ageing but remained

constant when an electrical field was applied during ageing. For the other ageing cases the effect was opposite.

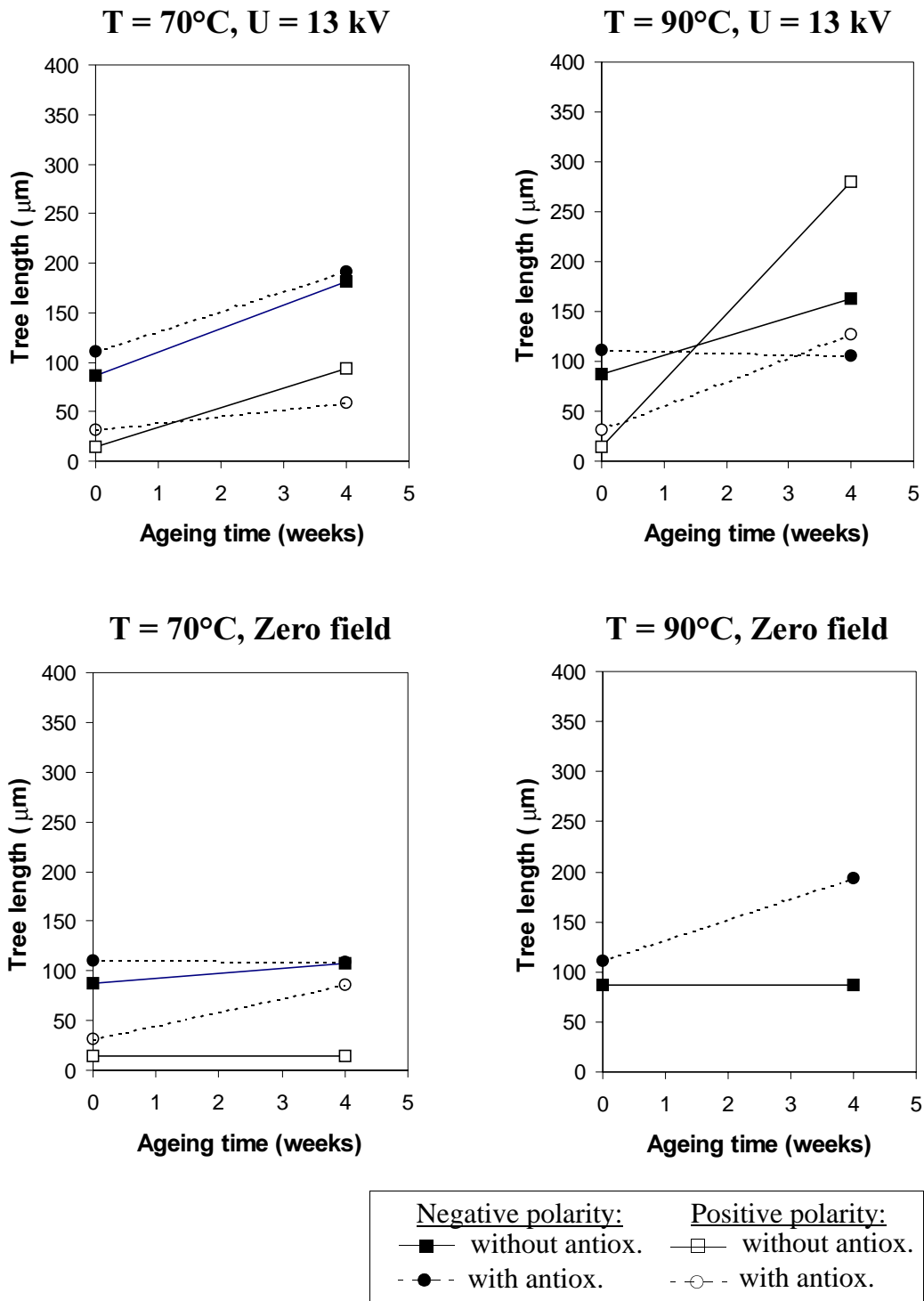


Figure 7.8 Mean electrical tree length before and after 4 weeks ageing at 70°C and 90°C.

Table 7.3 Analysis of variance performed to find which ageing cases gave a significant change in the length of the electrical trees. The shaded cells show the cases where the significance level was better than 90%.

| Ageing conditions: | Positive polarity | | Negative polarity | |
|--------------------------------|-------------------|--------------|-------------------|--------------|
| | without antiox. | with antiox. | without antiox. | with antiox. |
| 4 week, electrical 70°C (3,4) | 93.6 | 97.2 | 99.7 | 97.2 |
| 4 week, electrical, 90°C (7,8) | 100 | 98.4 | 95.3 | 12 |
| 4 week thermal, 70°C (5,6) | 8.1 | 74.6 | 63.2 | 4.2 |
| 4 week thermal 90°C (9) | - | - | 2.6 | 88.3 |

7.4 Discussion

7.4.1 DC breakdown voltage

Strong polarity effect

The DC breakdowns occurred in the range from 20 - 60 kV depending on polarity, material and ageing conditions. If the electrostatic field at the needle tip is calculated (using Equation 2.3) with applied voltage $U = 20$ kV and $r_{\text{needle}} = 6$ μm , a value of 1140 kV/mm is obtained. The ‘intrinsic’ breakdown strength of polyethylene at 70°C is about 350 kV/mm [77] and thus the calculated electrostatic field is more than 3 times higher than the intrinsic strength. This means that for all cases homocharge accumulated around the needle and reduced the local electric field to values below the intrinsic breakdown level. The DC breakdown testing revealed that the breakdown voltage was 40 - 150% higher with negative compared to positive polarity. Such a polarity effect has been observed by several workers previously [49 - 51] and, as discussed in Section 2.5 and 2.6, the effect is explained by higher homocharge concentrations at the needle with negative compared to positive polarity causing a larger reduction of the local electric field.

The antioxidant additive reduced the breakdown level

LDPE with antioxidant had a 16 - 26% lower negative breakdown voltage than the material without antioxidant, both before ageing and after 4 weeks at 70°C. In Section 6.4.1 it was shown that in a homogenous field the two materials had an equal breakdown strength at 70°C. Thus the observed difference must be related to the conditions in the inhomogenous field region. If a smaller amount of negative charge was present around the needle in the case of LDPE with antioxidant, this would give a lower breakdown strength due to less efficient screening of the needle. The space charge measurements performed in Chapter 5 may support this explanation. From Figure 5.7 we see that during ageing of LDPE with antioxidant at $E = 100$ kV/mm and $T = 70^\circ\text{C}$, positive charge was formed throughout the insulation with a maximum close to the cathode. If this type of positive charge formation took place in the high field region around the negative needle, the net negative charge would be reduced and thus a less efficient screening obtained.

Improved breakdown level after thermal and electrical ageing at 70°C

4 weeks electrical and/or thermal ageing mainly affected the DC breakdown level in the case of LDPE without antioxidant. The increased negative breakdown level after 4 weeks at 70°C may be related to the annealing and corresponding increase in Young's modulus that was observed after thermal ageing at 70°C (see Figure 4.6). As discussed both in Section 2.4 and 5.4 the breakdown strength of LDPE depends on Young's modulus at 70°C. The change in electromechanical breakdown level due to the change in Young's modulus can be calculated from Equation 2.2. Figure 7.9 shows the calculated percentage change in breakdown level compared with the change obtained from the breakdown tests. After 4 weeks at 70°C there is a good agreement between the change calculated from Young's modulus and the measured change in LDPE without antioxidant. In LDPE with antioxidant there was no such agreement. The measured breakdown level was unaltered after ageing even though Young's modulus increased. This indicates that the space charge situation arising due to the antioxidant caused breakdown at a level below the electromechanical critical field. This is also supported by the fact that the breakdown level in the material with antioxidant was about 20% lower than in LDPE without antioxidant despite the two materials having equal elastic modulus.

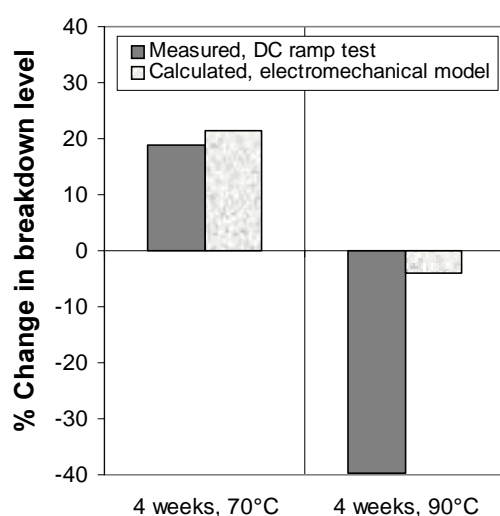


Figure 7.9 Percentage change in breakdown level due to thermal ageing measured with the DC ramp test and calculated from the electromechanical model. The values of Young's modulus obtained in Chapter 4 was used in the calculation. *LDPE without antioxidant.*

Another question is why the same improvement of the breakdown voltage due to annealing was not observed in the case of positive applied voltage. This may be explained as follows: With positive polarity the accumulated charge is confined to a small region around the needle and the region with high electric field is also limited. Compression of this small fraction of the insulation does not cause electromechanical instability and breakdown first occurs when the field around the needle reaches the intrinsic breakdown level.

Oxidation of LDPE without antioxidant -> reduced breakdown level

After 4 weeks at 90°C the breakdown voltage of the test objects without antioxidant was reduced by as much as 40% in the case of negative polarity. The oxidation measurements clearly demonstrated that this reduction in breakdown voltage was related to a heavy oxidation of the material. The oxidized material had become brittle, but Young's modulus was unaltered and could not account for the large reduction in breakdown level, see Figure 7.9. The reduction was most probable caused by the oxidation products giving rise to enhanced high field conduction and corresponding Joule heating as discussed in Section 2.2.2. The reduction in breakdown voltage is in agreement

with results obtained by Chen et al. [25]. They found that the breakdown strength of LDPE was reduced by 30% after 15 days at 100°C.

No effect of oxidative degradation was observed in the case of positive applied voltage. Again this may be related to the poor screening which confines the high electrical field to a small region around the needle. The carbonyl concentration decayed towards the needle as can be seen from Figure 4.10. Thus the carbonyl concentration was low in the region with high electric field and no significant increase in the high field conduction occurred. This can be further illustrated by estimating the field distribution from the needle in the case of positive and negative polarity. The field estimation is based on equations developed by Mason [49]. It is assumed that the negative homocharge caused a needle extension of 0.2 mm while the positive homocharge only caused an extension of 0.04 mm. The estimated field distributions for the two polarities are shown in Figure 7.10. and we see that the field in the region with high carbonyl concentration is about 4 times higher with negative compared to positive polarity.

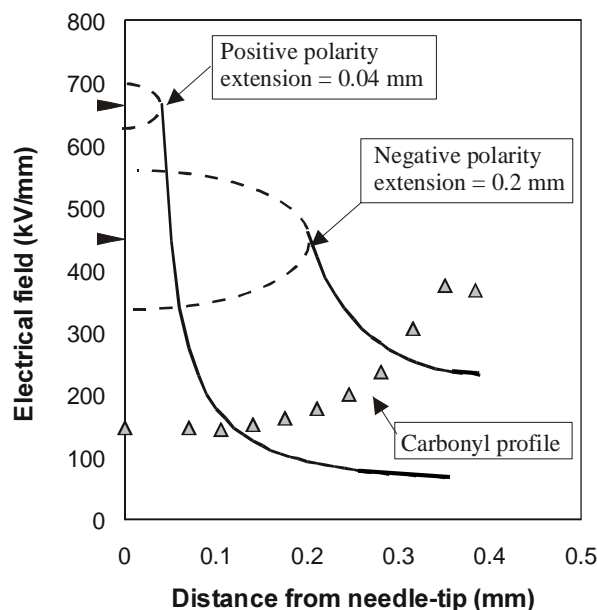


Figure 7.10 Illustration of the field distribution in the region with heavy oxidation in the case of 25 kV positive and negative voltage applied to the needle. The dashed lines indicate the needle extension due to accumulated homocharge.

7.4.2 Electrical treeing

Short-circuit trees initiated at breakdown

The observed electrical trees were most probably formed when breakdown occurred at one needle, i.e. short-circuit trees. The possibility of DC treeing during the voltage rise period may be rejected on the basis of the needle experiments with polyethylene done by Ieda et al. [50]. They found that with a voltage rise speed of 100 V/sec the tree initiation voltage was 80 kV in the case of positive polarity and far above this with negative polarity. The experiments were performed at 30°C but from the temperature dependence of the intrinsic breakdown strength we can expect a positive tree initiation voltage of at least 30 kV at 70°C. Thus with a needle to plane distance of only 0.4 mm the breakdown and tree initiation level coincide and breakdown probably occurred immediately when treeing was initiated at a needle. When tree initiation and breakdown took place at one needle, the accumulated homo-charges around the other two needles gave rise to a very high electrical field around the needle tip and a short-circuit tree was formed if the electrical field exceeded the intrinsic breakdown strength.

Inspection of the unaged test objects revealed electrical trees at all needles in the case of negative polarity while only a few trees were observed for positive polarity. As discussed in the previous section less homocharge accumulates around the needle with positive polarity, and therefore a lower electrical field arises at short-circuit giving less probability of tree formation. The mean treelength for negative polarity was about 100 μm which is in good agreement with the short-circuit results obtained by Ieda et al. [50] at 70°C after 15 minutes prestress with 50 kV.

Longer electrical trees after electrical ageing at 70 and 90°C

In general the number of electrical trees and the mean electrical tree length increased after electrical ageing at 70 and 90°C. In most cases the increased tree length was not related to a corresponding increase in breakdown voltage. There were less changes in the mean tree length after thermal ageing and this indicates that the change was related to the applied field during ageing. A suggestion is that homocharge drifted away from the needle during the four week ageing period and got trapped in the bulk of the insulation. Before DC testing the objects were short-circuited for one hour and the charge in the

proximity of the needles was removed due to a high driving field. The field decay away from the needle and the charge trapped in the bulk may thus have remained after short-circuit. When breakdown occurred this trapped charge may have played a part in the tree formation process.

The most pronounced effect of ageing on electrical treeing was observed in LDPE without antioxidant aged 4 weeks electrically at 90°C with positive applied voltage. A mean tree length of 280 μm was obtained and this was 70% longer than for any of the other ageing cases. It seems likely that this large increase was related to the heavy oxidation of the material. But why was the same large increase in treelength not observed in the case of negative voltage (mean tree length 160 μm)? This could be related to the difference in mobility of the positive and negative homocharges. As discussed in Section 2.5 the negative homocharge consists of injected electrons while the positive charge is a result of ionization and electron extraction in the high field region. From this it is reasonable to assume that the negative homocharge has a higher mobility than the positive charge. When the negative charge around the needle reaches a certain concentration and extension, charge will begin to move towards the plane electrode and disappear. Due to lower mobility the positive charge remain distributed throughout the whole insulation and the charge far away from the needle contribute to tree formation in the heavily oxidized material. Figure 7.11 illustrates this model together with the other test cases for LDPE without antioxidant aged with applied electrical field.

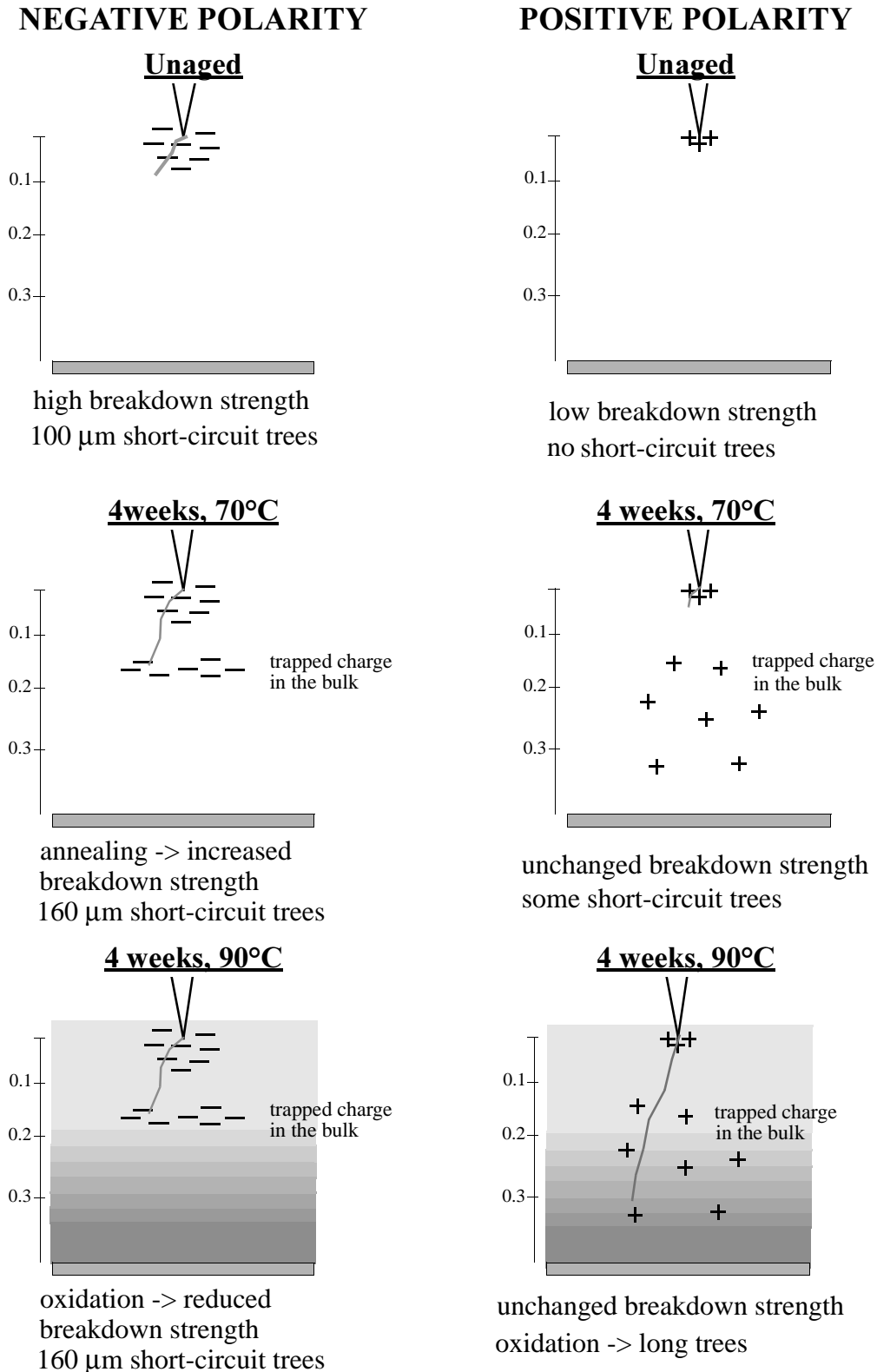


Figure 7.11 Proposed models for breakdown and tree formation in LDPE without antioxidant before and after electrical ageing. The grey shading illustrates the oxidation profile.

7.5 Conclusions

From the results discussed in this chapter the following conclusions can be made in relation to the four hypotheses presented in Chapter 1.

Effect of oxidation:

Heavy oxidation of LDPE without antioxidant was observed after 4 weeks ageing at 90°C. The oxidation gave a large reduction in DC breakdown strength, probably due to enhanced high field conduction.

Effect of the antioxidant additive:

The degree of oxidation remained unchanged in LDPE with antioxidant after thermal ageing at 90°C. Thus the protection was effective and the DC breakdown strength remained unchanged. LDPE without antioxidant performed better than LDPE with antioxidant until the oxidation process accelerated. The poorer performance of LDPE with antioxidant was probably a result of positive charge accumulation at the cathode.

Effect of protrusions when ageing with constant DC voltage:

When a constant DC voltage was applied homocharge accumulated around the needles and reduced the inhomogeneous electrical field. No sign of enhanced polymer degradation around the needles was observed after 4 weeks ageing. The DC breakdown strength was unchanged or even increased as long as the oxidation level remained low.

Effect of protrusions at failure / fast grounding:

When failure occurred at one needle during the DC breakdown test, electrical trees were often initiated from the remaining two needles in the test object. The number and length of these short-circuit trees increased after electrical ageing at 70 - 90°C.

Chapter 8

POLARITY REVERSAL TESTING OF SAMPLES WITH NEEDLE-PLANE ELECTRODE GEOMETRY

8.1 Introduction

The fourth hypothesis formulated in Chapter 1 states that defects in a HVDC insulation system are particularly critical during abrupt grounding or polarity reversal. The results obtained in Chapter 6 supported this hypothesis for the case of abrupt grounding, and in this chapter the effect of polarity reversals during ageing will be further investigated.

8.2 Experimental procedures

Cup-shaped test objects with three needle prints were prepared from LDPE with and without antioxidant as described in Section 3.2.3. The needle prints had a bend radius of $6 \pm 1.5 \mu\text{m}$ and the distance from needle to plane was $0.5 \pm 0.1\text{mm}$. All experiments were performed at a temperature of 70°C . The polarity given always refers to the needle electrode.

Short term DC polarity reversal breakdown test

The short term DC polarity reversal breakdown voltage was evaluated by applying the voltage sequence shown in Figure 8.1 to unaged test objects. The starting level at the needle electrode was -16 kV and after 5 minutes the polarity was reversed to $+16\text{ kV}$. The rate of reversal was 13 kV/second . After finishing the cycle at $\pm 16\text{ kV}$ the voltage level was incremented by 1 kV . This continued until the voltage reached 20 kV which was the maximum output of the voltage source. If breakdown had not occurred the cycling continued at $\pm 20\text{ kV}$. 80% of the breakdowns occurred before or during the

first cycle at 20 kV. The choice of 5 minutes DC stressing time at each polarity was based on the results by Ieda et al. [50] showing that the homocharge concentration around a needle in polyethylene reached a maximum level after 5 minutes of DC prestress at $T = 60^\circ\text{C}$ (see Figure 2.5).

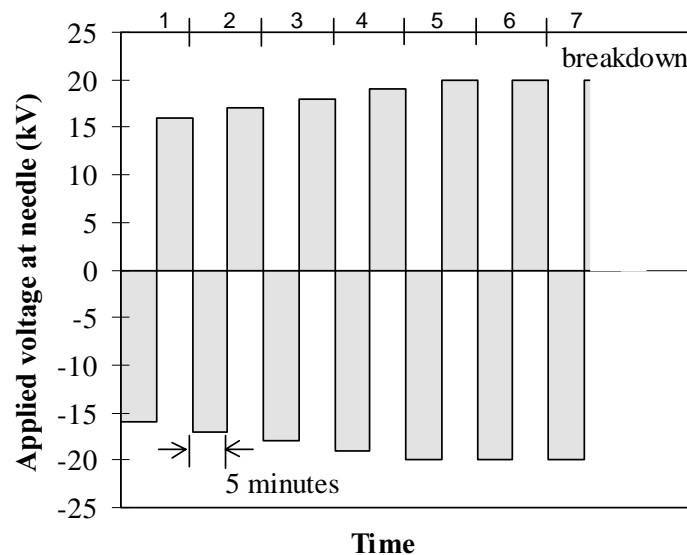


Figure 8.1 The DC polarity reversal breakdown test. The cycle number is given in the top of the figure. The voltage rate at reversal was 13 kV/sec. Breakdown always took place when changing from negative to positive polarity as indicated in the figure.

Long term ageing

During long term ageing the polarity was reversed between ± 8 kV every 5 minute at a rate of 13 kV/second. The test objects were kept in an air-ventilated oven at 70°C for a period of 4 weeks which corresponds to 4000 polarity reversal cycles. After ageing the test objects were subjected to a DC ramp test without polarity reversal. The test was performed following exactly the same procedure as described for unaged needle objects in Section 7.2. Negative polarity was used since the results in Chapter 7 showed that the effects of ageing were more pronounced in this case. Before the breakdown test the objects were kept short-circuited for one hour at 70°C to remove accumulated charge.

After the breakdown tests had been performed all test objects were microtomed in 250 μm slices and the areas around the needles were inspected with optical and infrared microscopy.

8.3 Results

8.3.1 DC polarity reversal breakdown test

The results from the polarity reversal breakdown test were analysed by Weibull statistics and the resulting 63% breakdown voltage is shown in Table 8.1. Both the material with and without antioxidant obtained a characteristic breakdown voltage of 20 kV. The scatter in the data was low as indicated by the high β -values. One test object with and one without antioxidant had no breakdown during the first cycle at 20 kV. These objects were given the value $U > 20$ kV and included as suspended data in the statistical analysis. In the object with antioxidant failure occurred after 7 cycles at 20 kV while the object without antioxidant survived 30 cycles after which the test was terminated.

Breakdown always occurred after changing from negative to positive polarity at the needle. In LDPE without antioxidant breakdown took place immediately after reversal or at the positive edge while in the case of the material with antioxidant the average time to breakdown was 93 seconds.

Table 8.1 DC polarity reversal breakdown voltage. $U_{63\%}$: characteristic breakdown voltage, β : Weibull shape factor, n/s: total number of data/suspended data, t: average time to breakdown from the last polarity reversal

| Material | $U_{63\%}$ (kV) | β | n/s | t (sec.) |
|---------------------|-----------------|---------|-----|-------------|
| without antioxidant | 19.8 | 21 | 5/1 | 0 |
| with antioxidant | 20.0 | 18 | 5/1 | 93 ± 24 |

Electrical trees were present at all needles after the breakdown test, also in the test object where breakdown did not occur. Figure 8.2 shows typical tree structures in test objects with and without antioxidant. The tree length was measured in the direction of the applied field (vertical) and at a right angle to the field (horizontal) as indicated in the figure. We see that in LDPE without antioxidant the tree extended almost twice as far in the horizontal direction as in the vertical direction while in LDPE with antioxidant the tree extension was similar in the two directions. A longer tree extension in the horizontal direction was observed in 60% of the test objects without antioxidant and in 20% of the test objects with antioxidant. This is reflected in Figure 8.3 which shows the average tree length for the two materials. We see that in LDPE without antioxidant the average tree length was 1.5 times longer in the horizontal than the vertical direction. In LDPE with antioxidant the horizontal and vertical tree length was similar.

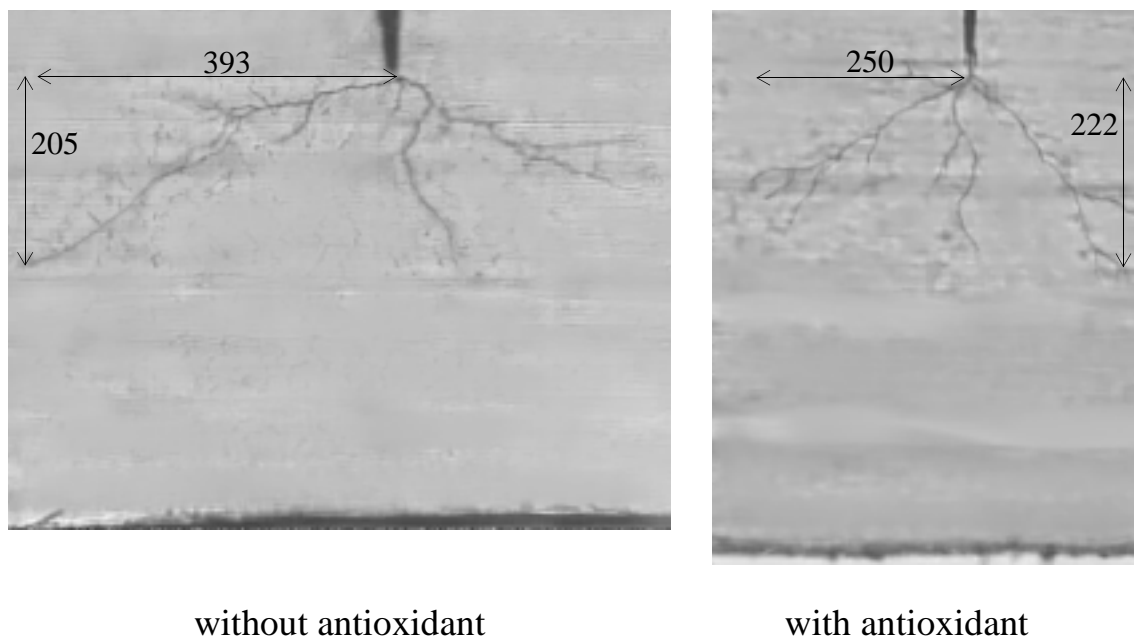


Figure 8.2 Microscope image of electrical trees formed during polarity reversal breakdown testing. The numbers give the tree length in the direction of the applied field and at a right angle to the field in micrometer.

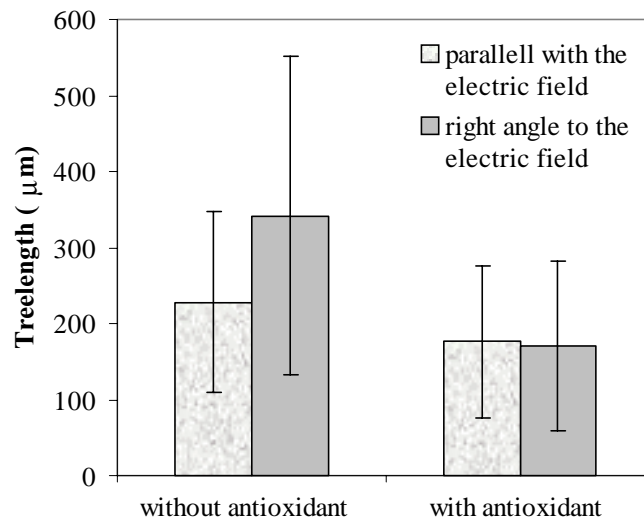


Figure 8.3 Average tree length after DC polarity reversal testing.

8.3.2 4 weeks DC polarity reversal ageing

The effect of the 4 weeks ageing with polarity reversals on the DC breakdown voltage is shown in Figure 8.4. The values for unaged materials tested with negative voltage are included as a reference. These values were previously presented in Chapter 7.3.1. In LDPE without antioxidant the negative breakdown voltage increased by 15% due to the ageing while in LDPE with antioxidant the breakdown voltage was reduced by 25%. Thus after 4 weeks polarity reversal ageing at 70°C LDPE without antioxidant had a 83% higher breakdown voltage than the material with antioxidant.

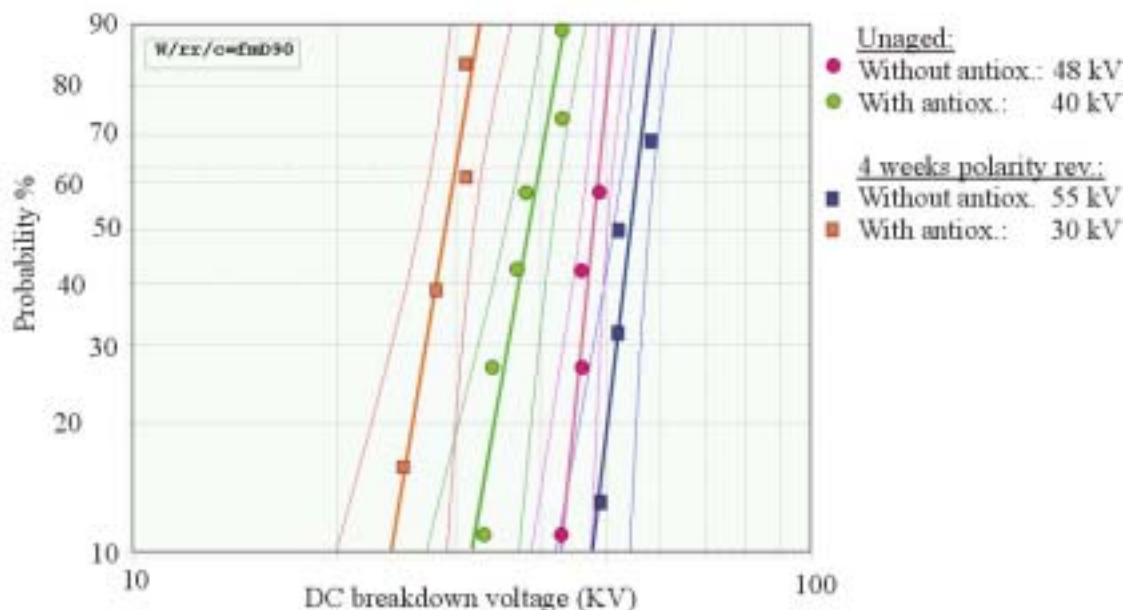


Figure 8.4 Weibull plot of DC breakdown voltage obtained before and after 4 weeks polarity reversal ageing at ± 8 kV and 70°C . Negative voltage applied during testing. The 90% confidence limits are shown and the 63% breakdown voltage is given in the legend.

The degree of oxidation after the polarity reversal ageing was measured by FTIR microscopy as described in Section 4.3.3. The number of carbonyl groups was unaltered both in the vicinity of the needle electrodes and the plane electrode, thus there was no evidence of accelerated oxidation caused by the polarity reversals.

Electrical trees were present at all inspected needles after the DC breakdown test. Figure 8.5 shows the average tree length in the direction of the applied field compared with the values obtained for unaged test objects and test objects aged 4 weeks with constant negative voltage. We see that in LDPE without antioxidant the mean tree length after polarity reversal ageing was the same as after ageing with constant negative polarity; about twice the length obtained for unaged test objects. In LDPE with antioxidant the mean tree length after 4 weeks polarity reversal ageing was the same as before ageing. In both materials the electrical trees had a similar extension in the vertical and horizontal direction.

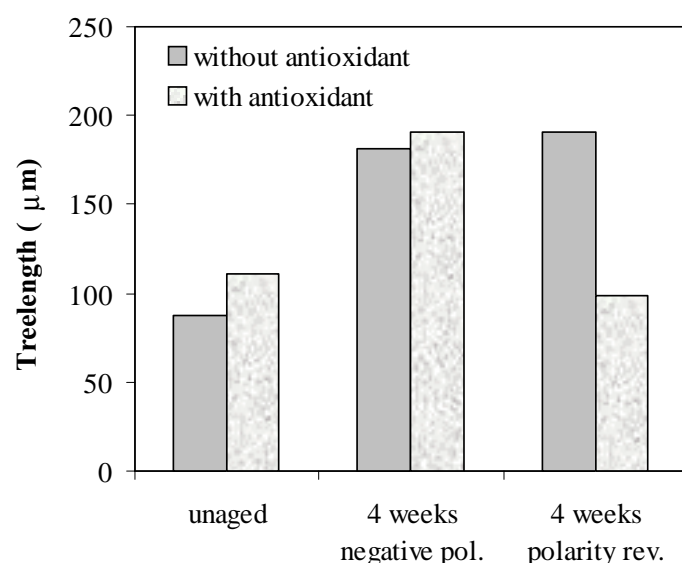


Figure 8.5 Average length of the electrical trees generated during the DC ramp test with negative polarity. Comparison of values for unaged test objects, objects aged 4 weeks at a constant voltage of -13 kV and objects aged with polarity reversal every 5 minute.

8.4 Discussion

8.4.1 Short term polarity reversal breakdown test

Polarity reversal more critical than constant DC voltage

The short term polarity reversal test resulted in a characteristic breakdown level of 20 kV for both materials. This is 25% lower than the level obtained in the DC ramp test with positive polarity in Chapter 7.3.1. The lower breakdown level is related to the high field arising around the needle tip at polarity reversal. Homocharge accumulates during the period of constant DC voltage and when the polarity is reversed in less than 1 second the accumulated charge is converted to heterocharge resulting in a high local electric field. Breakdown always occurred after changing from negative to positive polarity. This was expected since the results reported in Chapter 7 showed that more homocharge accumulated around a needle with negative compared to positive polarity. Thus when the polarity was reversed from negative to pos-

itive a higher field arised than in the opposite case, and the probability of breakdown was higher.

Breakdown delayed 1 - 2 minutes after reversal in LDPE with antioxidant

In LDPE without antioxidant breakdown took place immediately after reversal while in LDPE with antioxidant the time to breakdown was 1 - 2 minutes. This difference may be related to positive charge formation around the needle during the negative half-cycle in LDPE with antioxidant. Such positive charge formation in the case of needle with negative polarity was previously discussed in Section 7.3.1. The positive charge may have reduced the electrical field after reversal from negative to positive polarity and prevented an immediate breakdown. Even if complete breakdown was avoided electrical trees were probably initiated at reversal as will be further discussed in the next section. The electrical trees acted as an extension of the needle and reduced the insulation thickness by up to 50%. Thus breakdown may have been initiated from the extended needle after a few minutes even if the applied voltage was 25% lower than the positive breakdown voltage measured in Chapter 7. The proposed models for breakdown in LDPE with and without antioxidant is illustrated in Figure 8.6.

Electrical trees initiated at polarity reversal

After the polarity reversal tests electrical trees were present at all needles and the mean tree length for LDPE with antioxidant was 180 μm . In contrast electrical trees were only observed at 1 of 10 needles when breakdown tests with constant positive polarity were performed (see table 7.2). This gives a strong indication that the electrical trees observed after the polarity reversal tests were formed during reversal, not at breakdown. This is also supported by the fact that electrical trees were present at all needles, also in the test object where breakdown did not occur. The trees were probably initiated during some of the first reversals from negative to positive polarity and then continued to grow each time a new reversal took place.

There was a tendency of the electrical trees to extend longer in the horizontal direction than in the direction of the applied field, especially in LDPE without antioxidant. This can be related to the local field distribution around the needle immediately after polarity reversal. The field distribution is deter-

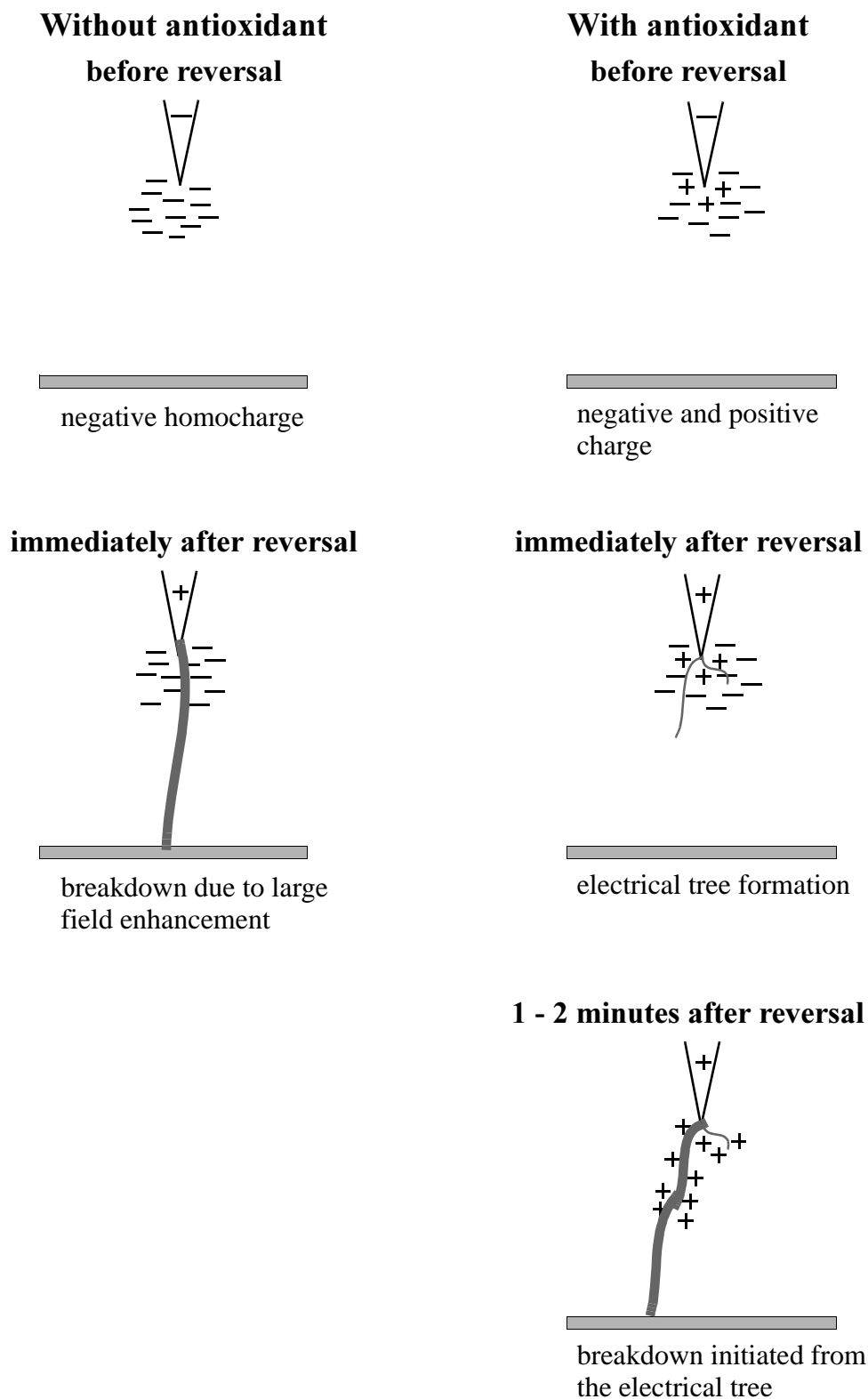


Figure 8.6 Schematic illustration of the proposed models for polarity reversal breakdown in LDPE with and without antioxidant.

mined by the distribution of the accumulated charge and therefore the maximum field gradient may appear in other directions than parallel with the applied field. When an electrical tree has been formed it is the field around the tip of the tree that determines the further growth direction. Due to the long, thin geometry of the tree it is most probable that the electrical field gradient has its maximum in the front of the tree. Therefore the electrical tree is likely to continue to grow in the initial direction.

8.4.2 Long term ageing

LDPE without antioxidant -> no effect of 4000 polarity reversals

The 4 weeks polarity reversal ageing increased the DC breakdown voltage of LDPE without antioxidant by 15%. This was unexpected since 4000 reversals at a fast rate of 13 kV/second was thought to be tough conditions that would lead to a reduced breakdown level. The voltage was reversed between +/- 8 kV, i.e. $\Delta U = 16$ kV. It is possible that this voltage difference was too low to initiate electrical trees during ageing. This is supported by results from Ieda et al. [50] showing that the short-circuit tree length decay towards zero when the negative pre-stress voltage is less than 25 kV. The electrical trees observed after breakdown were very similar in length and shape to those observed after ageing with constant negative voltage. This is also an indication that no electrical trees were formed during ageing. No tree initiation combined with improved mechanical strength due to the annealing effect may then explain why the breakdown level increased after ageing. The effect of improved mechanical strength on the breakdown level was discussed in Chapter 7.4.1.

LDPE with antioxidant -> 25% reduction after 4000 polarity reversals

LDPE with antioxidant behaved very differently; the negative DC breakdown voltage was reduced by 25% after the polarity reversal ageing. It was argued above that electrical trees were not initiated during ageing of LDPE without antioxidant. These arguments should also be valid for LDPE with antioxidant and therefore the reduced breakdown strength was probably caused by another process taking place during ageing. One possible explanation is that positive charge was generated during ageing which contributed to a less efficient screening of the needle in the succeeding DC breakdown test with negative polarity. The positive charge was generated in each negative

half-cycle and moved out of the high field region in each positive half-cycle. After 4000 cycles a large amount of positive space charge may have been distributed throughout the insulation. One question that arise from this proposed model is why a similar reduction of the DC breakdown voltage was not observed after 4 weeks ageing with constant negative polarity. The answer to this may be that with constant needle polarity an equilibrium between positive and negative charge was established and no further increase of the positive charge concentration took place.

8.5 Conclusions

The breakdown level obtained when applying DC polarity reversals was 20% lower than the level obtained when applying a constant positive DC voltage at the needle. Electrical trees were generated at all needles during the short term polarity reversal tests. Both these results confirm that polarity reversals may be critical if protrusions are present in the insulation system.

The DC breakdown strength of the test objects with antioxidant was reduced by 25% after a 4 week ageing period with 4000 polarity reversal cycles. This reduction was ascribed to positive charge generation in the negative half cycles giving rise to a less efficient screening of the needle in the following DC breakdown test.

Chapter 9

DISCUSSION

The main purpose of this work has been to obtain increased knowledge on which factors are controlling the endurance of an extruded polymeric insulation under HVDC conditions. LDPE was selected as insulating material and was subjected to thermal and DC electrical ageing in homogenous and inhomogenous fields. The effect of the ageing on electrical properties like space charge accumulation, DC breakdown strength and electrical tree initiation was investigated and related to changes in morphology, oxidation level and antioxidant concentration. In this chapter the four hypotheses presented in the introduction will be discussed on the basis of the results obtained.

1. Thermal oxidation has a negative effect on the long term electrical properties of LDPE.

Heavy oxidation was observed in LDPE without antioxidant after about 6 weeks at 70°C or 4 weeks at 90°C. This oxidation clearly affected the electrical properties. The DC breakdown voltage of the test objects with needle electrodes was reduced by 40% after 4 weeks ageing at 90°C. The probability of breakdown also seemed to increase when the oxidation process accelerated during long term ageing of test objects with and without iron particles. The reduced breakdown level was explained by the enhanced high field conduction with corresponding increased joule heating due to the oxidation.

The results demonstrated that thermal oxidation is detrimental to the insulation and must be avoided. Normally this is solved by adding an antioxidant to the material, but as discussed below the antioxidant itself may also have a negative influence on the electrical properties. The characterisation results presented in Section 4.3.3 showed that oxidation was inhibited in the

test objects where thicker aluminium electrodes had been deposited. The thicker electrodes acted as a barrier against oxygen and slowed the oxidation process significantly. This indicates the possibility that a oxygen tight outer sheet combined with a low operating temperature could be a sufficient protection against oxidation. Antioxidant is also necessary to prevent oxidation during the manufacturing process, but oxidation at this stage could possibly be prevented by operating in a nitrogen atmosphere.

2. The antioxidant additive prevents thermal oxidation but is a source of space charge accumulation in the insulation which may have a negative effect on the long term performance.

The protective effect of the antioxidant SantanoxR was clearly demonstrated when test objects with needle electrodes were subjected to 4 weeks ageing at 90°C. After ageing the DC breakdown strength of the material with antioxidant was unaltered while LDPE without antioxidant experienced a large reduction as mentioned above. The test objects with antioxidant were subjected to thermal ageing for up to 3000 hours at 70°C and 670 hours at 90 °C, but increased carbonyl content due to oxidation was never observed. Still, the measurements of antioxidant concentration presented in Chapter 4 showed that a loss of the antioxidant was taking place in the surface regions due to both migration and consumption of the antioxidant molecules. Some of the test objects with an insulation thickness of only 0.2 mm were almost completely depleted of antioxidant after 1500 hours of ageing at 70°C. Therefore the protection obtained with an antioxidant additive is time limited. The protection time depend on factors such as insulation thickness, oxygen availability and the ageing temperature.

Before oxidation LDPE without antioxidant showed a better performance than the material with antioxidant. In the case of test objects with needle electrodes, the material without antioxidant obtained a 20 - 36% higher negative DC breakdown voltage than the material with antioxidant. When the same test objects were subjected to 4 weeks ageing with polarity reversals the resulting negative breakdown level of LDPE without antioxidant was twice the level of LDPE with antioxidant. The long term ageing of test objects with and without iron particles showed that 60% of the objects with antioxidant failed during the first hour of ageing while only 30% of the test objects without antioxidant failed in this initial period. Enhanced space charge accumulation due to the antioxidant additive was probably the cause of the poorer performance. The space charge measurements presented in Chapter 5 showed a faster charge accumulation rate in LDPE with antioxi-

dant compared to the material without antioxidant. An electrode field enhancement of up to 75% was obtained in LDPE with antioxidant under certain ageing conditions, while the electrode field modification in LDPE without antioxidant never exceeded 45%.

The obtained results support the formulated hypothesis. The material was protected from oxidation, although only for a limited time, but it showed a poorer performance during and after electrical and thermal ageing due to space charge accumulation.

3. Inclusions in the insulation or protrusions at the electrodes are detrimental to the insulation and reduce the insulation life time under DC electrical ageing.

In this work irregular iron particles were used to investigate the effect of inclusions in the insulation and needle electrodes represented extreme protrusions at the electrode. The included particles reduced the short term DC breakdown strength, but during long term DC ageing no difference was observed between test objects with and without particles. The lack of particle influence was probably due to screening of the particles by accumulated space charge. The test objects with needle electrodes were subjected to 4 weeks electrical and thermal ageing but no accelerated degradation was observed in the vicinity of the needles. The DC breakdown level was unaltered or even higher than before the ageing started. This was also associated with accumulation of homocharges around the needle which reduced the high electrical field.

These results contradicts the hypothesis stated. None of the irregularities seemed to cause an accelerated degradation and reduced life time as long as a constant DC voltage was applied. When the voltage changed abruptly the situation was completely different as will be discussed below.

4. Defects in the insulation system are particularly critical during polarity reversal or abrupt grounding.

When the DC breakdown level of the test objects with three needle electrodes were evaluated, breakdown occurred at one needle and the two other needles experienced an abrupt grounding. In the case of negative polarity this abrupt grounding always resulted in electrical tree initiation at the other needles. The electrical trees had lengths varying from 50 - 300 μm and the longest trees were obtained when the test objects had first been subjected to

electrical and thermal ageing. The tree formation was caused by the high electrical field arising when the accumulated homocharge around the needle was converted to heterocharge at grounding. The electrical field exceeded the intrinsic breakdown strength of the material and a local breakdown was initiated.

The test objects with included iron particles also experienced an abrupt grounding when failure occurred at one site in the insulation, but no electrical trees were observed from the particles. The field enhancement was probably lower and confined to a much smaller region than in the case of the needle electrodes which may explain the absence of tree formation.

The test objects with needle electrodes were subjected to a short term polarity reversal breakdown test. The obtained breakdown level was 25% lower than with constant positive polarity and 60% lower than with constant negative polarity. Electrical trees were observed around all needles after the test, also in test objects where breakdown did not occur. Thus it was clear that the electrical trees were generated and were growing during polarity reversal. 4 weeks ageing with polarity reversal every 5 minute was also performed. The material without antioxidant was not affected by this ageing, and the negative breakdown level was the same as after ageing with constant polarity. The absence of degradation was explained by the applied voltage being below the threshold level for tree initiation. In LDPE with antioxidant the negative breakdown level was 25% lower after polarity reversal ageing compared to ageing with constant polarity. This was not ascribed to degradation during ageing, but to positive space charge generation caused by the antioxidant.

These results have shown that irregularities may be critical if the insulation is subjected to abrupt grounding or polarity reversal. Electrical trees may be initiated due to the high electrical field arising around the irregularity on reversal or grounding. Polarity reversals can be avoided with modern converter technology, but one can not be completely guarded against failure. From a practical point of view this means that failure and abrupt grounding at one site of an extruded HVDC cable may initiate electrical trees at protrusions throughout a whole cable length.

Chapter 10

CONCLUSIONS

In this work low density polyethylene has been subjected to thermal and electrical ageing under HVDC conditions with the purpose of gaining increased knowledge to which factors influence the life time of an extruded insulation. The following main conclusions can be drawn from the work:

- Thermal oxidation reduced the DC breakdown level of LDPE significantly. This was probably a result of enhanced high field conduction and localized Joule heating caused by the oxidation products. From these results it was evident that oxidation must be avoided in HVDC cable insulation. It was observed that oxidation was prohibited when the thickness of the electrodes increased.
- The antioxidant additive prevented thermal oxidation. The protection time was limited as loss of the antioxidant due to diffusion and consumption was observed after 4 weeks thermal ageing at 70 and 90°C. The antioxidant additive caused faster space charge accumulation and larger field modifications at the electrodes. The DC breakdown level of the test objects with needle electrodes was reduced by 16 - 26% due to the antioxidant. After ageing with polarity reversals the breakdown level was 50% lower in test objects with than without antioxidant. The obtained results indicate that the possibility of eliminating the antioxidant additive completely should be considered due to its negative influence on the electrical properties.
- Included iron particles reduced the short term DC breakdown strength of LDPE, but during long term ageing no difference was observed between test objects with and without particles. This was ascribed to screening of the particles by accumulated space charge.

- Polarity reversal or abrupt grounding initiated electrical tree growth from the needle electrodes. This was caused by the high electrical field arising when the homocharge around the needle was converted to heterocharge on grounding or reversal. The length of the electrical trees increased after thermal and electrical ageing. These results indicate that abrupt grounding or polarity reversal of an extruded HVDC cable may initiate electrical trees from protrusions present at the electrode-insulation interfaces.

REFERENCES

- [1] A. Nyman, B. Ekenstierna; *The Baltic cable HVDC project*, CIGRÉ paper 14-105, 1996
- [2] F. Rüter, J. L. Parpal, S. G. Swingler; *A review of HVDC extruded cable systems*, CIGRÉ paper P2-03, 2000
- [3] M. S. Khalil; *International Research and Development Trends and Problems of HVDC Cables with Polymeric Insulation*, IEEE Electrical Insulation Magazine, Vol. 13, No. 6, pp. 35 - 47
- [4] M. Bryggeth, K. Johannesson, C. Liljegren, L. Palmqvist, U. Axelsson, J. Jonsson, C. Tørnkvist; *The development of an extruded HVDC cable system and its first application in the Gotland HVDC light project*, JiCable, pp. 538 - 542, 1999
- [5] K. Terashima, M. Asano, K. Watanabe, M. Yoshida, H. Kon; *Research and development of DC XLPE cable and associated factory joint*, JiCable, pp. 543 - 548, 1999
- [6] T. Tanaka, K. Kunii, T. Nakatsuka, H. Miyata, T. Takahashi; *High performance HVDC polymer cable*, JiCable, pp. 874 - 879, 1999
- [7] X. Bourgeat, M-H. Luton; *Results of tests using continuous high voltage on low density polyethylene insulation*, JiCable, pp. 694 - 696, 1995
- [8] S. Whitehead; *Dielectric Breakdown of Solids*, Clarendon Press, pp. 60, 1951
- [9] F. W. Billmeyer; *Textbook of polymer science*, John Wiley & Sons, Inc., Chapter 10, 1984
- [10] L. A. Dissado, J. C. Fothergill; *Electrical degradation and breakdown in polymers*, IEE Materials and devices, Series 9, Peter Peregrinus Ltd. on behalf of IEE, Chapter 9, 1992
- [11] J. J. O'Dwyer; *The Theory of Electrical Conduction and Breakdown in Solid Dielectrics*, Clarendon press, Oxford, 1973
- [12] T. J. Lewis; *Electrical Effects at Interfaces and Surfaces*, IEEE Trans. Electr. Insul., Vol. EI-21, No. 3, pp. 289 - 295, 1986
- [13] H. J. Wintle; *Conduction processes in polymers*, Chapter 3 in Engineering Dielectrics, Volume IIA, Electrical properties of solid insulat-

- ing materials: Molecular structure and Electrical behaviour, ASTM special technical publication 783, 1983
- [14] M. Ieda; *Electrical Conduction and Carrier Traps in Polymeric Materials*, IEEE Trans. Electr. Insul., Vol. EI-19, No. 3, pp. 162-178, 1984
- [15] D. M. Taylor, T. J. Lewis, *Journal of Physics D*, Vol. 4, pp. 1346 - 1357, 1971
- [16] L. A. Dissado, J. C. Fothergill; *Electrical degradation and breakdown in polymers*, IEE Materials and devices, Series 9, Peter Peregrinus Ltd. on behalf of IEE, Chapter 2, 1992
- [17] F. H. Kreuger; *Industrial High DC Voltage*, Chapter 4, Delft University Press, 1995
- [18] J. P. Crine, S. Haridos, K. C. Cole, A. T. Bulinski, R. J. Densley, S. S. Bamji; *Oxidation and Thermal Resistance of HMW-PE and XLPE H. V. Cables*, Int. Symp. Electr. Insul., pp. 219 - 224, 1988
- [19] T. Kelen; *Polymer Degradation*, Van Nostrand Reinhold Company, Chapter 6, 1983
- [20] C. Banmongkol, T. Mori, T. Mizutani, M. Ishioka, I. Ishino; *Effects of Oxidation on Electrical Conduction and Breakdown of Low-Density Polyethylene Films with Different Densities*, Jpn. J. Appl. Phys., Vol. 37, No. 3A, pp. 872 - 877, 1998
- [21] T. Mizutani, Y. Suzuoki, M. Hikita, Han Sang Ok, Kim Jong Seuk; *High field conduction and breakdown of polyethylene - oxidation effects*, Annual report IEEE Conf. Electr. Insul. Dielectr. Phenomena, pp. 54 - 59, 1991
- [22] M. Ieda, T. Mizutani, Y. Suzuoki, Y. Yokota; *Study of Space Charge Effects in Polyethylene by Thermal-pulse Current Techniques. Effects of oxidation*, IEEE Trans. Electr. Insul., Vol. 25, No. 3, pp. 509 - 514, 1990
- [23] Y. Suzuoki, T. Furuta, H. Yamada, S. O. Han, T. Mizutani, M. Ieda, N. Yoshifuji; *Study of Space Charge in Polyethylene by Direct Probing. Effects of oxidation*; IEEE Trans. Electr. Insul., Vol. 26, No. 6, pp. 1073 - 1079, 1991
- [24] T. Tsurimoto, M. Nagao, M. Kosaki; *Effect of Oxidation on Localized Heat Generation and Dielectric Breakdown of Low-Density Polyethylene film*, Jpn. J. Appl. Phys., Vol. 34, No. 12A, pp. 6468 - 6472, 1995

-
- [25] G. Chen, A. E. Davies; *Effect of Thermo-oxidative ageing on electrical performance of low density polyethylene*, IEEE 5th Int. Conf. on Cond. and Breakdown in Solid Dielectr., pp. 651 - 655, 1995
- [26] T. Kelen; *Polymer Degradation*, Van Nostrand Reinhold Company, Chapter 10, 1983
- [27] G. A. Cartwright, A. E. Davies, S. G. Swingler, A. S. Vaughan; *Effect of an antioxidant additive on morphology and space-charge characteristics of low-density polyethylene*, IEE Proc. Sci. Meas. Technol., Vol. 143, No. 1, pp. 26 - 34, 1996
- [28] T. Mizutani, Y. Suzuoki, Y. Matsukawa, A. Oganessian, K. Hattori, H. Kon, M. Ieda, T. Suzuki; *Space Charge and High Field Phenomena in Polyethylene*, Annual report IEEE Conf. Electr. Insul. Dielectr. Phenomena, pp. 55 - 60, 1992
- [29] N. Nibbio, T. Uozumi, N. Yasuda, T. Fukui; *The effect of Additives on Space Charge in XLPE Insulation - Crosslinking Reagent and Antioxidant*, IEEE Int. Symp. Electr. Insul., pp. 559 - 562, 1994
- [30] A. Gustafsson, P. Carstensen, U. H. Nilsson, A. Campus, A. A. Farkas, K. Johannesson; *A Study of Crosslinked Polyethylene for HVDC Cables*, Nordic Insul. Symp., pp. 61 - 68, 1999
- [31] J. B. Howard; *DTA for Control of Stability in Polyolefin Wire and Cable Compounds*, Polym. Engin. and Sci., Vol. 13, No. 6, pp. 429 - 434, 1973
- [32] H. E. Bair; *Exudation of an Antioxidant Additive from Thin Polyethylene Films*, Polym. Engin. and Sci., Vol. 13, No. 6, pp. 435 - 439, 1973
- [33] J. L. Parpal, C. Guddemi, Hinrichsen; *Antioxidant concentration distribution measurements in XLPE cable insulation by PIXE analysis, FTIR and UV spectroscopy*, JiCable, pp. 824 - 828, 1999
- [34] B. Andreß, P. Fisher, H. Repp, P. Röhl; *Diffusion losses of additives in polymeric cable insulation*, IEEE Int. Symp. Electr. Insul., pp. 65 - 67, 1984
- [35] L. E. Nielsen, R. F. Landel; *Mechanical properties of polymers and composites*, 2. ed., Marcel Dekker Inc., Chapter 2, 1994
- [36] H. W. Moll, W. S. LeFevre; *Some "Temperature-Young's Modulus" Relationships for Plastics*, Industrial and Engineering Chemistry, Vol. 40, pp. 2172, 1948

- [37] W. G. Oakes; *The electric strength of some synthetic polymers*, Proc. Instn. Electrical Engineers, Vol. 96 I, pp. 37 - 43, 1949
- [38] K. Stark, C. G. Garton; *Electric strength of irradiated polythene*, Nature, Vol. 176, pp. 1225, 1955
- [39] J. J. O'Dwyer; *The Theory of Electrical Conduction and Breakdown in Solid Dielectrics*, Clarendon press, Oxford, chapter 8.4, 1973
- [40] D. C. Bassett; *Principles of Polymer Morphology*, Cambridge University Press, pp. 132 - 133, 1981
- [41] F. Severini, R. Gallo, S. Ipsale; *Environmental Degradation of Stabilized LDPE. Later Stages*, Polym. Degrad. and Stability, Vol. 17, pp. 57 - 64, 1987
- [42] H. M. Gilroy; *Long term Photo- and Thermal Oxidation of Polyethylene*, Durability of Macromolecular Materials, Vol. 95, pp. 63 - 74, 1978
- [43] M. Ieda; *Dielectric Breakdown Process of Polymers*, IEEE Trans. Electr. Insul., Vol. EI-15, No. 3, pp. 206 - 224, 1980
- [44] L. A. Dissado, G. Mazzanti, G. C. Montanari; *The Role of Trapped Space Charge in the Electrical Aging of Insulating Materials*, IEEE Trans. Dielectr. Electr. Insul, Vol. 4, No. 5, 1997
- [45] J. David Mintz; *Failure Analysis of Polymeric-Insulated Power Cable*, IEEE Trans. Power Apparatus and systems, Vol. 103, No. 12, pp. 3448 - 3453, 1984
- [46] F. H. Kreuger; *Endurance tests with polyethylene insulated cables*, CIGRÉ 21-02, 1968 session, pp. 1 - 10, 1968
- [47] M. Fukuawa, T. Kawai, Y. Okano, S. Sakuma, S. Asai, M. Kanaoka, H. Yamanouchi; *Development of 500 kV XLPE Cables and Accessories for Long Distance Underground Transmission Line. Part III: Electrical properties of 500 kV Cables*, IEEE Trans. Power Delivery, Vol. 11, No. 2, pp. 627 - 634, 1996
- [48] G. Chen, A. E. Davies; *The Influence of Defects on the Short-term Breakdown Characteristics and Long-term dc Performance of LDPE Insulation*, IEEE Trans. Dielectr. Electr. Insul, Vol. 7, No. 3, pp. 401 - 407, 2000
- [49] J. H. Mason; *Breakdown of solid Dielectrics in Divergent Field*, Proc. IEE, Paper No. 127 M, pp. 254 - 263 (1955)

-
- [50] M. Ieda, M. Nawata; *DC treeing breakdown associated with space charge formation in polyethylene*, IEEE Trans. Electr. Insul., Vol. EI-12, No. 1, pp. 19 - 25 (1977)
- [51] H. Kawamura, M. Nawata; *DC Electrical Treeing Phenomena and Space Charge*, IEEE Trans. Dielectr. Electr. Insul., Vol. 5, No. 5, pp. 741 - 747 (1998)
- [52] M. Mammeri, C. Laurent, M. Nedjar; *Dynamics of Voltage Polarity Reversals as the Controlling Factor in Space-charge Induced Breakdown of Insulating Polymers*, IEEE Trans. Dielectr. Electr. Insul., Vol. 4, No. 1, pp. 44 - 51, 1997
- [53] N. Shimizu, C. Laurent; *Electrical Tree Initiation*, IEEE Trans. Dielectr. Electr. Insul., Vol. 5, No. 5, pp. 651 - 659, 1998
- [54] K. Uchida, N. Shimizu; *The effect of Temperature and Voltage on Polymer Chain Scission in High-field Region*, IEEE Trans. Electr. Insul., Vol. 26, No. 2, pp. 271 - 277, 1991
- [55] N. Shimizu, K. Uchida, K. Horii; *Initiation Mechanism of Electrical Tree - Chain Scission by Injected Charge and Role of Oxygen*, Annual report IEEE Conf. Electr. Insul. Dielectr. Phenomena, pp. 419 - 424, 1987
- [56] M. Mammeri, C. Laurent; *Influence of Space Charge Buildup on the Transition to Electrical Treeing in PE under AC voltage*, IEEE Trans. Dielectr. Electr. Insul., Vol. 2, No. 1, pp. 27 - 35, 1995
- [57] J. Bezille, J. Becker, H. Janah; *Electrical breakdown strength evolution of HV XLPE cable after long-term test. Correlation with physical properties*, Ji cable, pp. 212 - 214, 1995
- [58] S. T. Hagen, *AC Breakdown Strength of XLPE Cable Insulation*, Dr. thesis, NTNU, 1993
- [59] N. H. Ahmed, N. N. Srinivas; *Review of Space charge Measurements in Dielectrics*, IEEE Trans. Electr. Insul., Vol. 4, No. 5, pp. 644- 656, 1997
- [60] J. Densley, R. N. Hampton; *Space Charge Measurements Techniques: A review*, Electra No. 187, pp. 75 - 89, 1999
- [61] T. Takada, T. Maeno, H. Kushibe; *An Electric Stress-Pulse Technique for the Measurement of Charges in a Plastic Plate Irradiated by an*

- Electron Beam*, IEEE Trans. Electr. Insul., Vol. EI-22, No. 4, pp. 497 - 501
- [62] T. Maeno, T. Futami, H. Kushibe, T. Takada, C. M. Cooke; *Measurement of Spatial Charge Distribution in Thick Dielectrics using the Pulsed Electroacoustic Method*, IEEE Trans. Electr. Insul., Vol. 23, No. 3, pp. 433- 439, 1988
- [63] B. Sanden; *XLPE Cable Insulation Subjected to HVDC Stress. Space Charge, Conduction and Breakdown Strength*, Dr. thesis NTNU, 1996
- [64] D. A. Skoog, J. J. Leary; *Principles of Instrumental Analysis*, 4th edition, Saunders College Publishing, pp. 266 - 269, 1992
- [65] D. A. Skoog, J. J. Leary; *Principles of Instrumental Analysis*, 4th edition, Saunders College Publishing, pp. 126 - 127, 1992
- [66] F. M. Rugg, J. J. Smith, R. C. Bacon; *Infrared Spectrophotometric Studies on Polyethylene. II. Oxidation*, J. Polym. Sci., Vol. XIII, pp. 535 - 547, 1954
- [67] M. U. Amin, G. Scott; *Photo-initiated Oxidation of Polyethylene, Effect of Photo-sensitizers*, European Polymer Journal, Vol. 10, pp. 1019 - 1028, 1974
- [68] F. W. Billmeyer; *Textbook of Polymer Science*, John Wiley & Sons, Inc., pp. 242-243, 1984
- [69] K. Karlsson, C. Assargren, U. W. Gedde; *Thermal Analysis for the Assessment of Antioxidant Content in Polyethylene*, Polymer Testing, Vol. 9, pp. 421 - 431, 1990
- [70] K. Uchida, T. Kawashima, T. Uozumi, Y. Inoue, S. Fukunaga; *Effects of Morphology on Space Charge Distribution in Polyethylene*, Int. Symp. Electr. Insul. Materials, pp. 231 - 234, 1995
- [71] K. S. Suh, H. H. Koo, S. H. Lee, J. K. Park; *Effects of Sample Preparation Conditions and Short Chains on Space Charge Formation in LDPE*, IEEE Trans. Dielectr. Electr. Insul., Vol. 3, No. 2, pp. 153 - 160, 1996
- [72] F. Oldervoll, E. Ildstad; *Space Charge, Oxidation and Morphology Changes in Low Density Polyethylene During High Voltage DC Ageing*, Conf. rec. of the IEEE Int. Symp. Electr. Insul., pp. 477 - 480, 2000

- [73] T. Mizutani, Y. Suzuoki, H. Kon; *Effects of oxidation and antioxidants on space charge in polyethylene*, Annual report IEEE Conf. Electr. Insul. Dielectr. Phenomena, pp. 89 - 92, 1995
- [74] S. Mbarga, D. Malec, N. Zebouchi, Hoang-The-Giam; *Study of space charge effect on dielectric DC breakdown of synthetic insulators with the pressure wave propagation method*, J. of Electrostatics, Vol. 40&41, pp. 355 - 361, 1997
- [75] J. K. Nelson; *Breakdown Strength of Solids*, Chapter 5 in Engineering Dielectrics, Volume IIA, Electrical properties of solid insulating materials: Molecular structure and Electrical behaviour, ASTM special technical publication 783, pp. 461 - 469, 1983
- [76] B. Wunderlich, M. Dole; *Specific Heat of Synthetic High Polymers. VII: High Pressure Polyethylene*, J. Polym. Sci., Vol. 24, pp. 201 - 213, 1957
- [77] W. G. Lawson; *Effects of temperature and techniques of measurement on the intrinsic electric strength of polythene*, Proc. IEE, Vol. 113, pp. 197 - 202, 1966
- [78] G. E. P. Box, W. G. Hunter, J. S. Hunter; *Statistics for experimenters*, John Wiley & Sons, Chapter 6, 1978

